UNIVERSITY OF ILLINOIS
URBANA

AERONOMY REPORT NO. 22

STUDIES OF IONOSPHERIC ABSORPTION MEASUREMENTS

by
J. S. Shirke

October 1, 1967

Supported by
National Aeronautics and
Space Administration
Grant NsG-511

Aeronomy Laboratory
Department of Electrical Engineering
University of Illinois
Urbana, Illinois

CITATION POLICY

The material contained in this report is preliminary information circulated rapidly in the interest of prompt interchange of scientific information and may be later revised on publication in accepted aeronomic journals. It would therefore be appreciated if persons wishing to cite work contained herein would first contact the authors to ascertain if the relevant material is part of a paper published or in process.

A E R O N O M Y R E P O R T

N O. 22

STUDIES OF IONOSPHERIC ABSORPTION MEASUREMENTS

by
J. S. Shirke

October 1, 1967

Supported by
National Aeronautics and
Space Administration
Grant NsG-511

Aeronomy Laboratory
Department of Electrical Engineering
University of Illinois
Urbana, Illinois

ABSTRACT

Several aspects of ionospheric absorption measurements undertaken recently are presented in this report. The studies are divided basically under four topics.

In Chapter 1 the phenomenon of the so-called 'winter anomaly' in ionospheric absorption is described. Following a brief review of the principal features of the anomaly, the various ground-based techniques normally available for the detection of the anomaly are discussed.

A criterion for the detection of the anomaly is presented, based on the ground-based measurements of vertical incidence absorption on short radio waves. The criterion has been successfully tested at Wallops Island, Virginia, by carrying out two series of rocket measurements during normal and anomalous conditions in the winter of 1965 through 1967. A comparison is undertaken of the results obtained from the rocket experiments with those derived from the ground-based techniques, and the two sets of measurements are observed to be consistent. The winter anomaly is observed to be caused mainly due to enhancements in electron number density in the lower ionosphere, and various aspects of the enhancement are discussed.

For an operating frequency of 3.03 MHz a substantial part of the total absorption is shown normally to be arising above 110 km, depending largely on the virtual height of reflection of the echo. The average anomalous absorption originating much below the 110 km level is shown to be about 8 dB at its noon maximum. Nevertheless the particular event investigated using a rocket launch during the winter of 1965-1966 is shown to be considerably larger in magnitude than the average, and that in the winter of 1967 much weaker.

Various other aspects of the normal and anomalous winter absorption are discussed, including the diurnal variation of absorption on the normal and anomalous days. The relative amplitudes of the deviative and nondeviative absorption components are also investigated as a function of altitude during normal and abnormal conditions.

Chapter 2 deals with the latitudinal variation of vertical incidence absorption along the 75° W longitude. The results are derived from measurements on board the USNS Croatan using mobile equipment during the 1965 expedition. The results so obtained are compared with those derived from the measurements at Wallops Island described in the first chapter. The effects of the latitudinal variation of the earth's magnetic field have been taken into account, using the classical magnetoionic theory.

A departure has been noted from the expected latitudinal pattern of absorption and has been presented as a geomagnetic anomaly. The major features of the anomaly are shown to be the following:

1. A reduction in absorption around the geomagnetic equator in the afternoon hours; and
2. The appearance of a broad zone of increased absorption around geomagnetic latitudes of 18° persisting until late evening hours.

That the day-to-day variability in ionospheric absorption is not the cause of the observed anomaly is confirmed from early morning observations which agree very well with the expected latitudinal pattern of absorption. The existence of the anomaly has been shown to be consistent with observations noted at other stations in the eastern hemisphere.

In Chapter 3 a study is undertaken of the global distribution of ionospheric absorption on the ordinary and extraordinary modes of propagation.

The computer source program for the evaluation of the various indices is reproduced in the Appendices wherein two cases are shown. The first is applicable generally at all latitudes except under pure transverse or pure longitudinal propagation conditions. The other case is applicable for the transverse ordinary mode propagation. A typical output from the computer for a fixed location is also reproduced.

In Chapter 4 are presented some of the preliminary results of vertical incidence ionospheric absorption measurements at Urbana, Illinois. The observed absorption on 3.03 MHz has been shown to be very often largely deviative in nature. The diurnal and seasonal variation of this absorption has been estimated and is shown to be different from that normally expected for the corresponding nondeviative absorption.

The reflection coefficient of the sporadic E layer has been evaluated and its influence on the absorption characteristics of the normal E layer discussed.

Finally, some of the plans are presented for future work on vertical incidence measurements at the local station.

The generalized magnetoionic theory was used in the computations. A program adaptable for a 7094 computer has been developed to evaluate the absorption values at several selected latitudes along the 75° E and 75° W longitudes. At each location the absorption indices on the two magnetoionic modes were evaluated at each one km height interval from 56 to 110 km. The electron density model used in the computations was derived from a rocket experiment described in Chapter 1 for a normal winter day. The same is true with the electron collision frequency model. The variations in absorption characteristics investigated are then purely due to the variations in the terrestrial magnetic field.

Various features of the analysis are presented. Certain peculiarities are noted in the distribution of absorption close to the level of reflection of the waves. The geomagnetic anomaly described in Chapter 2 is suggested to be arising as a natural outcome of the generalized theory.

The frequency dependence of absorption is investigated as a function of altitude at different locations. A modification is suggested in the classical inverse frequency dependence of absorption.

Various aspects of the differential absorption between ordinary and extraordinary modes of propagation of waves are investigated as a function of latitude as well as altitude. The corresponding variations in the reflection coefficient of partially reflected waves from the lower ionosphere are also considered and the feasibility of conducting partial reflection experiments at different locations discussed.

Finally, the Faraday rotation characteristics of radio waves are investigated as a function of latitude and the changes taking place are compared with the corresponding changes in the absorption profiles.

ACKNOWLEDGEMENTS

The author wishes to thank Professor S. A. Bowhill, for the helpful discussions during the course of this work. The measurements described on board the ship were carried out by Mr. G. W. Henry.

The work described in this report was supported by the National Aeronautics and Space Administration under grant NsG-511.

The author was on leave of absence from the Physical Research Laboratory Ahmedabad 9, India, during the period of this work.

TABLE OF CONTENTS

TABLE OF CONTENTS (cont'd)

LIST OF ILLUSTRATIONS

LIST OF ILLUSTRATIONS (cont'd)

LIST OF ILLUSTRATIONS (cont'd)

1. WINTER ANOMALY IN IONOSPHERIC ABSORPTION

1.1 Introduction

The 'winter anomaly' in ionospheric absorption of radio waves has been shown by several investigators to be confined to middle latitudes where an excess absorption occurs on certain days in winter, above the amount expected from the relationship between ionospheric absorption and solar zenith angle.

In order to clarify the nature of the anomaly, it was decided to launch a few rockets equipped with suitable payloads and to make direct measurements of electron density, collision frequency of electrons and the mesospheric temperatures during anomalous and normal winter conditions.

It became essential to establish a criterion for the detection of the anomalous event from ground-based measurements. Experiments were therefore undertaken at Wallops Island, Virginia, using ground-based techniques to identify days of anomalous type during the winter of 1965 through 1967. Rocket experiments were performed based on the criteria; some of the results of these measurements are presented in the following, and a comparison undertaken of the ground-based and rocket results. Initially, however, some of the main features of the winter anomaly are reviewed and the techniques available for the detection of the anomaly surveyed.

1.2 Principal Features of the Anomaly

Ever since the discovery of the phenomenon by Appleton in 1937 considerable speculation has persisted as to the cause of the anomaly. The region of enhanced attenuation has not been identified, nor have the relative roles of the electron collision frequency and electron density in producing the anomaly been clarified. The phenomenon has been associated with the pressure ridges in the troposphere (Gregory, 1965), and with stratospheric warming

events (Shapley and Beynon, 1965). Beynon and Jones (1965) have attributed the phenomenon partly to changes in the collision frequency of electrons with neutral particles and partly to changes in the electron density. More recently, Sechrist (1967) has related it to changes in the electron density arising out of changes in the nitric oxide concentration; these being caused in turn by temperature inversions near the mesopause.

There is considerable geographic latitude dependence of the anomaly both in intensity and occurrence frequency; with no detectable anomaly at Ahmedabad (23° N, 73° E) (Shirke, 1959, 1962), a maximum is found around Sverdlovsk 57° N close to the same longitude zone as Ahmedabad (Thomas, 1961). In the American zone, Thomas suggests that the maximum incidence of the winter anomaly is near Washington 39° N. He shows that the winter anomaly effects are present to some extent at Churchill 59° N but its incidence is masked by auroral phenomena.

A strong dependence of the phenomenon on the sunspot activity is noticed with over 80 percent of the days being anomalous at the latitude of Slough (Appleton and Piggott, 1954) during the maximum of sunspot activity. Shapley and Beynon (1965) have shown a much lower occurrence frequency, once every five to eight days, at Lindau during a different solar epoch.

It is clear from the work of several investigators (Appleton and Piggott, 1954; Dieminger, 1955; Beynon and Davies, 1955; Lange-Hesse, 1953; Davies and Hagg, 1955) that the magnetic activity index cannot be used as a day-to-day criterion for the detection of the anomaly. However, a positive correlation exists between increase in the magnetic index and the winter anomaly when both are averaged for over four months (Thomas, 1961; Bossolasco and Elena, 1963).

1.3 Techniques of Detecting the Anomaly

1.3.1 Low Altitude Partial Reflections

Gardner and Pawsey (1953) have shown that it is often possible to receive backscattered echoes of transmitted pulses from low ionospheric levels provided sensitive recording equipment is available. The appearance of low-altitude echoes on fixed-frequency transmission or on ionograms has been correlated with the winter anomaly as seen from the work of Dieminger (1955), Appleton and Piggott (1948, 1954), Beynon and Davies (1955), Gnanalingam and Weekes (1955) and others.

In order to investigate this feature of the anomalous winter absorption in further detail, the output of a sensitive receiver was monitored on several occasions at Wallops Island. A technique similar to that used by Belrose and Burke (1964) was developed. Herein a pair of short pulses was transmitted once every two seconds. The pair consisted of an ordinary and an extraordinary pulse separated by an interval of about 0.07 seconds. The antenna receiving the ionospheric echoes on the two pulses was made to follow the polarization of the transmitting antenna by means of a relay system. The output of the receiver was then displayed on an oscilloscope such that the echo corresponding to the extraordinary mode was observed on the upper half of the screen; the ordinary echo appeared in the lower half with reversed polarity.

Normally no perceptible echo returns were observed from the lower ionosphere in spite of the high transmitter power. On a few occasions, however, echoes were observed from as low an altitude as 50 km. It has been confirmed from vertical incidence absorption measurements described later, that these events occurred on the anomalous type winter days.

A typical A-scope photograph taken on 10 January 1966, is reproduced in Figure 1.1. The horizontal scale giving the altitude of the echo is shown

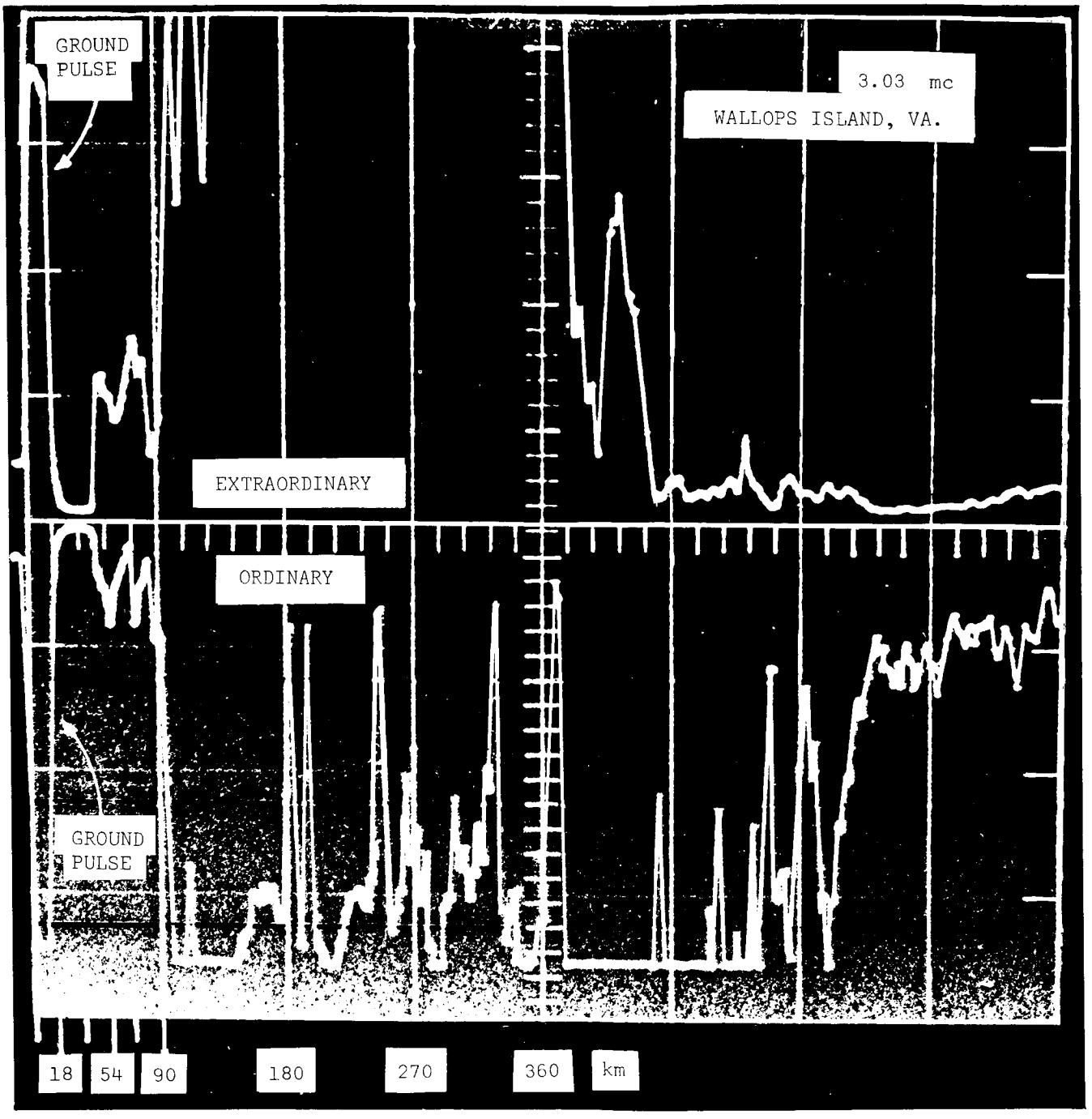

Figure 1.1 A noontime A-scan record of single pulse transmission made at Wallops Island on 10 January 1966. The extraordinary echoes are observed on the topside of the central line whereas the ordinary are seen below the same but with reversed polarity.

at the bottom. A receiver desensitizing pulse prevents any echoes from appearing below about 50 km.

Concentrating on the low-altitude region, the amplitude of the extraordinary echoes, shown on the topside of the central line dividing the face of the picture tube, is observed to be larger than the ordinary for altitudes below 80 km. Above this level the extraordinary wave is seen to be growing weaker compared to the ordinary. Observations during the above event, as also on another occasion, have shown that at a given time echoes with larger amplitudes are confined to specific altitude regions in the lower ionosphere. Besides, at a given altitude there is considerable fluctuation in the intensity of the reflected echo as a function of time.

One of the main features of these observations however, is that the low-altitude reflections start becoming perceptible only around 1100 hours local time and continue to increase in intensity towards noon. The appearance of the low-altitude echoes is expected to depend on the sensitivity of the equipment and on the noise level at a given time and location. The present evidence shows that, in addition to the above two factors, the conditions for the appearance of partial reflections become favorable as the anomalous absorption approaches its diurnal maximum.

Thus, an improvement in the detection threshold for partial reflection from low altitudes may well provide a criterion for the identification of an anomalous winter day. Nevertheless, the practical application of this feature would be limited. One would have to wait until the anomalous conditions have developed substantially to make a detectable improvement in the strength of the partial reflections. Alternatively, extremely sensitive equipment utilizing large transmitter power would have to be used to bring down the detection threshold of the echoes. This, however, is not always practicable.

1.3.2 Ionosonde Measurements on f_{min} and Lower E-Region Echoes

The above discussion was restricted to transmissions using very large powers. A typical ionosonde is usually not sensitive enough to record partially reflected echoes in the very low altitude range. A fairly sensitive ionosonde, for instance the Magnetic AB model J5, at times shows echoes beginning at 80 km and above. One such instrument is operated at Wallops Island, Virginia, by the Environmental Science Services Administration for the National Aeronautics and Space Administration. Several of the ionograms made on this equipment during the winter of 1965-66 were examined for possible clues as to the detection of the winter anomaly.

Figure 1.2 shows four of these ionograms made during two days, both known to be of the anomalous winter type from vertical incidence absorption measurements. The ionograms designated (a) and (b) were made on 16 December 1965 within an interval of 15 minutes. Those denoted by (c) and (d) were made on 10 January 1966 and were spaced at 20 minute intervals.

It is interesting to note that only two of these ionograms (b) and (d) show an echo at the low-frequency end of the ionogram. The echo is seen to lie between 92-102 km on ionogram 1.2 (d) and about 10 km lower on 1.2 (b). Further, the echo at the low-frequency end of the ionogram is completely absent in the ionograms (a) and (c) made a few minutes earlier on both days. Either the absorption below these levels had increased, or the gradient in electron density which could have been the cause of the partial reflection, had decreased within the short interval between ionograms.

Further, the minimum frequency f_{min} at which the trace begins at a higher level in the ionograms is very nearly identical in all four cases and is close to 1.5 mc/s. This suggests that the absorption below the reflection level of

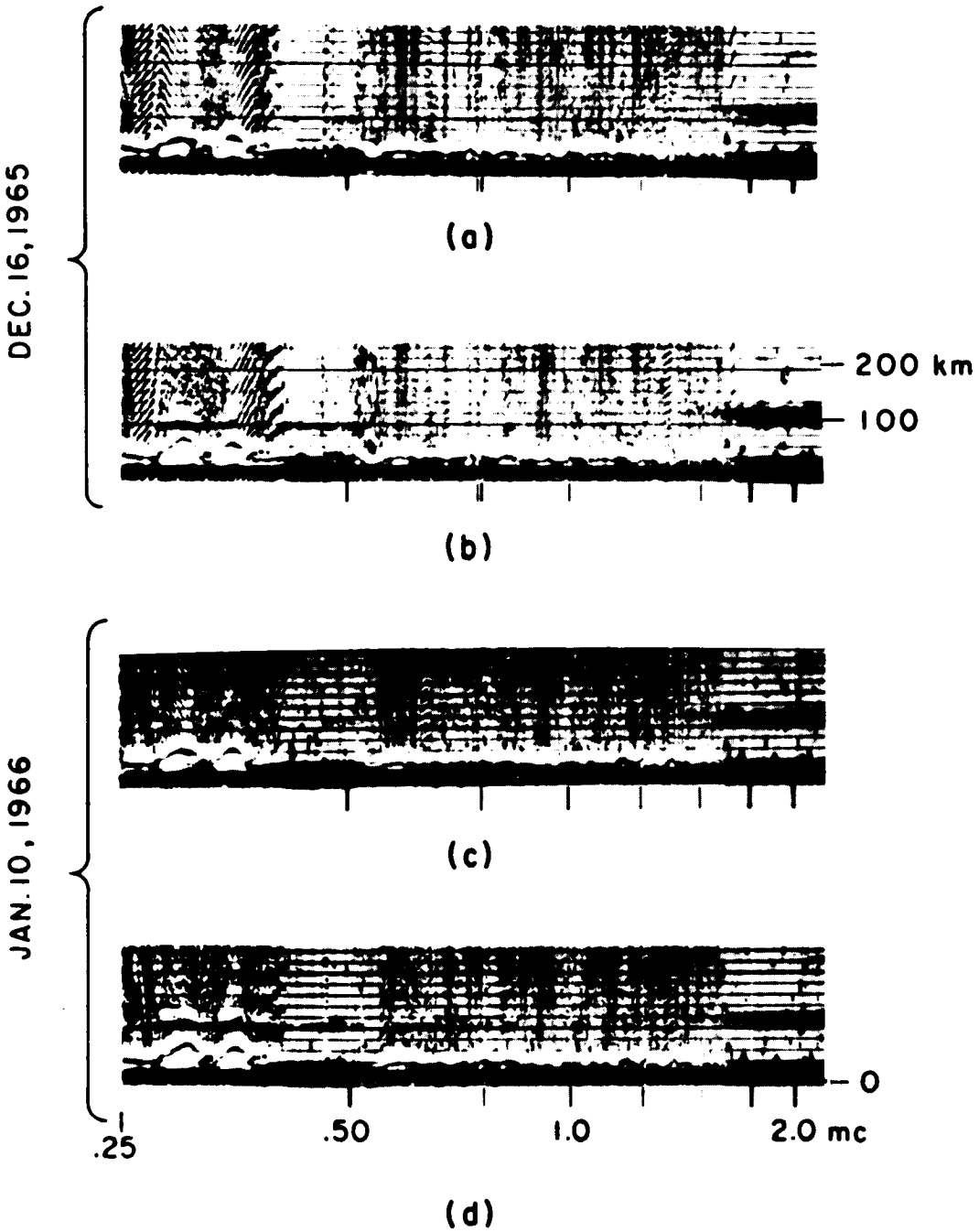

Figure 1.2 Vertical incidence ionograms made at Wallops Island on 16 December 1965 at times (a) 1215 (b) 1230 EST and on 10 January 1966 at (c) 1140 and (d) 1200 EST. Note, a separation of 8 km exists between the lower most height marker and the start of the ground pulse which needs to be taken care of in determining the virtual heights of echoes.

1.5 mc/s has not altered appreciably from one instance to the other. It may be concluded, therefore, that appearance of a layer below 100 km on an ionogram during an anomalous absorption event is often intermittent in nature, probably due to fading as well as oblique incidence, and is not always representative of the absolute plasma density at that altitude.

The rocket launched at noon on 10 January 1966 encountered a large gradient of ionization beginning at 82 km (Bowhill et al., 1967). If the echoes were to be formed by partial reflection caused in turn by the gradient in electron density, then we should have expected a strong reflection beginning at the 82 km level. However, none were observed at this altitude in either ionogram 1.2(c) or 1.2(d), the lowest level of the trace being 92 km in 1.2(d). Other ionograms made in quick succession at this time did not show the existence of a layer beginning at 82 km. This shows that for some reason genuine electron density gradients could be masked at times at low levels in the ionosphere and would not be discernible on ionograms.

Inspection of several ionograms shows that echoes are observable in the altitude region 90 to 100 km rather frequently. This includes days which are considered to be normal. Calculations of electron densities, based on the maximum frequencies reflected, at times agree fairly well with the expected values of plasma densities at these levels, suggesting that the reflections are from regular layers. However, there are occasions when the reflected frequency far exceeds that derived from the expected plasma density, suggesting that the reflections are partial in nature. Oblique incidence echoes from low altitudes might also be contributing substantially in this altitude region and it is usually hard to distinguish one type of reflection from the other. The appearance of echoes in this altitude region cannot be considered to be conclusive as to the existence or otherwise of the anomalous winter absorption conditions.

Returning to ionogram (b) in Figure 1.2 wherein an echo was seen in the altitude range 82-92 km, it was the only occasion during about two weeks of observations in the winter of 1965-66 that an echo was observed at these low altitudes in the ionograms. As noted earlier, this day was identified as one of the anomalous winter type. It may well be then that the appearance of echoes in this altitude range is positively correlated with the existence of the winter anomalous conditions. The converse, however, does not seem to be true, as is evident from the rest of the ionograms shown in Figure 1.2. The nonexistence of a layer between 82-92 km altitude range then should not necessarily imply the absence of anomalous conditions.

The minimum frequency recorded on the ionogram (f_{min}) has often been taken as an index of absorption. However, the interference due to the broadcast band often makes the reading of f_{min} difficult. Besides, the appearance of a layer discussed earlier in the 90-100 km region below the usual E-region level can cause further confusion in estimating the f_{min}. The presence of the lower layer would have to be ignored while computing the f_{min} on the E-region echo if f_{min} is to serve as an index of absorption. This is often difficult. Especially so when the two layers are not well resolved. A situation similar to that described above is often encountered when the zenith angle of the sun is large.

Keeping the sensitivity of the equipment constant is yet another requirement if f_{min} is to be related from one day to the other. The use of f_{min} in providing a criterion for the winter anomaly is therefore limited and not recommended.

1.3.3 Vertical Incidence Absorption Measurements

In view of the limitations in the techniques discussed so far in positively identifying the anomaly, it was decided to rely mainly on vertical

incidence absorption measurements. A schedule of operation was therefore drawn in advance of the expected dates of rocket launches. The criteria for the detection of the anomaly were drawn by Shirke and Rao (1967) based on these measurements taking into account the various factors that might normally influence the absorption recordings. Some details of these measurements are therefore incorporated in the following.

1.4 Experimental Setup for Vertical Incidence Measurements

The ground-based measurements were conducted using a pulsed transmitter tuned to 3.03 mc/s and having a peak power of 50 Kw. The pulse width was adjustable between 50 to 100 μsec. A pulse repetition frequency of 2 cps was used. The measurements were made using the ordinary mode of propagation. Two identical but independent antenna systems were used for transmission and reception of signals. Each system consisted of four half-wave dipoles situated at the four sides of a square array, the opposite sides being connected in parallel. The output from the two pairs of antennas thus formed were then combined after adding a suitable phase delay in one of the outputs. Circular polarization of either polarity could be achieved by proper choice of the delay.

The output of a high gain receiver was displayed on an oscilloscope and the desired echo was selected using a variable position gate. The gated output was then integrated using a circuit with a time constant of 45 seconds and fed to a pen recorder. In order to accommodate a larger range of amplitude variation of the echo a fraction of the output was fed back as AGC to the previous stages of the receiver.

The system was calibrated using the output from a standard signal generator which was modulated by a square pulse to simulate the ionospheric echo. The pulsed output of the signal generator was fed into the receiver

through an RF attenuator. The receiver output as observed on the pen recorder was calibrated in terms of the attenuator settings in the range of signals normally expected from the ionosphere.

Usually echo amplitudes were seen to be undergoing large fluctuations with periods ranging from one to ten minutes. For computation of absorption a period of ten minutes was found suitable, in general, to give a reasonable estimate of the median echo amplitudes. From successive measurements made, when conditions permitted, on the first and second order echoes it was possible to deduce an equipment constant which could then be used when only the first hop reflections were available.

1.5 Results of Absorption Measurements (1965-66 Winter Series)

A rocket (NASA code name 14.247) equipped with a composite payload (Bowhill, 1965) designed for the investigation of the winter anomaly phenomena was scheduled to be launched on 15 December 1965 as a part of the U.S. IQSY program, this being the final IQSY Quarterly World Day. Vertical incidence ionospheric absorption measurements were commenced at Wallops Island six days prior to the launch date. Measurements were made usually throughout the sunlit periods. It was confirmed from these observations that the ionospheric conditions were not anomalous on the day the launch was made. It became necessary to look for another day which would be of the anomalous type. In order to establish the criterion for the anomaly, measurements were continued until 20 December 1965. During this period various types of ionospheric conditions were encountered including 5 days with anomalous winter absorption. This provided an opportunity to study the diurnal variation of absorption under normal and abnormal conditions.

With a view to launch another rocket (code name 14.248), a second set of ground-based measurements was commenced on 4 January 1966. The rocket equipped with a payload identical to that used in the previous launch was kept ready every day until 10 January 1966. On this day the set criterion was satisfied and the rocket was launched at 1214 EST corresponding to a solar zenith angle of 60°, the same as in the previous case. The rocket measurements confirmed the existence of anomalously high absorption on this day. The analysis of the ground-based data leading to the launch of the rocket (14.248) is presented in the following.

1.5.1 Development of a Criterion for Detection of Winter Anomaly

A pair of typical records made during the ground-based measurements is reproduced in Figure 1.3. The nature of fading of the receiver signals on the two occasions is not identical. The record on the top corresponds to an echo returned from a regular ionospheric layer while that at the bottom is made during the presence of a blanketing type of sporadic E (Es). While the reflections from regular layers exhibit large amplitude fluctuations with a slow period of variation, the Es type reflections vary with a relatively short period and with a smaller range of amplitude. The nature of these records strongly suggests that the larger amplitude fluctuations originate above the level of normal Es.

A true-height analysis of some of the ionograms made during these measurements indicates that at the operating frequency the group retardation varies considerably from one day to the other, as also the virtual height of reflection of the echo. There is reason to believe that a large portion of the absorption taking place above the Es level is deviative in nature, caused by the retardation effects originating close to the level of reflection. Usually,

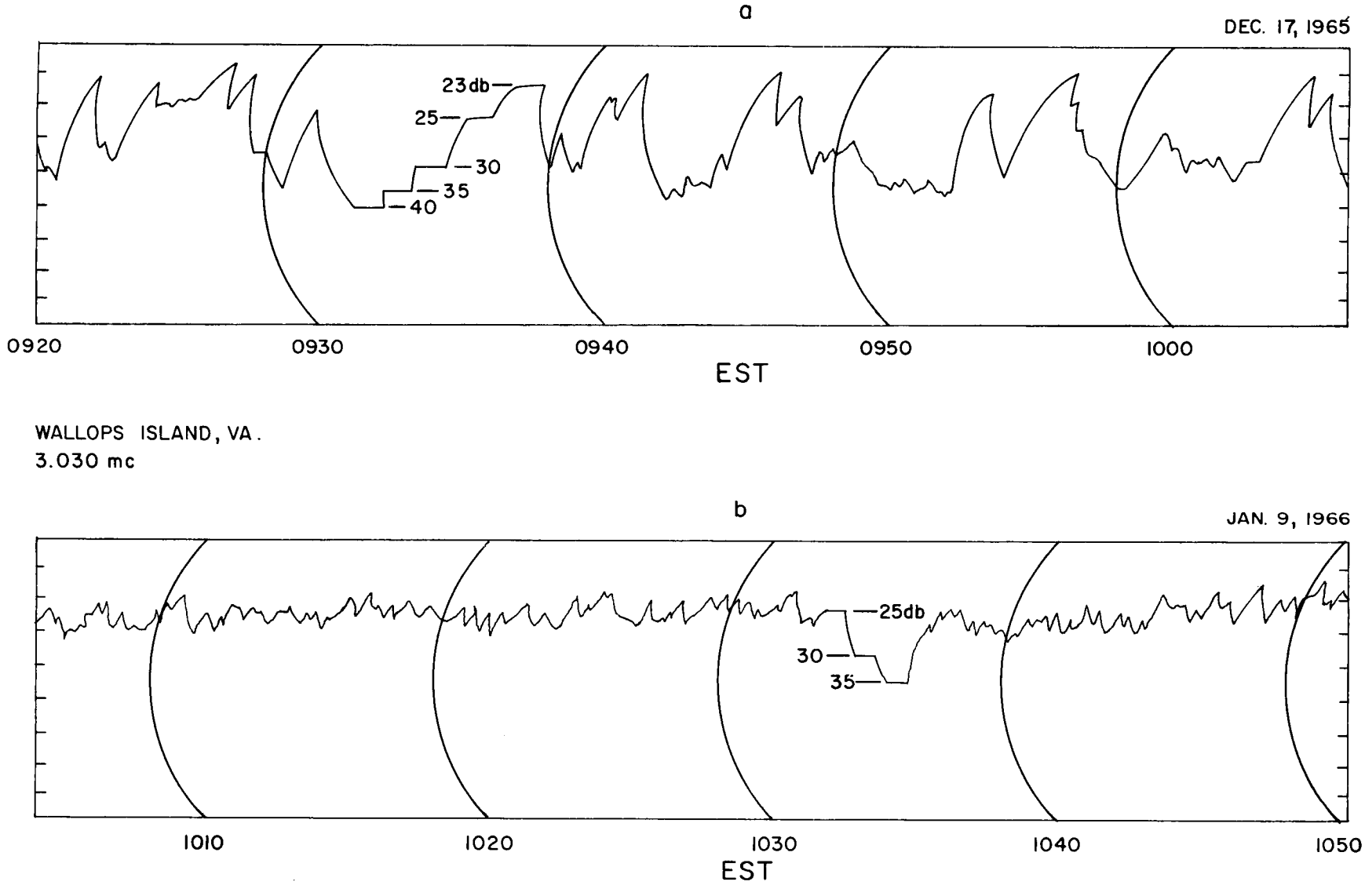

Figure 1.3 A pair of typical records reproduced from the automatic absorption recording equipment. The amplitude fluctuations in the one-hop transmissions from (a) F-region in the absence of any intervening Es layer and (b) a blanketing type Es layer.

measurements on a large number of frequencies would be required to isolate the absorption in the different ionospheric levels.

In the present study an approach has been employed wherein measurements on a single suitably chosen frequency, could be used to resolve the absorption in different ionospheric regions. The method relies on obtaining for a given local time and frequency, large variations in the virtual height of reflection of the echo from one day to another. Then the absorption below the lowest virtual height attained can be computed, provided significant changes have not occurred in the lower ionosphere from one day to another. The variable portion of the measured absorption can then be attributed to the changes in the virtual height of reflection of the echoes.

The application of the method of analysis described above has been shown in Figure 1.4. The average absorption for each day of observation for the three hours between 1030 to 1330 local time has been plotted as a function of the corresponding virtual height of reflection of the echoes on different days. The points are seen to lie very close to either one of the two dotted curves shown in the figure. There is reason to believe that those days for which the noon absorption lies close to the top curve are all of the anomalous winter type, while those falling close to the lower curve represent normal days.

In either category of days the absorption as seen from the two curves in Figure 1.4, is a linear function of virtual height in the region 110 to 190 km the absorption increasing with increasing altitude. Above 190 km there is a decrease in absorption with further increase in altitude. This might be explained on the following basis. Up to a certain altitude, the change in the virtual height of the echo is essentially due to a corresponding change in the group retardation close to the level of reflection with

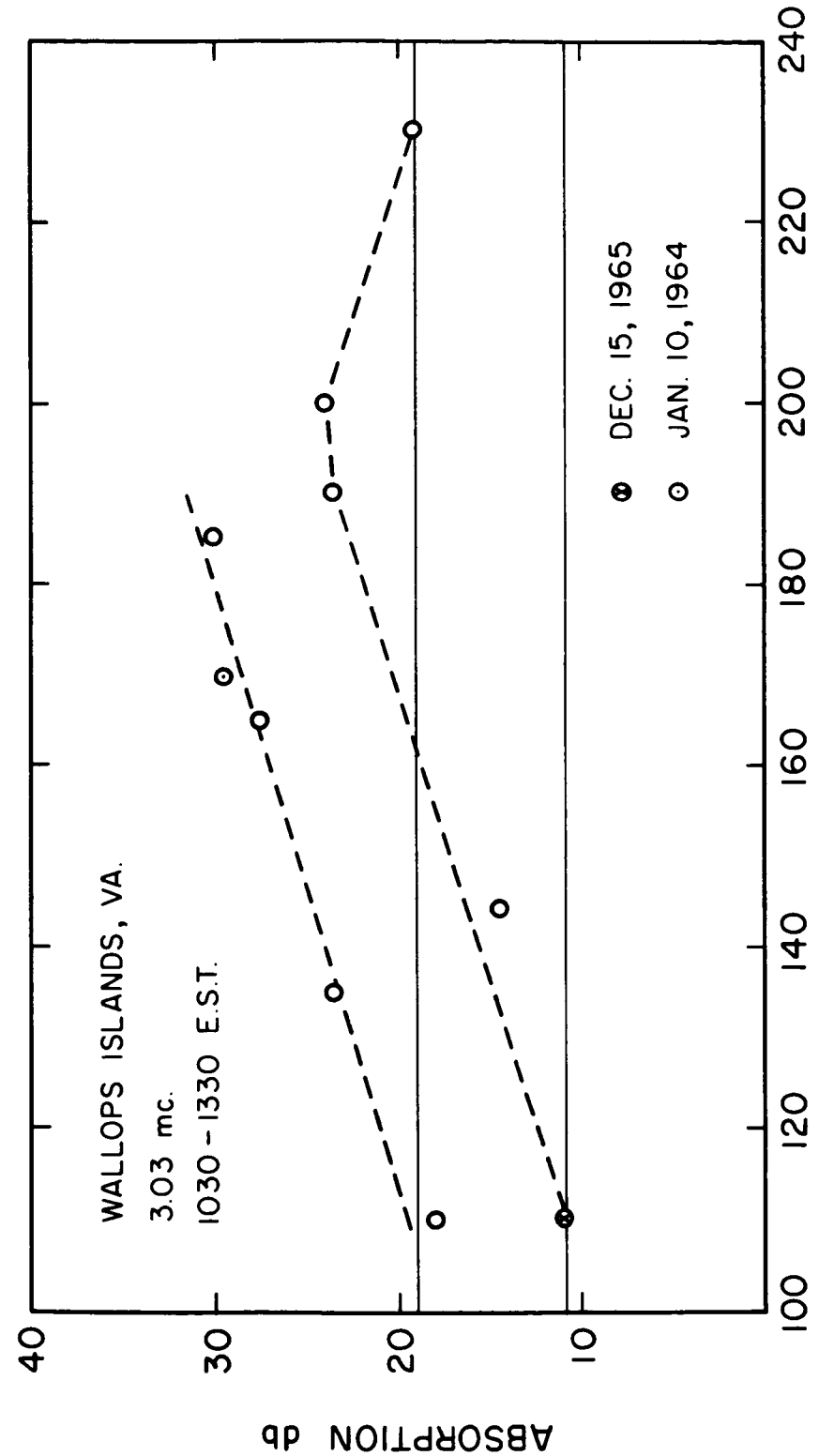

Figure 1.4 Absorption values averaged on individual days over 1030-1330 hours EST shown against the corresponding virtual heights of reflection of the echoes. The upper and lower dashed curves represent the anomalous and normal winter days respectively. The days on which rockets were launched have been identified.

relatively little change in the true height of reflection of the echo. The collision frequency of electrons with neutral particles would not alter substantially in this region therefore, and the absorption would be governed mainly by increases in the group retardation. Once the virtual height exceeds a certain value, in the present case 190 km, there would be a substantial change in the true height, the group retardation effects being relatively less. In effect the absorption would be less than before, the collision frequency having decreased with altitude. True height calculations at the operating frequency using some of the ionograms made during the above period of measurements supports the above conclusions.

In the range 110 to 190 km the absorption is seen to increase by 0.15 dB linearly for every 1 km increase in virtual height during both sets of days shown in Figure 1.4. Besides, the two curves are seen to run almost parallel to each other in the range of altitudes for which data are available on both sets of days. This strongly suggests that the cause of the winter anomaly lies somewhere below 110 km which is the lowest level of virtual height achieved during the present measurements. Further, the separation between the two curves is close to 8 dB throughout the common range of data points, indicating that the average excess absorption due to the anomaly is of the order of 8 dB at its noon maximum.

Figure 1.4 also shows that the normal absorption at noon is 11 dB below the 110 km level. The excess absorption on the anomalous day adds to the normal absorption and was close to 19 dB below the 110 km level, as was observed on one of the days (16 December 1965) when the reflections were from a sporadic E layer situated at 110 km. On days when the virtual height of reflection is larger than 110 km the total noon absorption L expressed in dB can be computed using the relationship

$$L = 19 + (h' - 110) \times 0.15 \qquad (1.1)$$

where h' is the virtual height of reflection of the echo expressed in km.

The ideal period to apply the above criterion for the winter anomaly for use with a rocket launch under the anomalous conditions would be between 1000 and 1100 local time; the anomalous absorption would have increased appreciably by then, still allowing enough time to make final preparations for the launchings of the rocket at noon. This does not imply that launchings should be restricted to noon; the anomalous absorption would be relatively less at other times of the day and would correspondingly be more difficult to detect.

Once the criterion has been set, any short period of observation should normally suffice to detect the presence of the anomaly; however, it is preferable to continue observation throughout a one-hour period such as between 1000 to 1100 local time. This is to avoid spurious increases in absorption due to causes such as focus fading, intervening sporadic E layer etc. It is unlikely that such causes would remain undetected throughout the one-hour period.

The above criterion was drawn at a time when the sunspot number was very low. At other times of the sunspot cycle due allowance would have to be made for the change in the solar activity.

1.5.2 Diurnal Variation of Absorption on an Anomalous Day

The above discussion was restricted to the noon absorption. The diurnal variation of absorption on the anomalous winter day is investigated in the following. In Figure 1.5 is plotted the absorption on 10 January 1966, a typical anomalous winter day, as a function of the cosine of the solar zenith

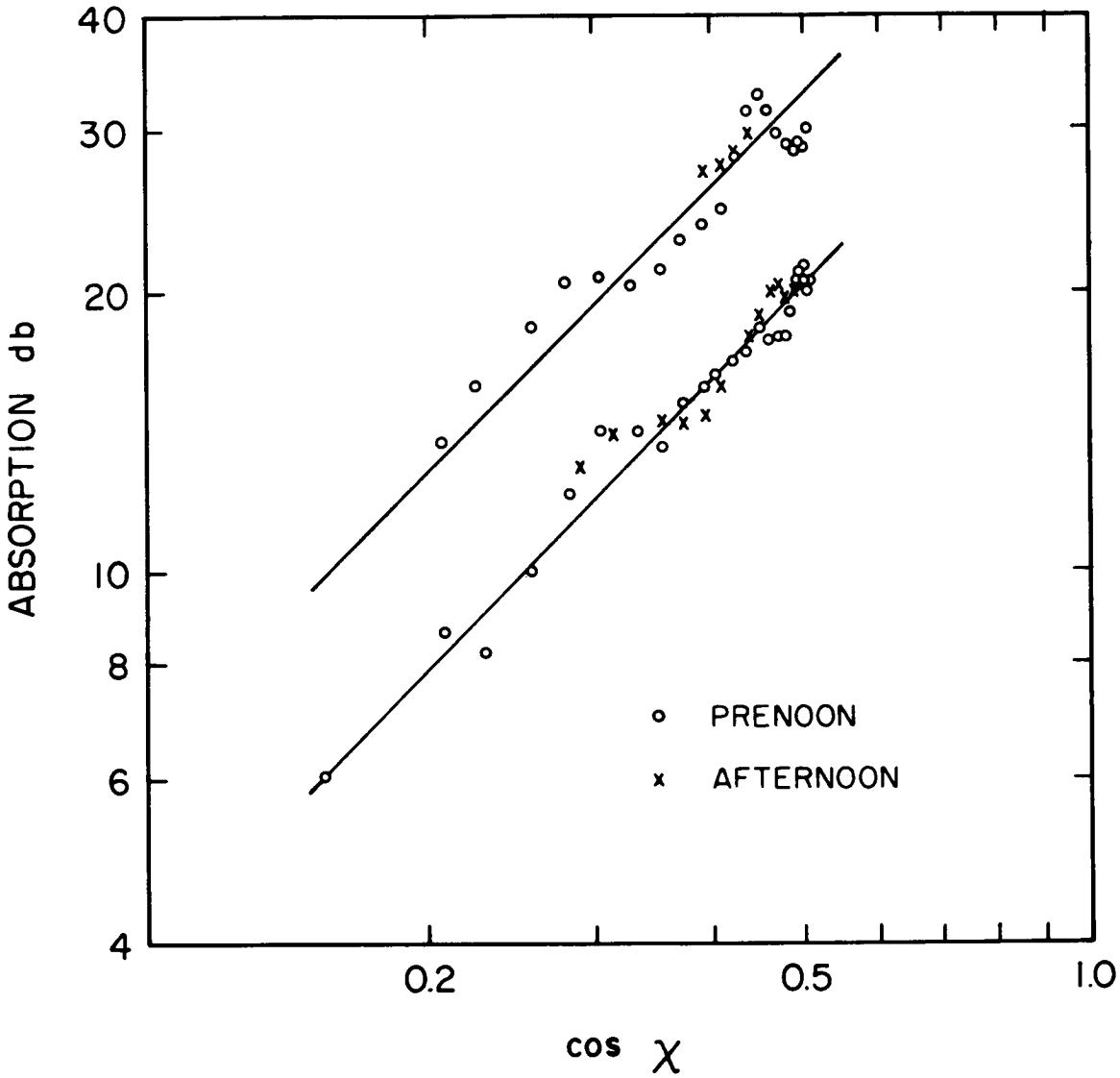

Figure 1.5 The absorption as it varies as a function of the cosine of the solar zenith angle is shown. Logarithmic scale has been used on either axis. The lower values correspond to control days; the larger values are for 10 January 1966, a typical winter anomalous day.

angle. Since it is hard to find a normal day with the virtual height of reflection remaining constant throughout, it has not been possible to make a direct comparison of the diurnal variation on a normal day with an abnormal winter day. Instead, the average diurnal variation of absorption on all the other days for which data has been available has been computed and compared with the abnormal winter day. These days have been referred to as 'control days' in the following discussion. On one of the control days the measured absorption was by far the largest and has therefore been excluded while computing the averages. It was a day of the anomalous winter type; the virtual height had remained close to 190 km through the day. As a result, the absorption below, as well as above, the 110 km level was large on this occasion.

Figure 1.5 also shows the diurnal variation of absorption on the 'control days' along with the variation on the abnormal day. The median values of absorption obtained for each successive 10-minute interval are used for the plot on the abnormal day. The average for a 10-minute interval around a given local time on all the control days is used to obtain successive points for the other plot. To reduce scatter a 3-point running mean has been taken. The two sets of points corresponding to the abnormal winter day and the control days seem to be close to two straight lines. Since the graph is plotted using logarithmic scales, the relationship between the measured absorption and the solar zenith angle can be expressed by

$$L = K (\cos \chi)^{\eta} \qquad (1.2)$$

where

L is the absorption in dB

χ is the solar zenith angle

K and n are numerical constants.

The value of n is close to unity for both sets of points, the value of K being 66 and 42 dB, respectively, corresponding to the abnormal and control days. These values of absorption would also correspond to the overhead sun, the value of n being unity. As can be seen from the plots, the absorption on the anomalous winter day under investigation obeyed the same law of variation as on the control days. The excess absorption on this occasion at least is seen to increase gradually with decreasing solar zenith angle. Whether a similar situation exists on other anomalous winter days will be discussed in a later section.

1.5.3 Comparisons of Results Obtained from Ground-Based and Rocket Techniques

As noted earlier, two rockets, 14.247 and 14.248, were launched during the above set of measurements. The results of these measurements will be presented in a paper by Mechtly and Shirke (1967). In the following, the rocket-derived electron density and collision frequency profiles are utilized to compute the corresponding vertical absorption profiles on the two events. A frequency of 3.03 MHz has been used since this was the frequency of operation for the ground-based experiments. Finally, the rocket-derived results are compared with those obtained from the ground-based measurements.

For the rocket 14.248 the electron density data was available only up to 93 km. A true height analysis has therefore been undertaken of an ionogram made at Wallops Island close to the launch time of the rocket. The electron density profile is extended to higher altitudes using the results

of the true height analysis. Since a single profile is involved, a manual 10-point method given by Schmerling (1958) is used. The ratios of the sampling frequencies appropriate for the Wallops Island location were obtained from Schmerling and Ventrice (1959). In this analysis no attempt has been made to correct the true heights for the underlying ionization below the threshold frequency of the ionogram. The electron density values close to 100 km will therefore be slightly in error. However with increasing altitude the retardation effect due to the underlying ionization will reduce considerably and will not be of a major consequence close to the reflection level of 3.03 MHz waves.

On the day rocket 14.248 was launched there was considerable fluctuation in the virtual height of reflection of 3.03 MHz waves as seen from several ionograms made between 1030 to 1230 hours EST. The average virtual height between the 2-hour period remained close to 165 km. In Figure 1.6 is shown the ionogram made at 1200 EST at Wallops Island redrawn on a different scale. Also shown is the true height profile evaluated using the procedure noted earlier. On an average, the true heights are seen to be about 70 km lower than the corresponding virtual heights in the 3.0 to 6.0 MHz frequency range. The true height corresponding to the 3.03 MHz is seen to be 116 km.

In Figure 1.7 is shown, as a function of altitude, the ratio of the electron number densities corresponding to the two rockets 14.248 and 14.247. The largest enhancement in the electron number density of 47 is noticed around 82 km during the anomalous event over the normal conditions. The average enhancement in electron density is seen to be close to 3.5 below the 80 km level. Above 82 km, the ratio of electron number densities falls smoothly. The same is seen to be close to unity at 102 km, indicating that the enhancement on the anomalous day had restricted itself to altitudes below 102 km.

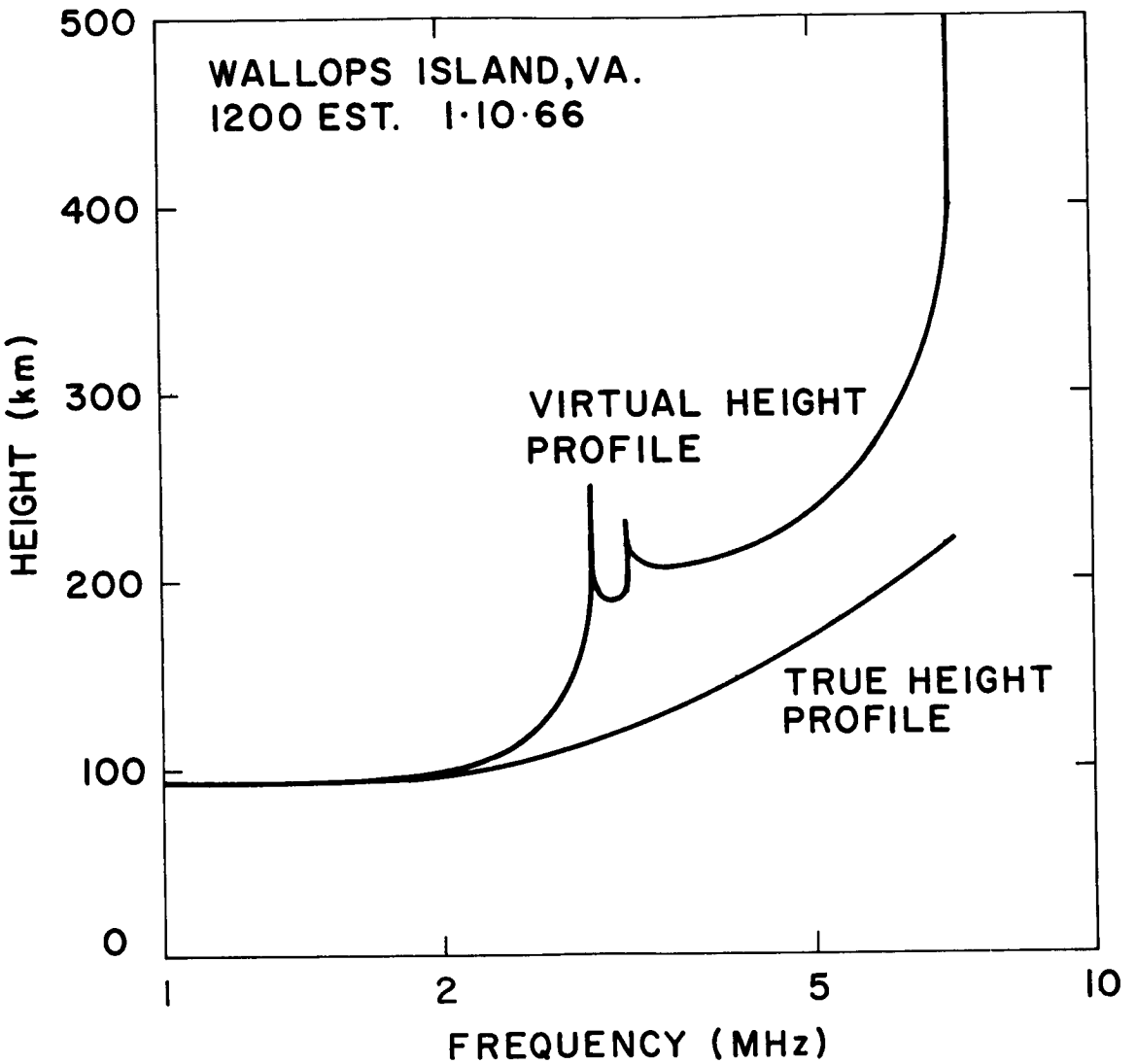

Figure 1.6 True height analysis of ionogram made at 1200 EST at Wallops Island (Virginia) on January 10, 1966.

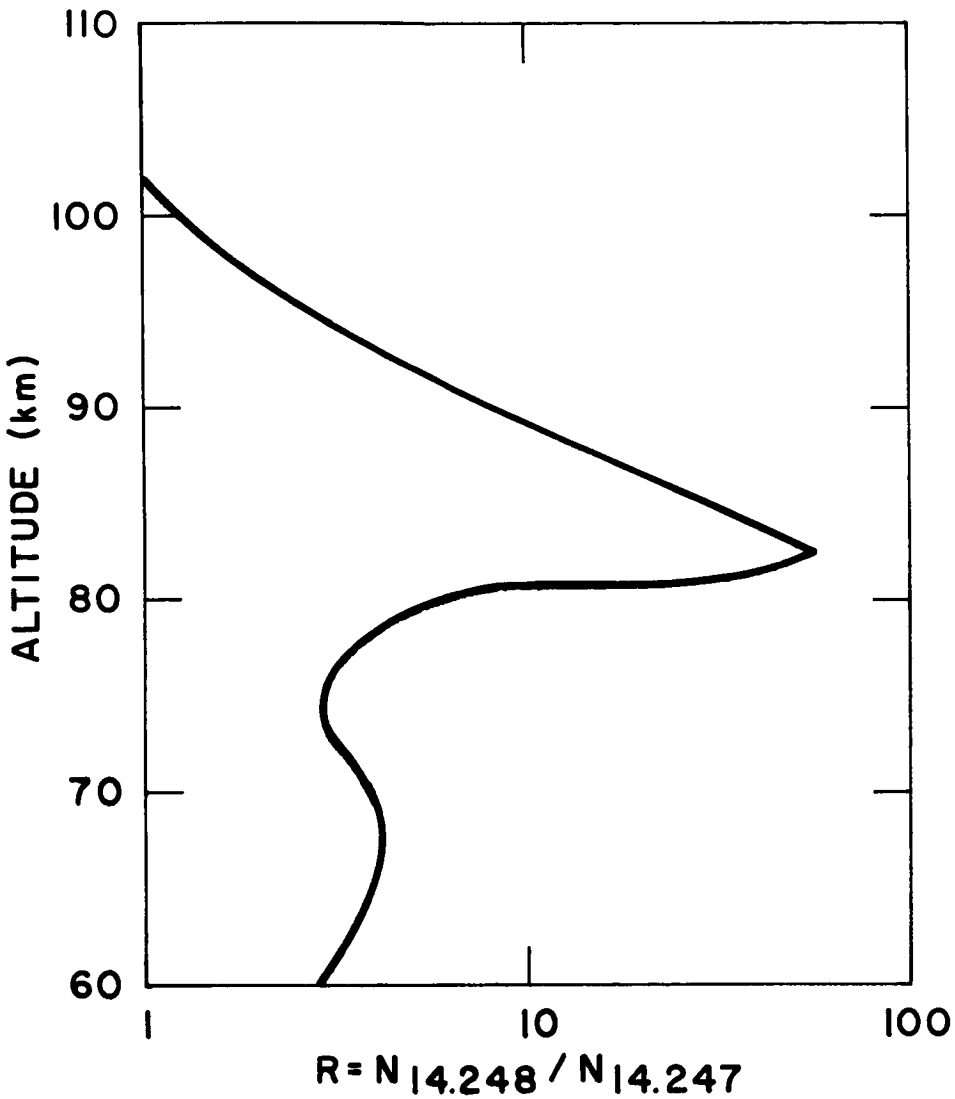

Figure 1.7 Ratio of electron density derived from rocket launches 14.248 and 14.247 shown as a function of altitude.

At altitudes close to 95 km a strong sporadic E layer was detected by the rocket experiments. Since this is not a usual feature, the peak in ionization at this level is intentionally suppressed in the calculation of the ratios, and also in subsequent calculations.

The propagation experiments in the rocket were performed on a frequency of 3.385 MHz, which is different from that used for the ground-based experiment. In order to compare the results derived from the two techniques, the ordinary wave absorption on 3.03 MHz is theoretically calculated using the profiles derived from the other experiments. The generalized Appleton and Hartree formulas given by Sen and Wyller (1960) have been used to evaluate the absorption over successive intervals of 1 km during which the electron density and collision frequency values are presumed to have remained constant.

A program adaptable for the 7094 computer available at the University of Illinois has been drawn to evaluate and sum up the absorption from 55 km up to the level of reflection of the waves. The refractive index corresponding to each height interval is also evaluated. The program is listed in Appendix I and will be described in some detail in Chapter 3.

The electron density profiles derived from the two rocket experiments and extended using the ionosonde measurements for 14.248 were fed in as input to the computer. As noted earlier a sharp Es layer was noticed around 95 km during the launch of rocket 14.247. The 3.03 MHz waves were totally reflected from this level. As a result, the absorption values were very low close to the launch time of the rocket. The Es layer must have existed for a very short duration as seen by the increase in absorption both a little prior to and after the launch time. Since the main purpose of the analysis is to investigate the normal behavior of the ionospheric absorption

characteristic rather than the transient one, the peak in the ionization corresponding to the Es layer has been suppressed while feeding the electron density profile to the computer.

For rocket 14.247 the electron collision frequency at any given altitude was found to be a function of the corresponding pressure value of p given by the CIRA (1965) model. The constant of proportionality was 6.74×10^5 where p was expressed in units of (Newtons/meter^2). Measurements during 14.248 did not permit evaluation of this constant unambiguously. The same collision frequency model was derived from 14.247 was therefore applied for the 14.248 analysis.

The absorption per km derived as a function of altitude is shown in Figure 1.8 for the electron density and collision frequency profiles discussed above. It is interesting to note that absorption has remained fairly low up to an altitude of 85 km on the normal day. In fact it is less than 10 percent of the total absorption evaluated up to the reflection level of 110 km on the anomalous winter day. The absorption is about 3.5 times larger throughout the altitude region below 81 km. A sharp increase in absorption is seen a km or so above this level. The maximum absorption on the anomalous day is seen around 90 km and is of the order of 1.68 dB/km. It is interesting to note that though the maximum enhancement in electron density was around 82 km, the maximum of absorption is located about 8 km above this level.

The curve showing the total absorption for 14.247 has a maximum at 97 km. This is due to a corresponding minima in the electron density at this altitude. But for this exception the absorption curves for 14.247 rise with increase of altitude; close to the 110 km level the absorption has increased sharply. This is due to the increase in the deviative absorption becoming large at these altitudes.

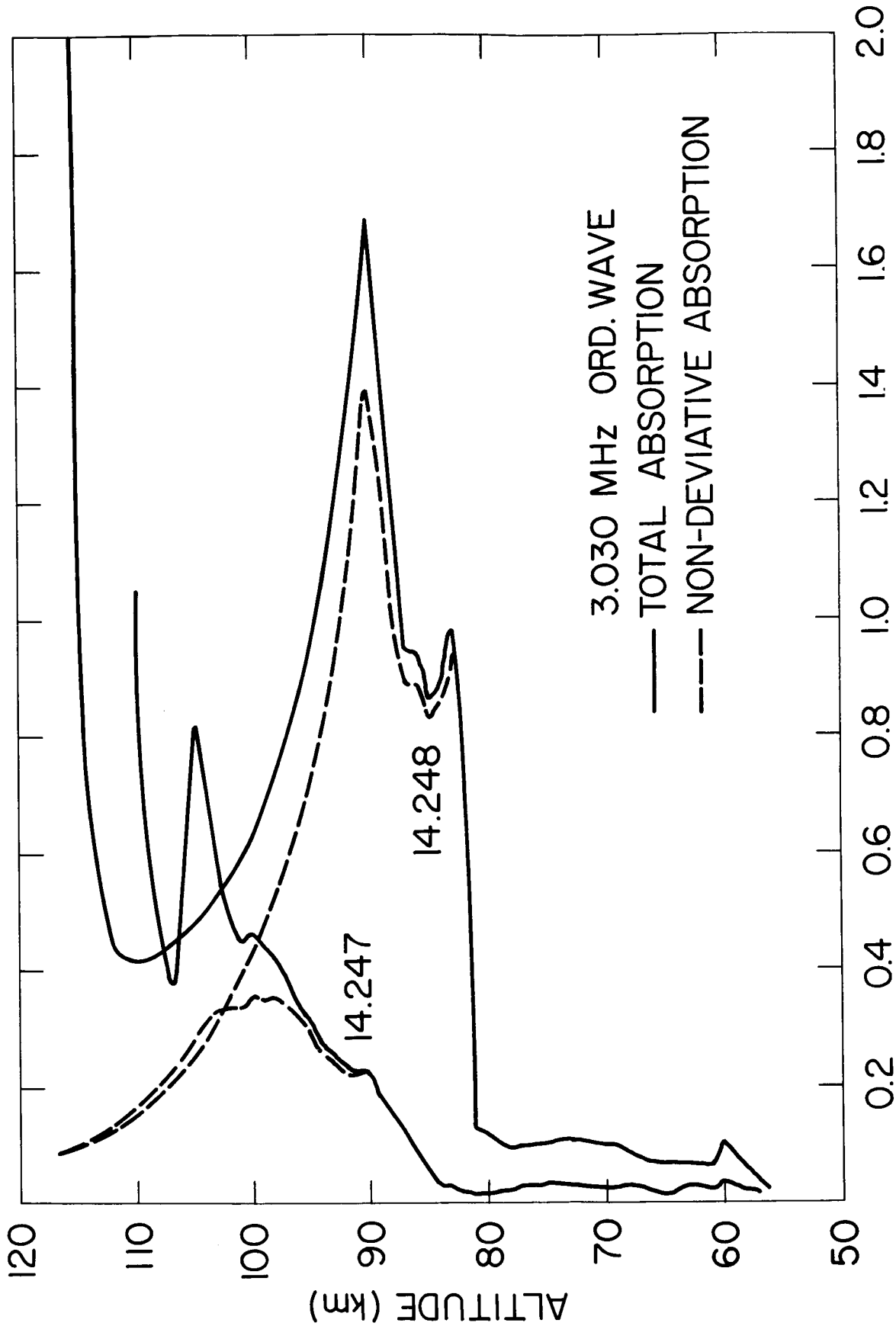

Figure 1.8 Ordinary mode absorption per km on 3.03 MHz derived from rocket launches 14.248 and 14.247. The nondeviative component of the total absorption is shown by the broken curves.

Also shown in the diagram are the values of the nondeviative absorption as a function of altitude. These have been computed using the product of the electron number density, the electron collision frequency and a constant. It is observed that the total absorption is mainly nondeviative up to an altitude of 90 km. Above this level it starts departing from the total absorption value. The separation of the two curves showing the total and the nondeviative components gives the contribution due to the deviative component of absorption to the total.

The nondeviative absorption corresponding to 14.247 is seen in the diagram to have a maximum around 99 km decreasing on either side of this level. For 14.248 the corresponding level is at 90 km, a shift of about 9 km over the normal day. Similarly, the deviative attenuation is seen appearing at such low levels as 82 km. With increasing altitude the deviative absorption is seen increasing, forming about 30 percent of the total at 100 km. Above 112 km it is seen rising very sharply as the level of reflection is approached.

On adding up the area under each of the curves the corresponding total absorption up to any desired altitude can be computed. For 14.247 the total absorption up to 110 km adds up to 11 dB out of which 6 dB is nondeviative. The average absorption measured on this occasion between 1030-1330 EST was 10.8 dB which agrees very well with that computed above. As can be seen from the diagram, the total absorption below 95 km for 14.247 is less than 3 dB. This explains the extremely low values of absorption measured for a short duration close to the launch time of 14.247, when a sporadic E layer appeared at this altitude and was responsible for total reflection of the 3.03 MHz signals from this altitude.

Corresponding to 14.248 the nondeviative absorption adds up to 22.6 dB up to the level of 116 km. The corresponding deviative absorption which can account for the observed retardation, works out to a value close to 10 dB. This brings the total absorption on this occasion to 32.6 dB. As noted earlier, the virtual height of reflection for the 3.03 MHz signal was fluctuating considerably during the few hours close to the launch time with corresponding changes in the deviative attenuation. The average absorption measured during the two hours preceding launch was close to 29 dB. The computed and measured values of absorption therefore seem to agree within the experimental accuracy of these measurements and lend mutual support to these observations made by the two different techniques.

Compared to the normal day, the enhancement in the nondeviative component is seen to be close to 16.6 dB during the anomalous event. The average enhancement corresponding to a solar zenith angle of 60° was estimated earlier from Figure 1.4 to be 8 dB for over 5 anomalous events observed during the two-week period of measurements. The enhancement in absorption is close to twice the average value for the 14.248 event. This suggests that this is one of the major events and by no means close to the average.

In conclusion it might be said that the winter anomaly appears to originate mainly due to changes in the electron number density at some altitude, rather than a change in the collision frequency model for the electrons.

1.6 Results of Absorption Measurements; 1967 Winter Series

1.6.1 Schedule of Operation

As noted in Section 1.1, one of the possible reasons proposed for the appearance of the 'winter anomaly' in ionospheric absorption is that of an inversion in the temperature gradient at the mesospheric levels.

In order to verify the above theory, it was planned to perform another series of coordinated rocket launchings using the University of Illinois propagation technique combined with the rocket-grenade experiment by the Goddard Space Flight Center. The experiments were scheduled to be performed during the last week of January or early February 1967.

It became necessary to establish the existence, or nonexistence, of the anomalous conditions on a given day from ground-based experiments so as to make possible the launch of the rockets as planned. Another series of ground-based vertical incidence absorption measurements was therefore undertaken at Wallops Island commencing on January 26, 1967, and continuing during the sunlit periods until February 3, 1967. The rocket (14.275), equipped with a payload consisting of propagation and allied experiments, was scheduled to be launched at a time corresponding to the solar zenith angle of 60°. This was to permit comparison of ionospheric conditions with those detected during the previous launch. The grenade experiment was to follow shortly thereafter.

It was planned to make another rocket-grenade experiment on a subsequent normal day so as to permit comparison of mesospheric temperatures during the normal and abnormal conditions.

1.6.2 Ground-Based Measurements Leading to Launch of Rockets

Taking account of the shortcomings experienced in the earlier series in making ground-based measurements of ionospheric absorption, a new system was designed and constructed to record the amplitude of ionospherically reflected echoes of signals transmitted from the ground. The major improvements incorporated in the new system included a dynamic range of 55 dB, a 16 cm wide chart paper with a fair amount of reading accuracy and use of circuits with improved stability of operation.

A procedure similar to that stated in Section 1.4 was followed in scaling the records. The results of the measurements are plotted in Figure 1.9 wherein the diurnal variation of the absorption is shown for the period of observation. The lowest values of absorption were observed on the very first day of observations and successively increased on subsequent days until January 31. Thereafter the values started decreasing on successive days. In Figure 1.10 is shown the average absorption for the two hours between 10 to noon on successive days. The trend of variation of absorption described above is clearly seen in the figure. The criterion discussed in Section 1.5.1 for the detection of the anomaly was met on January 31, 1967, and the rocket 14.275 was launched at $13^h\ 50^m\ 33^s$ EST, corresponding to a solar zenith angle of close to 60°. Another rocket with the grenades followed at $14^h\ 10^m$ EST which in turn was followed by an ARCAS meteorological rocket.

The ground-based vertical incidence measurements were continued on subsequent days. As seen in Figure 1.10, the average absorption for the two-hour period noted earlier kept decreasing on subsequent days until on February 3, 1967, the average dropped to 13 $\pm$ 2 dB. Normal conditions were believed to have been restored on this day and the second grenade rocket was launched at 1250 EST and was followed by an ARCAS meteorological rocket at 1325 EST.

During the launch of 14.275 difficulties were experienced by way of a substantial decrease in absorption following noon. Since the scheduled launch was to be at a solar zenith angle of 60°, doubts were raised as to whether the intensity of the anomalous event would be large enough to record any enhancements during the launch. A strong interference was present at the time from a nearby S.S.B. transmitter and it was difficult to ascertain whether the fall in absorption was due to genuine ionospheric causes or due to the

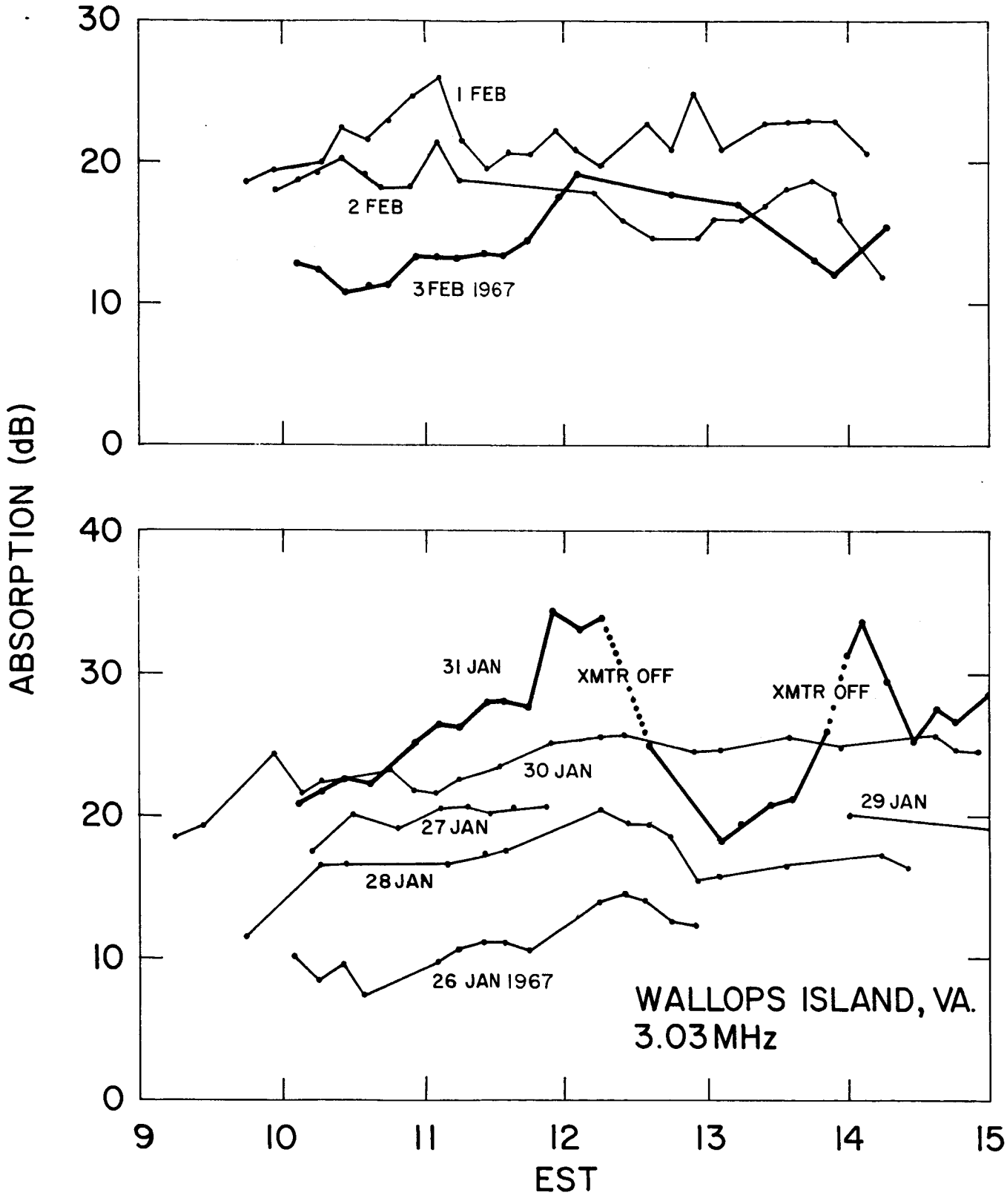

Figure 1.9 Diurnal variation of absorption on different days measured at Wallops Island during winter of 1967.

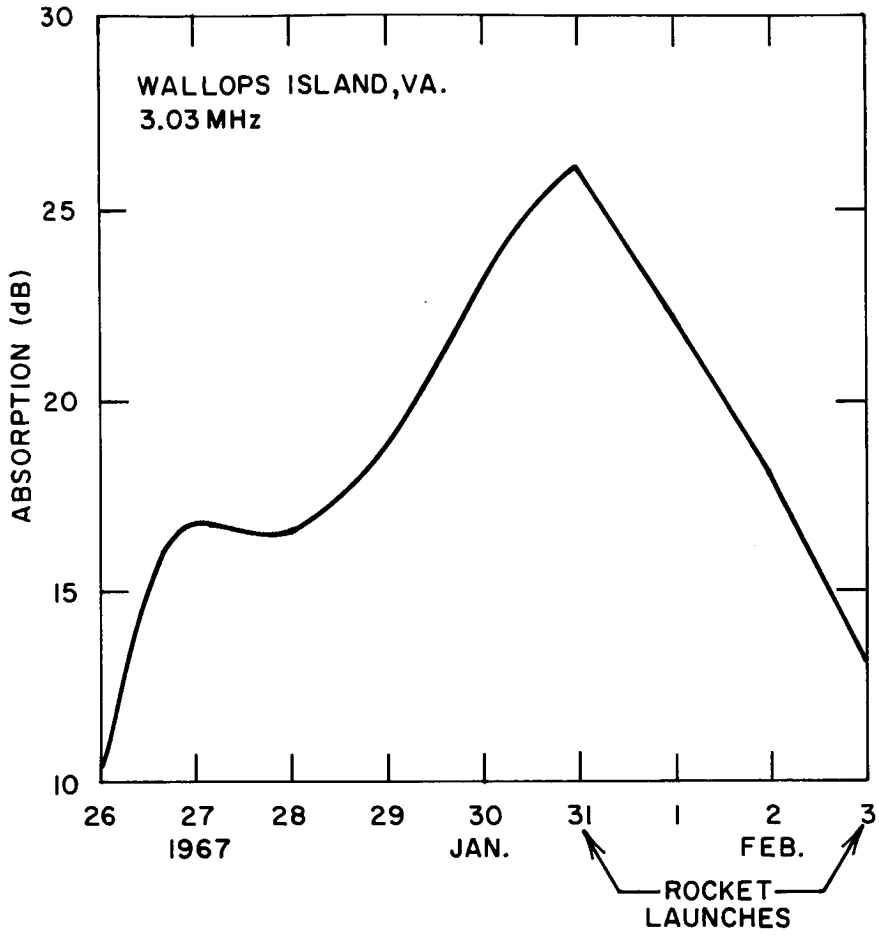

Figure 1.10 Average absorption between 1000-1200 EST on successive days during winter of 1967.

interference. At one stage the rocket countdown was held up due to the above reason. Finally, however, an upward trend in absorption was noticed and a decision was made to go ahead with the launch. Other considerations which led to the decision were the strong partial reflections from very low altitudes seen on the ionograms made at the station, and the fear that another event of the same intensity might not appear in the near future it being close to the end of the winter anomaly season.

On February 3, the absorption level was low as noted earlier. Around noon however, a sudden increase of about 5 dB of absorption was noticed. The meteorological conditions however had started deteriorating and it was necessary to launch the rocket prior to the scheduled time without waiting for the enhancement to subside. A postponing of the launch to the subsequent normal day was also considered. However, the forecast for the next few days indicated a worsening of the meteorological situation. The rocket carrying the grenades was therefore launched on this day at the time specified earlier. Thus, the difference in the instantaneous values of absorption during the two grenade launches was considerably lower than the difference at noon on the corresponding days.

1.6.3 Comparison of Ground-Based and Rocket Results

The data obtained from the rocket experiment are being analyzed. When completed, the results will be published in a separate communication by Mechtly *et al.*, (1967). However, the tentative values of the electron density and collision frequency available so far are utilized to compute the ordinary mode absorption on 3.03 MHz waves. Currently, the electron density values are available only up to 97 km. The calculations are therefore undertaken only up to that altitude. The computer program described in Section 3.3 is used to evaluate the absorption values. The procedure followed is identical to that

described in Section 1.5.3 and will not be repeated here. The collision frequency model derived from the rocket experiment is once again related to the CIRA (1965) pressure values and is given by

$$\nu_m = 7.35 \times 10^5 \, p$$

where p is pressure expressed in units of (Newtons/meter^2).

The results of the analysis are seen in Figure 1.11 wherein the absorption per km has been plotted as a function of altitude for the data from rocket 14.275. Also shown for comparison is the corresponding absorption derived from the 14.247 rocket described in the previous section as a representative of a normal day. The two curves are seen intersecting each other at altitudes 64 and 89 km. Below 80 km the absorption on 14.275 is about 7 to 8 times larger than that noticed for 14.247. The largest enhancement in absorption is noticed close to 82 km wherein the absorption during the anomalous event has increased 12-fold over the normal values.

Large though these enhancements are, the change in the total absorption up to the reflection level will be small compared to that observed in Figure 1.8 for the 14.248 launch. In fact, the total absorption in the region below 97 km works out to 6.7 dB for 14.275. The corresponding absorption on 14.247 is seen to be 3.6 dB which is only 3.1 dB lower than that observed for 14.275. It will be recalled that the enhancement over the normal was 16.6 dB, up to an altitude of 102 km during the 14.248 launch which is considerably larger than that for 14.275.

The enhancement in absorption seen for 14.275 is restricted to altitudes which are about 10 km lower than the corresponding altitudes for 14.248.

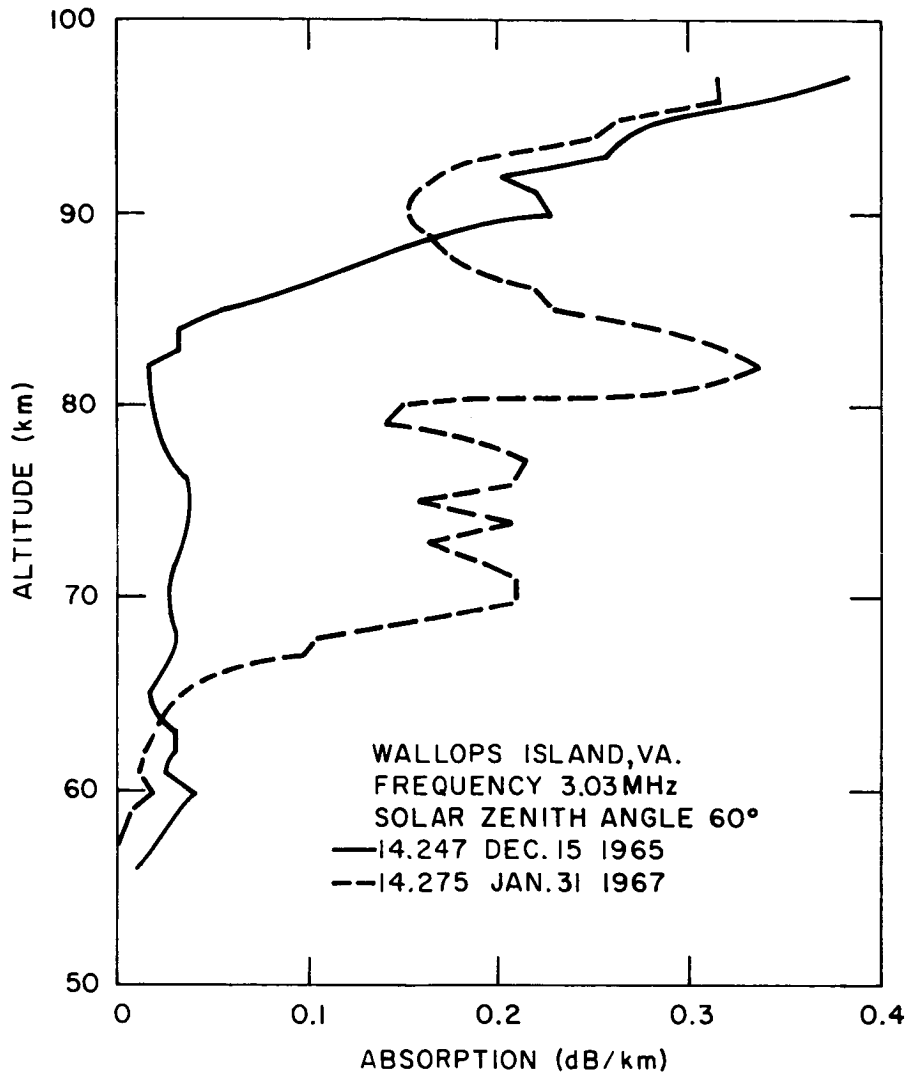

Figure 1.11 3.03 MHz ordinary wave absorption per km as a function of altitude corresponding to rocket launches 14.247 and 14.275.

It seems possible that the enhancement in electron density which is ultimately responsible for the enhancement in absorption is shifting downward following noon on January 31, 1967. This might explain the large decrease in absorption in the afternoon hours observed for the day in Figure 1.9. Whatever the cause creating the winter anomaly the evidence presented herein shows that all the events are not of equal magnitude. In view of the 8 dB of average enhancement in the low ionosphere during 5 anomalous events noticed during the 1965-66 winter, it appears that 14.248 represents a rather abnormal anomalous event whereas 14.275 represents a smaller than average event.

2. GEOMAGNETIC ANOMALY IN IONOSPHERIC ABSORPTION AT LOW LATITUDES OBSERVED ON BOARD USNS CROATAN

2.1 Introduction

Vertical incidence ionospheric absorption measurements have been reported from several low latitude stations during the last decade. Nevertheless, many of the problems associated with the ionosphere at low latitudes are far from solved. The seasonal anomaly in ionospheric absorption, for instance, refers to the much larger variation of absorption seen at midday through different seasons compared to the diurnal variation of absorption for a corresponding change in the solar zenith angles. At some of the very low latitude stations like Ibadan, the seasonal variation has been known to be more than twice as large as the corresponding diurnal variation (Skinner and Wright, 1956). Alternatively, no anomaly of the above kind has been detected at Ahmedabad (23° 01' N - 72° 36' E) (Shirke, 1959). The origin of the anomaly is yet to be traced. It also needs to be ascertained as to whether the seasonal anomaly is caused by abnormally low midday values of absorption in winter, or due to abnormally high values of absorption at noon in the equinoctial months.

Another anomalous feature pointed out recently by Beynon and Jones (1965) is the 'summer anomaly' in ionospheric absorption at some of the low latitude stations. The midday absorption for these stations in summer is found to be very low compared to what is expected from the measurements made at other times of the year. These features of the seasonal and summer anomalies referred to above appear at the outset to contradict each other. Thus, if the seasonal anomaly were to apply in summer, then the midday absorption in summer should be much larger than that in winter, the midday solar zenith angles being, in general, lower in summer than in winter. This, however, was not observed.

Fligel (1962) has suggested a geomagnetic control on ionospheric absorption based on the analysis of ground-based measurements at several stations in the eastern hemisphere. He has shown a zone of increased noon absorption around $\phi = 15^{\circ}$, Fligel's analysis is restricted to noontime and it needs to be ascertained how the distribution of absorption behaves at other times of the day.

The absorption measurements at low latitudes are restricted to specific geographic areas with very few observations available from the western hemisphere. Those available from other locations, again, are not made using identical frequencies for transmission nor at the same solar epoch. They are often restricted to periods close to noon and it is difficult to obtain a comprehensive picture of the various phenomena taking place over a wide range of latitudes at a given time. The diurnal variation of some of the peculiar features noted above in the distribution of ionospheric absorption has not been investigated adequately nor has the link, if any exists, between the diurnal and seasonal variation of the absorption at these latitudes been explored.

With the aim of investigating some of the problems listed above it was planned to make a latitude survey of the absorption values along the western coast of South America using mobile equipment mounted on board the ship USNS Croatan. The ship was equipped with rocket launch facilities and was used for the first mobile scientific expedition by the National Aeronautics and Space Administration as a part of the U.S. IQSY program. There were several other experiments performed on board the ship. The results of the absorption measurements alone are presented in this report.

The experiment was conducted during the latter half of April and early May 1965. During this period the ship covered geographic latitudes between 15° S

to 25° N. The seasonal variation of absorption is believed to be negligibly small during the short period of these observations. The average sunspot number at this time was close to 7. No magnetic disturbance of major consequence was reported from any of the magnetic observatories during this period. The experiment is therefore believed to have been performed under ionospherically quiet conditions.

The ship covered about 6° of latitude daily except when passing through the Panama Canal Zone. Unfortunately, the transmitter had to be put off on approaching the canal and some data were lost. Nevertheless, the trends in the latitudinal variation of absorption in this region are fairly clear from the data obtained from adjacent latitudes.

2.2 Technique of Measurements

The equipment used for the absorption measurements has been described by Henry (1966) and is dealt with very briefly in the following. Some of the results described herein are presented by Shirke and Henry (1967).

A pulse transmitter with a peak power of 50 kw was operated on a frequency of 3.03 mc/s. The pulsed-width was close to 50 μsec, the pulse repetition frequency being 0.5 cps. An antenna consisting of a pair of crossed dipoles was used to transmit the signals. The observations were confined to the ordinary mode of polarization. Transmission on this mode of propagation was achieved by introducing an appropriate delay circuit in one of the dipoles before mixing the outputs from the two dipoles.

A T-R switch was operated at the same pulse repetition frequency as the transmitter. This made possible the use of a single antenna system for transmission and reception of signals. A high-gain transistorized receiver was used for reception of the ionospheric echoes. The output of the receiver was fed to an oscilloscope with an A-scope type display and photographed using

a 35 mm film camera. Coordinated movements of the shutter and the film permitted one picture to be taken corresponding to each transmitted pulse. The time and frame number were recorded on individual frames for later identification.

An rf attenuator was incorporated in the input stage of the receiver. This was adjusted from time to time to prevent saturation of the receiver. A careful record of the attenuator gain-setting was maintained throughout the experiment. The receiver gain was kept at a constant level as far as possible; however, it had to be altered occasionally to accommodate the large variations in the echo amplitudes. Generally the measurements were confined to the first and second hop reflections only. It was then possible to evaluate an equipment constant which was used to obtain the absolute measure of ionospheric absorption, even in the absence of multiple reflections.

The use of an auxiliary oscilloscope permitted easy monitoring of the system. The time-base of the recording oscilloscope was calibrated and was used to obtain the virtual height of reflection of the echo. The measured attenuation was then corrected for the spatial component. The procedure for evaluating the dissipative absorption has been adequately dealt with by Piggott et al., (1957) and is not included here.

2.3 Diurnal Variation of Absorption Index

In Figure 2.1 is shown a typical diurnal variation of absorption as noted on April 23, 1965. The duration over which data are available is shown by the length of the dashes. A smooth curve has been drawn to fit the observations. Curves of a similar nature have been used in the following analysis for other days as well.

The schedule of operation specified one set of observations every 20 minutes. Each set consisted of readings for close to 10 minutes. It was an enormous

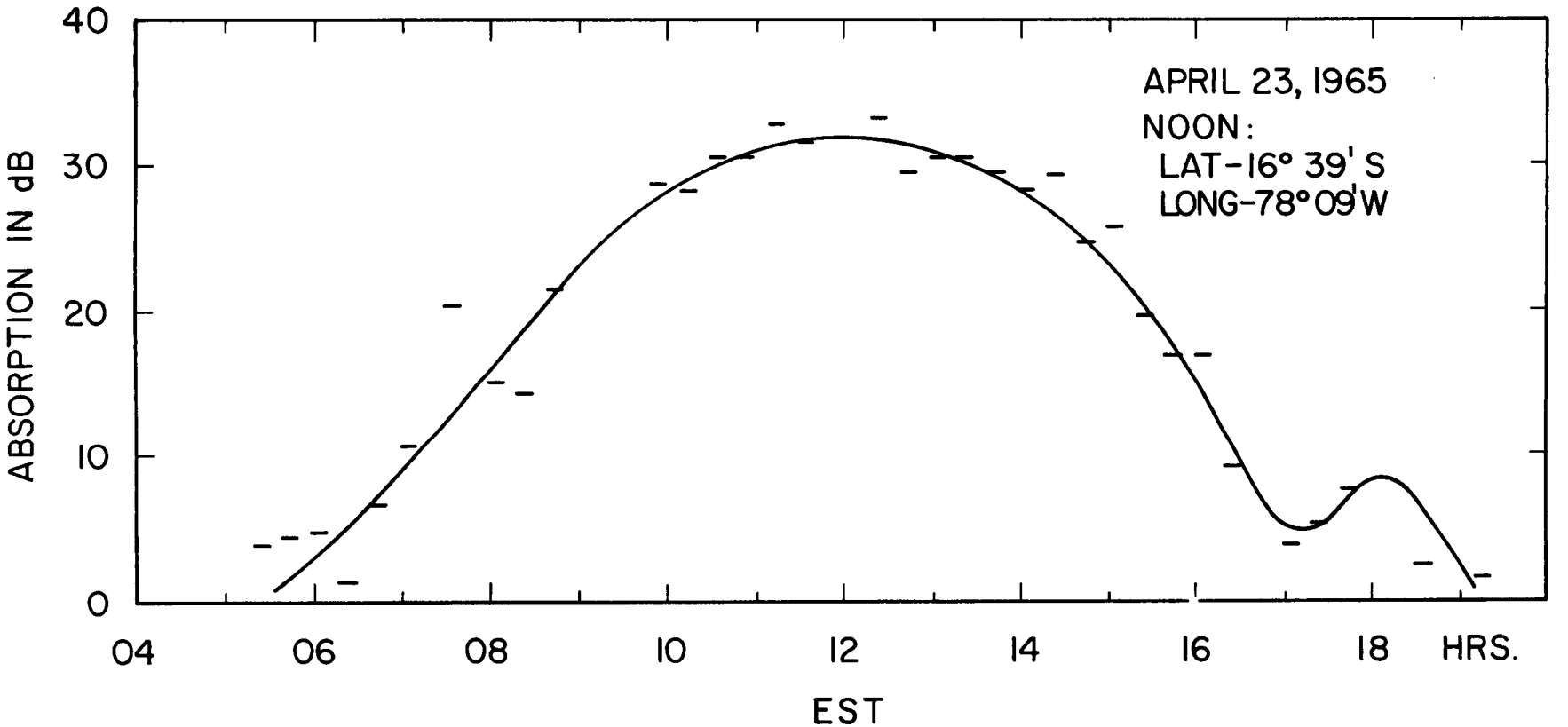

Figure 2.1 A typical diurnal variation of absorption is shown as observed on board the USNS Croatan. The dashes indicate the duration of each set of observations. The smooth curve drawn through these has been used for further computations.

task to reduce the large number of frames over which data were collected. A preliminary test was made to check whether it was justifiable to simplify the scaling procedure by restricting to only 10 percent of the available data. A median value of absorption was therefore determined for a 10-minute sampling interval, firstly, by noting the amplitudes from all the frames on which recording was available, and secondly by restricting to successive tenth frames only. This corresponds to reducing the pulse repetition frequency of the transmitter to one pulse every 20 seconds. No significant difference was noticed between the two median amplitudes thus derived. The reduced pulse rate was therefore considered to be acceptable for the purpose of the present analysis which restricts itself essentially to the gross features of the low latitude ionosphere.

One of the major limitations in the interpretation of ground-based ionospheric absorption measurements is usually the separation of the deviative and nondeviative components from the composite absorption. To overcome this difficulty a J5 type ionosonde manufactured by the Magnetic AB Corporation of Sweden was installed on board the ship and ionograms made at 15-minute intervals. Close investigation of these ionograms revealed that the daytime reflections were mostly from the E region. There were instances especially in the early morning hours when the reflections occurred from the F region with large deviative type absorption associated with it. The data for these periods have been excluded for the purpose of the present analysis.

Figure 2.2 shows the latitudinal variation of absorption for a few selected solar zenith angles separated by an interval of ten degrees. The forenoon and afternoon values are identified by different symbols. For a given solar zenith angle considerable latitudinal variation of absorption is clearly

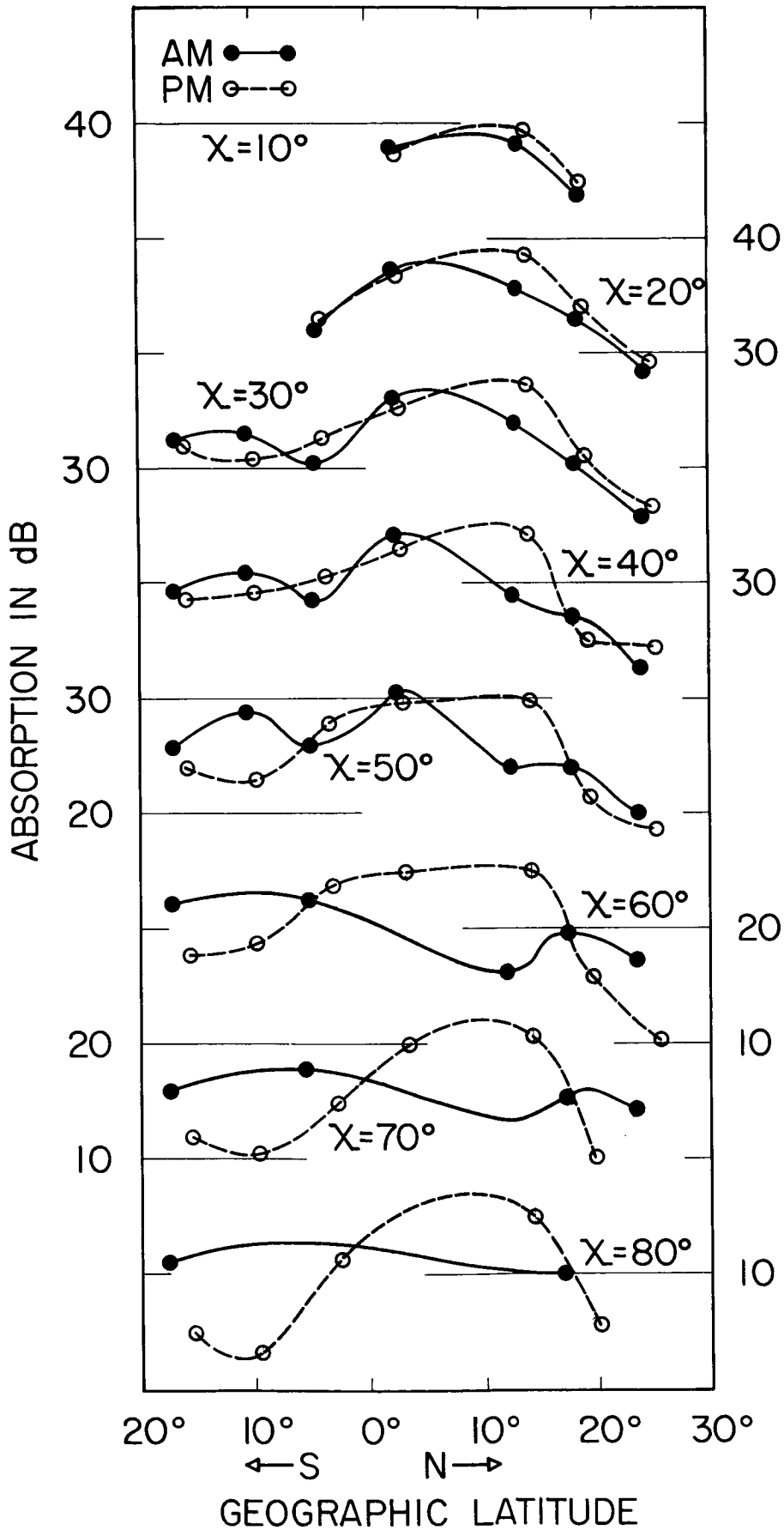

Figure 2.2 The latitudinal distribution of absorption is shown corresponding to specific solar zenith angles (χ). The forenoon and afternoon curves are identified. The dB scale appropriate for each curve is indicated by straight lines proceeding from the curve.

noticeable in the diagram. For instance, corresponding to the solar zenith angle of 70° in the morning, the maximum of absorption is 18 dB and is located around 8° S. Another maximum is situated around 20° N, while a minimum of 13 dB is seen close to 12° N. By the time the zenith angle reaches 10° the maximum of absorption has reached a value of 40 dB and is situated around 10° N. In the afternoon and late evening hours large values of absorption are seen persisting around 5° to 15° N latitudes. In the above discussion it might be noted that there are limited data points in the late evening hours. The distribution of absorption derived therefrom would therefore be less accurate than at other times of the day.

In Figure 2.3 is shown the variation of absorption on individual days plotted as a function of the cosine of the solar zenith angle. The plots are restricted to solar zenith angles less than 60°. Thereafter the E-layer critical frequency approaches the operating frequency and deviative type absorption predominates. The forenoon and afternoon values are denoted by separate symbols. Logarithmic scales have been used on either axis. In each case the data points are observed to lie close to a straight line. The slope of the lines, however, varies from one case to another. The variation of absorption L can therefore be expressed by the relationship

$$L = K (\cos \chi)^n \qquad (2.1)$$

where χ is the solar zenith angle and K and n are numerical constants. In each case then the value of n is a measure of how rapidly the absorption is varying as a function of the solar zenith angle. It will be noticed from the diagram that the index n varies not only from one day to another but also

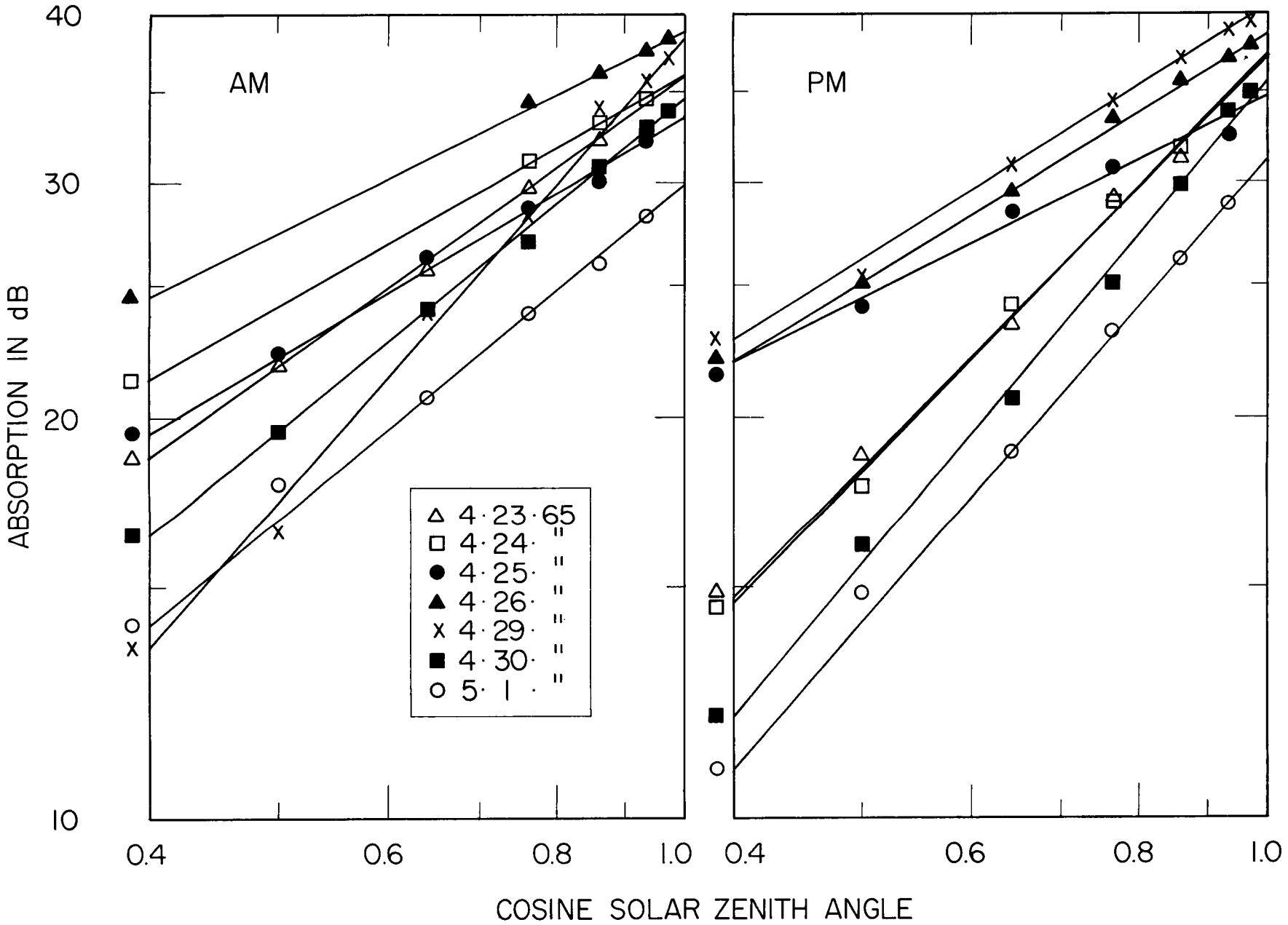

Figure 2.3 Absorption on individual days is plotted as a function of the cosine of the solar zenith angle (χ). Logarithmic scales are used on both axes. The slope of the line joining the points gives the index of absorption 'n'.

during the course of a single day. This, in turn, leads to a latitude anomaly in ionospheric absorption which will be presented shortly.

The latitudinal variation of the index n is shown in Figure 2.4. The morning and afternoon values are shown by separate curves. Smooth curves have been drawn through the data points. The two curves are seen intersecting each other several times constituting four latitude zones, each about ten degrees in width. The first zone lies between latitudes 15° to 5° south of the geographic equator. In this zone, the afternoon values of n are observed to be considerably larger than those in the forenoon. This results in abnormally low values of absorption by late evening. Incidentally, it may be pointed out that the geomagnetic equator, which appears to be the seat of an anomalous absorption feature, lies in the midst of this zone.

The boundaries for the adjacent zone lie five degrees on either side of the geographic equator. Within this zone the forenoon and afternoon values of the index n are very nearly identical to each other. As a result, there is no diurnal asymmetry of absorption around noon as was noticeable in the preceding zone. However, the average value of the index n in this zone is close to 0.6 which is by far the lowest value noted throughout the range of latitudes under investigation.

The third zone lies between geographic latitudes 5° to 15° N. These correspond to geomagnetic latitudes of 16° and 26° N respectively. In this zone, the pre-noon values of n are larger than the corresponding afternoon values. This indicates a rapid increase in absorption in the morning which does not subside equally rapidly in the afternoon. As a consequence, large values of absorption are seen persisting until late evening in this latitude zone.

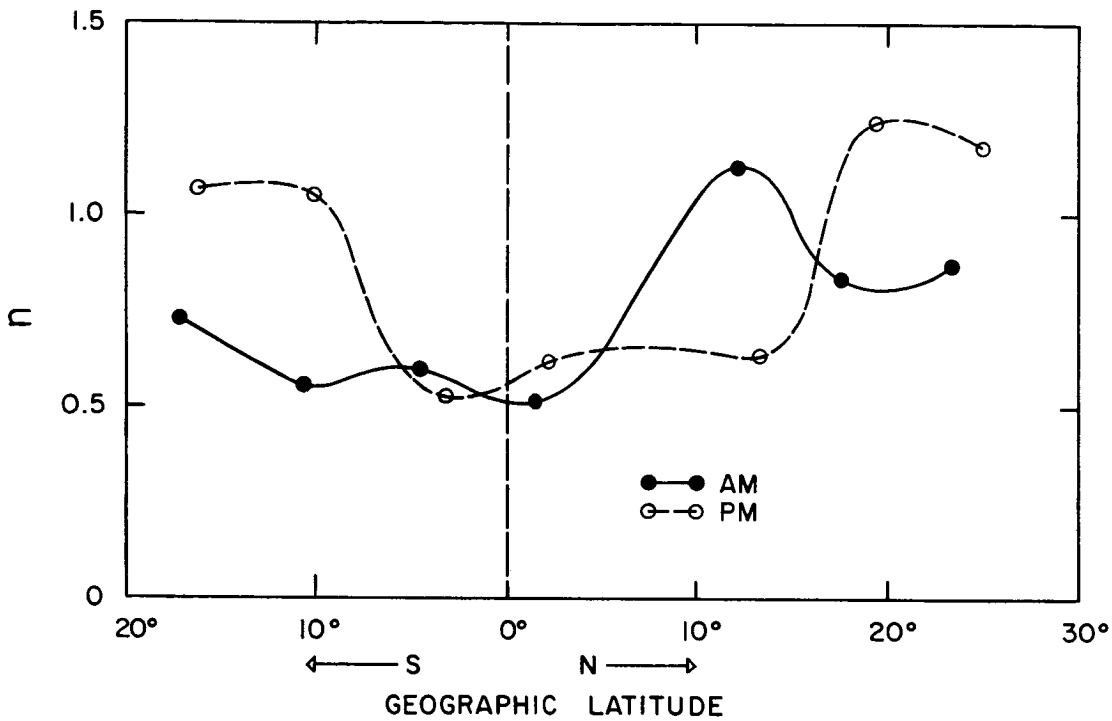

Figure 2.4 The latitudinal variation of the index of absorption 'n'. The forenoon and afternoon curves are identified.

A further reversal in the forenoon and afternoon curves of n is observed between 15° to 25° N. The forenoon rate of increase of absorption is moderate in this zone but the afternoon values are comparatively larger. As a consequence, the absorption is seen decreasing very rapidly in the afternoon. This forms a distinct contrast with the high values of absorption persisting in the late evening in the adjacent zone discussed earlier. The two zones grouped together represent a major feature of a latitude anomaly presented in the following.

2.4 Geomagnetic Anomaly in Ionospheric Absorption

At middle latitudes the ionospheric absorption of radio waves is known to vary symmetrically with respect to local noon except for a shift of a few minutes due to the relaxation effects in the ionosphere. Little symmetry around noon is observed in the absorption data in three out of four latitude zones described above. This indicates the presence of an anomalous feature in ionospheric absorption at low latitudes. In order to bring out the details of this feature, a latitudinal distribution of absorption has been extrapolated from the measurements made at a middle latitude station. The assumptions involved in these computations will be discussed later. A 'latitude anomaly' in ionospheric absorption is defined by the observed departures from the estimated values of absorption. Some features of this anomaly are presented in the following.

The station chosen for the comparison of absorption values was Wallops Island, Virginia (37° 50' N, 75° 20' W). It lies in the same longitude zone as the shipboard measurements. It is known that different types of anomalies in ionospheric absorption exist both at low as well as at high latitudes. A middle latitude station like Wallops Island is believed to be the least affected from either type of these anomalies. However, a phenomenon called the

'winter anomaly' in ionospheric absorption is known to exist at latitudes of Wallops Island whereby ionospheric absorption of radio waves increases considerably on some days in winter. In the present case, it has been ascertained (Shirke and Rao, 1967) that an anomaly of this kind did not exist at Wallops Island on the day; these data have been used in the computations.

The ionospheric absorption on a given frequency can be calculated using the magnetoionic theory given by Appleton (1937) and Hartree (1929). For the ordinary wave propagation making angle θ with the direction of the magnetic field the ratio A of quasi-transverse to quasi-longitudinal propagation is given by

$$A = \frac{XZ}{2\,(1+Y_L)^2 + Z^2} \Big/ \frac{XZ}{2\,(1+Z^2)} \tag{2.2}$$

where $X = \omega_N^2/\omega^2$, $Y_L = \omega_H \cos\theta/\omega$, and $Z = \nu/\omega$ are the functions of wave frequency ω, plasma frequency ω_N, gyrofrequency ω_H, and electron collision frequency ν.

It has been pointed out in Section 1.5 that more than 90 percent of the total absorption originates normally above 80 km. In this altitude region the collision frequency of electrons is much smaller than the operating frequency ω. Expression (2.2) can then be written as

$$A = \frac{1}{(1+Y_L)^2} \,. \tag{2.3}$$

In the derivation of the Appleton-Hartree equations a frictional term has been utilized which is believed to be independent of the electron velocity. Sen and Wyller (1960) have generalized the Appleton-Hartree equations so as to be applicable when the collision frequency of electrons is some function of

the electron velocity. Phelps and Pack (1959) laboratory results have shown for air the electron collision frequency is proportional to the energy of the electrons. For the ionospheric case where the Maxwellian velocity distribution of electron is applicable, Sen and Wyller have shown that in the asymptotic limit when the electron collision frequency far exceeds the operating frequency the Appleton-Hartree formulas can be retained, provided the collision frequencies used are two and a half times larger than before. The value of ratio A defined earlier for a pair of stations should therefore remain, moreover, the same whether the classical or the generalized formulas are used.

In Section 1.5 are given the results of the absorption measurements made at Wallops Island. On 15 December 1965 an average absorption of 11 dB was measured at the station corresponding to a solar zenith angle of 60° for an operating frequency of 3.03 MHz. In Figure 2.5 are shown curves based on expression (2.2) giving the absorption estimated as a function of geomagnetic latitudes for specific solar zenith angles 30°, 60° and 80°. The decrease in absorption with increase in latitude seen in the curves is due to the corresponding increase in the longitudinal component of the earth's magnetic field.

The estimated latitudinal variation of absorption shown in Figure 2.5 is based on the assumption that the profiles of the electron number density and that of the collision frequency of electrons with neutral particles, have both remained invariant as a function of latitude. In other words, these profiles are believed to be identical to those at Wallops Island throughout the low latitude range. The departure of the absorption measured on board the ship from that estimated for a corresponding latitude gives the extent of the latitude anomaly. This, in turn, is a measure of the extent to which the above assumption regarding the constancy of the profiles is inaccurate.

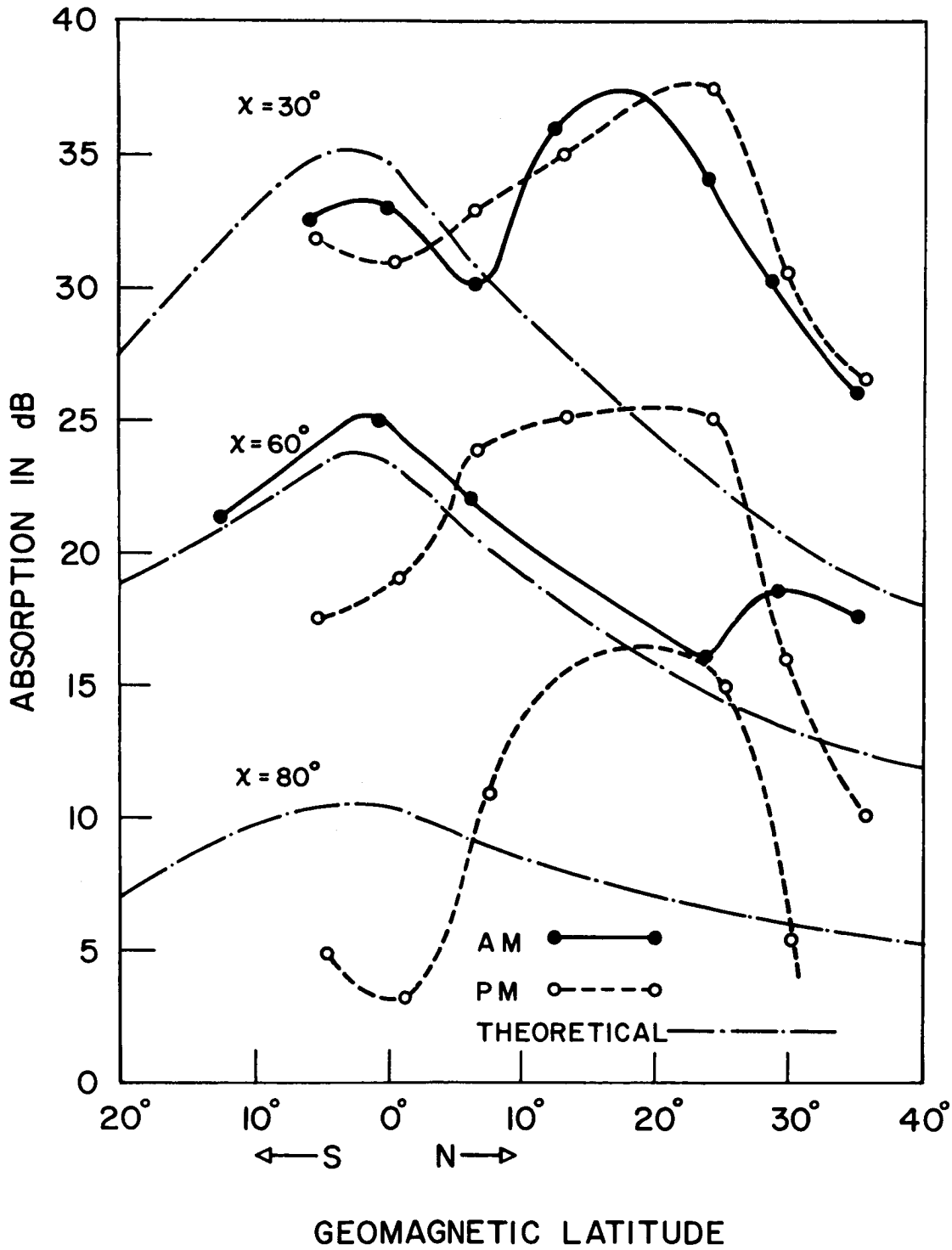

Figure 2.5 Absorption measured on board the USNS Croatan is shown as a function of the geomagnetic latitudes for each of the solar zenith angles 30, 60 and 80°. Also shown is the corresponding computed latitudinal variation of absorption presuming latitude invariant models of electron number density and electron collision frequency identical to those observed at a mid-latitude station.

Out of the three sets of curves shown in Figure 2.5 only the one corresponding to a zenith angle of 60° has been computed using the absorption value measured at Wallops Island. The absorption corresponding to zenith angles 80° and 30° has been computed from the above, using Equation (2.1) derived earlier. A value of n = 0.75 appropriate for middle latitude stations (Appleton and Piggott, 1954) has been used. The absorption measured on board the ship is also shown in Figure 2.5 for the three solar zenith angles listed above. The forenoon and afternoon values are shown by separate symbols.

With reference to Figure 2.5 and corresponding to a solar zenith angle of 60° in the morning, the calculated and observed distributions of absorption follow each other very closely on all days for which data is available except for a small departure beyond 24° latitude. This excellent agreement between observed and expected values proves that no day-to-day variation could have existed in the absorption values during the early morning hours. The variations developing later in the day and described in the following as features of an anomaly must therefore be genuine latitudinal variations in absorption. If day-to-day variability were to be the cause of these variations then these would have appeared in the morning hours as well.

With decreasing solar zenith angles an enhancement in absorption is seen shifting toward the lower latitudes, reaching a maximum around $\phi = 18°$. The enhancement is seen persisting until late evening in varying amplitudes in a latitude zone spread over ten degrees on either side of $\phi = 18°$. The data is not sufficient to indicate as to when the enhancement in this zone starts diminishing.

Another important feature of the anomaly is observed at latitudes close to the geomagnetic equator. Although the curves corresponding to solar zenith

angle of 30° in the morning do not show the presence of any major anomaly in this zone, a depression is seen developing in the afternoon at latitudes close to the magnetic equator. The trend for a decrease in absorption over the estimated values continues to grow toward evening and the absorption becomes fairly low by the time the solar zenith angle reaches 80°. Once again the data is not sufficient to indicate until what time the absorption continues to decrease.

For latitudes larger than $\phi = 30°$ the observed morning values of absorption are, in general, slightly larger than anticipated, while those in the evening lie below the estimated curve. This constitutes yet another feature of the latitude anomaly. As noted earlier, the sharp decrease in absorption in this zone forms a distinct contrast with the large value of absorption persisting until late evening in the adjacent zone.

2.5 Comparison of Shipboard and Eastern Hemisphere Measurements

One of the main objectives in choosing the 75° W longitude zone for the expedition was that the geographic and geomagnetic equators are separated widely in this area. It was an ideal place to test whether the latitude distribution of absorption is symmetrical with respect to one of these or not. It is obvious from the present data that there is no symmetry in the distribution of absorption with respect to the geographic equator at any time of the day. Evidence is presented in the following to show that the absorption varies relatively more symmetrically with respect to the geomagnetic equator.

Fligel (1962) has grouped the IGY ionospheric absorption data from over 22 stations situated mostly in the Indian zone. Out of these, only five stations fall south of the geomagnetic equator. It is therefore difficult to establish from these data alone whether the absorption values are symmetrical

with respect to the geomagnetic equator or not. This, however, is possible if we combine the data now available from the western zone with that from the east. The geomagnetic equator lies to the extreme geographic north in the eastern zone where the bulk of the stations making absorption measurements are situated; and to the extreme south in the western zone where the present measurements were made. As a result, two stations, one each from the two sections lying on the same geographic latitude, are separated by as much as 20° in geomagnetic latitudes. Comparison of data between the two sectors thus provides an excellent opportunity to test the existence or nonexistence of a geomagnetic control on ionospheric absorption.

With reference once again to Figure 2.5 and to the curves corresponding to solar zenith angle of 30° approaching noon, the shipboard measurements show a maximum of absorption around $\phi = +18^{\circ}$, which corresponds to 7° N geographic latitude. Fligel's analysis for the eastern zone shows a midday maximum around $\phi = 15^{\circ}$, which corresponds to about 25° geographic latitude. It is obvious, that the data from the two zones would match better on geomagnetic coordinates rather than on the geographic. Low values of absorption compared to those at $\phi = 18^{\circ}$ are observed around $\phi = 35^{\circ}$ in the data from both zones noted above. Similarly, a depression is seen toward the geomagnetic equator in the data from both sectors. A geomagnetic control of some kind on the distribution of absorption is thus confirmed from the two sets of measurements at low latitudes. The latitude anomaly may well be referred to as a geomagnetic anomaly. Fligel's noontime analysis, seems to form a special case of the geomagnetic anomaly presented in this report.

2.6 Discussion of Results

A brief review of some of the shipboard results follows in the light of some other anomalous features in ionospheric absorption reported from

low latitude stations. A link possibly existing between the various anomalies is also indicated. Once again referring to Figure 2.5 for latitudes close to the magnetic equator and for solar zenith angles of 30°, the absorption observed is a little lower than that predicted from the midlatitude station. Recalling that the shipboard data pertains to an equinoctial period, if we were to extrapolate from these measurements the winter noontime absorption for a low latitude station, then it turns out to be very low. This is so, because at low latitudes the observed seasonal index of absorption is usually as large as 1.7 as measured at Colombo (ϕ = 3° S) (S. Gnanalingam and P.H.J. Ratnasiri, private communication, 1965). This means that the latitude anomaly presented herein for the equinoctial data would have developed substantially by midday in winter, whereas it would have been just discernible at noon during the equinoxes. Besides, this shows that the origin of the seasonal anomaly lies in abnormally low values of absorption at noontime in winter and not in abnormally high values in the equinoxes.

During summer the midday absorption values at low latitudes are usually so low that they are discarded while computing the seasonal index. The low midday values in summer have been referred to as a 'summer anomaly' by Beynon and Jones (1965). An effect similar to that described above for winter might be occurring in summer as well, resulting in low midday values of absorption. In essence then, both the seasonal and summer anomalies in ionospheric absorption at low latitudes appear to be manifestations of the diurnal behavior of the low-latitude anomaly presented in this report.

It is customary for stations making absorption measurements to provide a single value for the index of absorption for the whole day. This is seldom accurate at the low latitude stations in view of the data presented here.

The asymmetric distribution of absorption around noon, as well as the geomagnetic latitude anomaly presented here, indicates that the absorption index could change considerably within the course of a single day. Besides, the value of the index alone offers no clue as to the initial or final value of absorption. Caution should therefore be exercised in giving excessive importance to isolated use of this index while discussing absorption measurements at low latitudes.

A geomagnetic anomaly in the F region has been known to exist in the same longitude zone as discussed here (Appleton, 1947). There are several features of the anomaly which seem to be similar in nature to those presented here. The F region anomaly is seen by way of large concentrations of electron number densities around $\phi = 15°$ persisting until late evening hours. One of the explanations for the existence of the phenomenon has been based on the transport of ionization from the equatorial regions via the geomagnetic lines of force to latitudes where maximum ionization is observed. It is possible, that some kind of a link exists between the very low and high altitude ionospheric regions. It is, however, very hard to conceive at this stage how such a link could be established and maintained for hours.

As noted earlier, the absence of any anomalous features in the early morning hours rules out the possibility of day-to-day variations causing the observed anomaly in absorption. The excellent agreement of the present results with the noon data from several of the eastern stations strongly supports the conclusion that these are genuine latitudinal variations.

The existence of a low latitude anomaly in the lower ionosphere has been established and its diurnal variation discussed in some detail. A possible link that might exist between the various anomalies known to appear

at low latitudes is also discussed. No comments have been offered as to the cause of the various anomalies. Whether the changes in absorption are produced by changes in the electron number density or in its collision frequency remains yet to be seen, as also the reasons why such changes should originate in the first place. Synoptic measurements of the lower ionosphere with rockets making *in situ* measurements of these parameters would greatly aid in solving these problems. A rigorous study of the deviative type absorption close to the level of reflection of the waves might also go a long way in explaining some features of the observed anomalous latitudinal variation of absorption.

3. WORLD-WIDE VARIATION OF IONOSPHERIC ABSORPTION, PARTIAL REFLECTION COEFFICIENTS AND FARADAY ROTATION OF RADIO WAVES

3.1 Introduction

A geomagnetic anomaly in the distribution of ionospheric absorption was presented in Chapter 2. Therein the latitudinal distribution of absorption measured on board the ship USNS Croatan was compared with that computed theoretically based on the measurements of total absorption made at a middle latitude station. The calculations were based mainly on the classical formulas given by Appleton and Hartree. The phenomena is investigated in further detail in the following. The effect of the earth's magnetic field on ionospheric absorption is studied by selecting several locations spaced at a regular latitude intervals. A single electron density profile derived from a rocket experiment is used to compute the absorption at small successive height intervals at each location. The collision frequency model used is also maintained constant with latitude. The computations are based on generalized magnetoionic formulas given by Sen and Wyller (1960).

Ever since Gardner and Pawsey (1953) demonstrated the partial reflection technique of deriving the electron densities in the lower ionosphere, the interest in this type of measurement has been growing. The technique relies on the measurement of the relative amplitudes of ionospherically scattered echoes on the ordinary and extraordinary modes of propagation. The absorption on the extraordinary mode varies considerably more than the ordinary depending on the earth's magnetic field. The reflection coefficients of the ordinary and extraordinary modes of the scattered waves also undergo considerable latitude variation due to changes in the magnetic field. The feasibility of making partial reflection measurements therefore differs widely from place

to place due to changes in the field values alone. A study of the world-wide distribution of absorption on the extraordinary mode of propagation has therefore been included in the analysis as also of the reflection coefficient of scattered waves on the two magnetoionic modes. The changes occurring in the Faraday rotation of rf waves as a function of latitude are also investigated and included in the following.

3.2 Ionospheric Absorption, Theoretical Considerations

According to the Appleton (1937) and Hartree (1929) magnetoionic theory, the absorption of radio waves in the ionosphere is due to the dissipation of the energy of electrons which are vibrating under the influence of the wave field when they make collisions with other particles. The complex refractive index and the state of polarization in a weakly ionized gas with an alternating field are given by the Appleton-Hartree theory. However, in the derivation of these formulas a fictional term has been utilized which is assumed to be independent of the electron velocity, ν, and the electron velocity distribution.

Laboratory experiments made by Phelps and Pack (1959) have shown that the collision frequency of electrons is a function very nearly of the square of their velocity. Under these circumstances, Sen and Wyller (1960) have deduced the formulas for the complex refractive indices and the state of polarization, utilizing a generalized conductively-tensor for the Lorentz gas. They show that in the ionospheric wave propagation the electric and magnetic field effects would be negligible. The electrons can therefore be assumed to have a Maxwellian velocity distribution. For such a case Sen and Wyller have shown that the elements of the conductivity-tensor are expressible in terms of the semiconductor integrals $C_p(x)$.

The integrals are defined by the expression

$$C_p(x) = \frac{1}{p!} \int_0^\infty \frac{\varepsilon^p}{\varepsilon^2 + X^2} \varepsilon \, d\varepsilon \qquad (3.1)$$

where $\varepsilon = m\nu^2/2KT$, and m is the electron mass, T the temperature and K the Boltzman's constant.

The two integrals which are of interest for the ionospheric case are $C_{3/2}(x)$ and $C_{5/2}(x)$. The integrals have been tabulated by Dingle et al., (1956-57) along with many other integrals. These have been extended further by Burke and Hara (1963) who have given the following approximations to the above integrals,

$$C_{3/2}(x) = \frac{X^4 + a X^3 + a_2X^2 + a_1X + a_o}{X^6 + b_5X^5 + b_4X^4 + b_3X^3 + b_2X^2 + b_1X + b_o} \qquad (3.2)$$

and

$$C_{5/2}(x) = \frac{X^3 + a_2X^2 + a_1X + a_o}{X^5 + b_4X^4 + b_3X^3 + b_2X^2 + b_1X + b_o} \, . \qquad (3.3)$$

In the above expressions the subscripted coefficients a and b are constants and the values of the constants have been tabulated by Burke and Hara.

For the general case except when the propagation of an electromagnetic wave is not transverse or purely longitudinal with respect to the magnetic field, Sen and Wyller (1960) have given the following expression for the complex refractive index n' which is equal to the ratio of C the velocity of light and U the phase velocity of the wave

$$n'^2 = \frac{C^2}{U^2} = \left(n - i \frac{ck}{\omega}\right)^2 = \frac{A + B \sin^2 \psi \pm \sqrt{B^2 \sin^4 \psi - C^2 \cos^2 \psi}}{D + E \sin^2 \psi} \qquad (3.4)$$

where n is the real part of the complex refractive index and (ck/ω) the imaginary part which gives the absorption indices for the angular wave frequency ω. k is the absorption coefficient. The positive and negative signs before the radical sign correspond to the ordinary and extraordinary modes respectively. ψ is the angle made by the direction of propagation with the magnetic field, i is the root of -1 and

$$\begin{aligned} A &= 2\varepsilon_I(\varepsilon_I + \varepsilon_{III}) \\ B &= \varepsilon_{III}(\varepsilon_I + \varepsilon_{III}) + \varepsilon_{II}^2 \\ C &= 2\varepsilon_I\varepsilon_{II} \\ D &= 2\varepsilon_I \\ E &= 2\varepsilon_{III} \end{aligned} \tag{3.5}$$

The fundamental elements ε_I, ε_{II} and ε_{III} of the generalized dielectric tensor are expressed as follows

$$\begin{aligned} \varepsilon_I &= (1-a) - ib \\ \varepsilon_{II} &= \tfrac{1}{2}(f-d) + \tfrac{1}{2}(c-e) \\ \varepsilon_{III} &= [-a - \tfrac{1}{2}(c+e)] + i\,[b - \tfrac{1}{2}(f+d)] \end{aligned} \tag{3.6}$$

where

$$a = \frac{\omega_o^2}{\nu_m^2} C_{3/2}\left(\frac{\omega}{\nu_m}\right)$$

$$b = \frac{5\omega_o^2}{2\omega\nu_m} C_{5/2}\left(\frac{\omega}{\nu_m}\right)$$

$$c = \frac{\omega_o^2(\omega-s)}{\omega\nu_m^2} C_{3/2}\left(\frac{\omega-s}{\nu_m}\right)$$

$$d = \frac{5}{2}\frac{\omega_o^2}{\omega\nu_m} C_{5/2}\left(\frac{\omega-s}{\nu_m}\right)$$

$$e = \frac{\omega_o^2(\omega+s)}{\omega\nu_m^2} C_{3/2}\left(\frac{\omega+s}{\nu_m}\right) \qquad (3.7)$$

$$f = \frac{5}{2}\frac{\omega_o^2}{\omega\nu_m} C_{5/2}\left(\frac{\omega+s}{\nu_m}\right) \quad .$$

In these expressions ν_m is the collision frequency for monoenergetic electrons and ω_o is the plasma density given by

$$\omega_o^2 = \frac{4\pi Ne^2}{m} \quad . \qquad (3.8)$$

Herein N, e, m and s are, respectively, the number density, charge, mass and gyrofrequency of electrons.

The real and imaginary parts of the complex refractive index can be separated by using the following expressions

$$\frac{C^2}{U^2} = \left(n - i\frac{ck}{\omega}\right)^2 = L - iM$$

then

$$n = \frac{1}{\sqrt{2}}\sqrt{L + \sqrt{L^2 + M^2}} \qquad (3.9)$$

and

$$\frac{ck}{\omega} = \frac{1}{\sqrt{2}}\sqrt{-L + \sqrt{L^2 + M^2}} \quad .$$

The formula applicable for the ordinary wave transverse propagation is given by Sen and Wyller as

$$\frac{C^2}{U^2} = \left(n - i\frac{ck}{\omega}\right)^2 = \varepsilon_I \text{ or } \frac{(\varepsilon_I + \varepsilon_{III})^2 + \varepsilon_{II}^2}{\varepsilon_I + \varepsilon_{III}}$$

which is the same as

$$\frac{C^2}{U^2} = 1 - \frac{\omega_o^2}{\nu_m^2} C_{3/2}\left(\frac{\omega}{\nu_m}\right) - i \frac{5\omega_o^2}{2\omega\nu_m} C_{5/2}\left(\frac{\omega}{\nu_m}\right) . \qquad (3.10)$$

The letters have the same meaning as noted earlier.

3.3 Computer 7094 Programming for Solving the Generalized Magnetoionic Equations

The evaluation of the real and imaginary parts of the complex refractive index using the expressions noted in Section 3.2 were undertaken by drawing suitable programs to feed a 7094 computer available at the University of Illinois. In all, three separate programs were drawn, one for the solution of Equation (4.4) in Section 4.2, applicable for the general case involving both the ordinary and extraordinary modes of propagation. The other two programs one each for the ordinary and extraordinary modes were applicable to the transverse case realized for vertical propagation at the dip equator. Only two of these programs have been reproduced in the Appendices I and III. The third program applicable for the transverse extraordinary propagation has not been included as the features are identical with the other two programs. Some features of Program I applicable to the general case are described in the following.

The first part of the program is to evaluate the semiconductor integrals $C_{3/2}(x)$ and $C_{5/2}(x)$ for appropriate values of x which is a function of ω, s and ν_m wherein ω is the angular operating frequency of the wave. For convenience in programming the integrals $C_{3/2}(x)$ and $C_{5/2}(x)$ are renamed as functions C32F(x) and C52F(x). The coefficients of the argument x used in the polynomials have been taken from Burke and Hara (1963) and have been reproduced at the end of Appendix I and have been renamed for convenience. Thus in Equation (3.2), A_4, A_3, A_2 and A_1 replace a_o, a_1, a_2 and a_3 respectively and

B6, B5, B4, B3, B2 and B1 replace b_o, b_1, b_2, b_3, b_4 and b_5. Similarly, in Equation (3.3), D1, D2, D3 replace a_o, a_1, and a_2 and E1, E2, E3, E4 and E5 replace b_o, b_1, b_2, b_3 and b_4, respectively. In Equation (3.7), a, b, c, d, e and f are called AB, BA, C, D, E and F respectively. In Equation (3.6), $\varepsilon 1$, $\varepsilon 11$ and $\varepsilon 111$ are complex quantities and are replaced by (E1R + 2EII), (E2R + 2 E2I) and (E2R + 2 E3I) respectively where i is equal to $\sqrt{-1}$. Equation (3.5) again involves complex quantities and the expressions A, B, C, D and E are replaced by (PR + iPI), (QR + iQI), (CR + iCI), (DR + iDI) and (ER + iEI). Finally, the quantity under the radical sign in Equation (3.4) is denoted by (GR + iGI). A new pair of variables RR and RI is introduced such that

$$RR + iRI = GR + iGI \quad . \tag{3.11}$$

For the ordinary wave the real part of the numerator in Equation (3.4) is designated as Z1, the imaginary part being Z2. The corresponding values for the extraordinary wave are called Z3 and Z4. Similarly, for the denominator the real part is denoted by Y1 and the imaginary part by Y2.

The quantities AKO and AKX denote, respectively, the ordinary and extraordinary absorption in dB per km for an up and down path in the ionosphere and are evaluated from the absorption coefficient derived through the solution of Equation (3.9). The corresponding real parts of the refractive indices are given by RKO and RKX, respectively.

The program is drawn so as to give as an output the above four quantities for each successive height interval of 1 km beginning from the lowest altitude of 56 km. The electron number density and collision frequency is presumed to have remained constant over the interval of 1 km. The largest height up to

which the program works is decided by a statement card indicating the number of desired height intervals. The frequency of propagation for which the above calculations are made can also be easily altered by replacing a single statement card in the program. Provision has been made to evaluate and list out the sum total of the absorption on each mode between any two pre-selected levels in the ionosphere. For any selected location the electron gyrofrequency and dip angle are fed in as input. Successive computations are made for any number of locations and listed on successive sheets. For convenience of identification, the geographic latitude, longitude, the dip angle and gyrofrequency of each location selected is printed out on top of each sheet. Provision has also been made to list out at the beginning of the program the electron number density and collision frequency as a function of height, as used in the program.

For the transverse case, applicable for the ordinary wave propagation at the equator, the input and output features of the program are very nearly identical to that for the general case discussed above. The program, however, is considerably simplified as the gyrofrequency does not play any role in the computations of the absorption indices. The computer source program for the transverse case is listed in Appendix II and is not discussed further.

In the discussion for the general case a prior knowledge is presumed for the gyrofrequency and the dip angle at a given location. In reality the quantities were evaluated for specific locations from a separate computer program written by Eckhouse (1964) and slightly modified to give the output in the desired form applicable for the current program. Considerable simplification is achieved in the procedure for evaluating the absorption and refractive indices by presuming a constant value of magnetic dip and gyrofrequency over the entire height range for a given location. The maximum error in the

absorption or refractive index calculation was estimated to be less than one percent over the entire height range of interest from 55 to about 110 km. In order to keep the error to a minimum the values of the dip angle and electron gyrofrequency appropriate to 75 km were used for each location.

3.4 Ionospheric Absorption on Ordinary Mode of Propagation

In Figure 3.1 is shown the latitudinal variation of the electron gyrofrequency and dip angle at 75 km altitude. The longitudes chosen are 75° east and 75° west, respectively. The geomagnetic equator lies to the extreme north close to the east longitude noted above and to the extreme south in the west longitude. The electron gyrofrequency is seen to have the lowest value of 0.77 MHz close to the dip equator in the western zone and close to 1.05 MHz in the eastern zone. Near the poles the frequency varies less slowly with latitude and has a value close to 1.55 MHz. Figure 3.2 shows the corresponding situation at 0° E and 0° W longitudes. The changes occurring in the absorption and refractive indices for the ordinary and extraordinary modes of propagation due to the above changes in the dip angle and gyrofrequency of electrons are investigated in the following.

In order to study the world-wide absorption characteristics as a function of the earth's magnetic field, vertical absorption profiles were derived at each 10° latitude interval on the two longitudes 75° east and 75° west. A single electron density profile as well as a single collision frequency profile for the electrons was used throughout the analysis. The electron density and collision frequency profiles were derived from a rocket experiment performed at a solar zenith angle of 60° at Wallops Island (Virginia) in the winter of 1965. Simultaneous measurements were performed using vertical incidence ground-based equipment. The absence of anomalous winter absorption

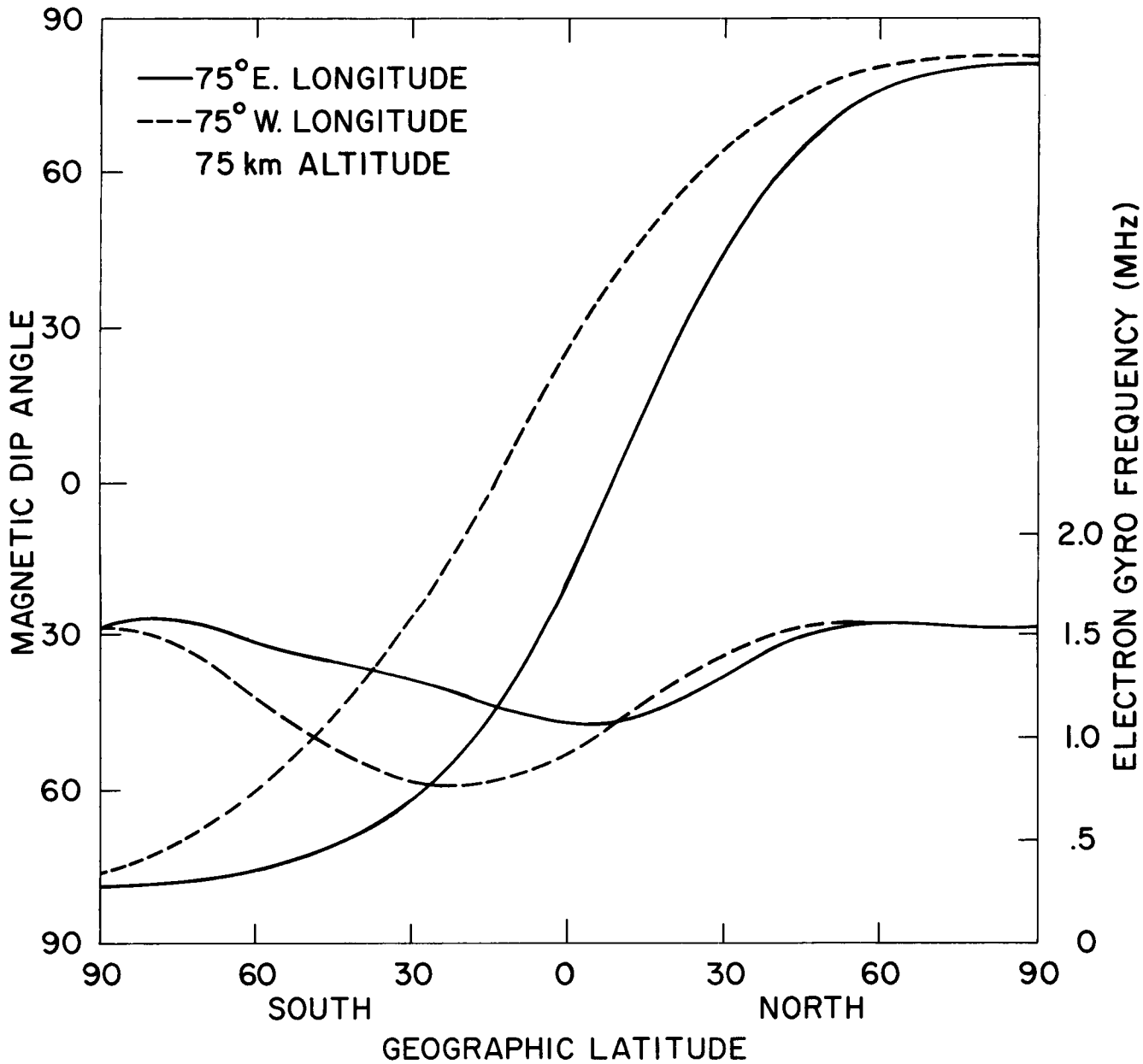

Figure 3.1 Variation along the 75° E and 75° W longitudes of the electron gyrofrequency and dip angle at an altitude of 75 km.

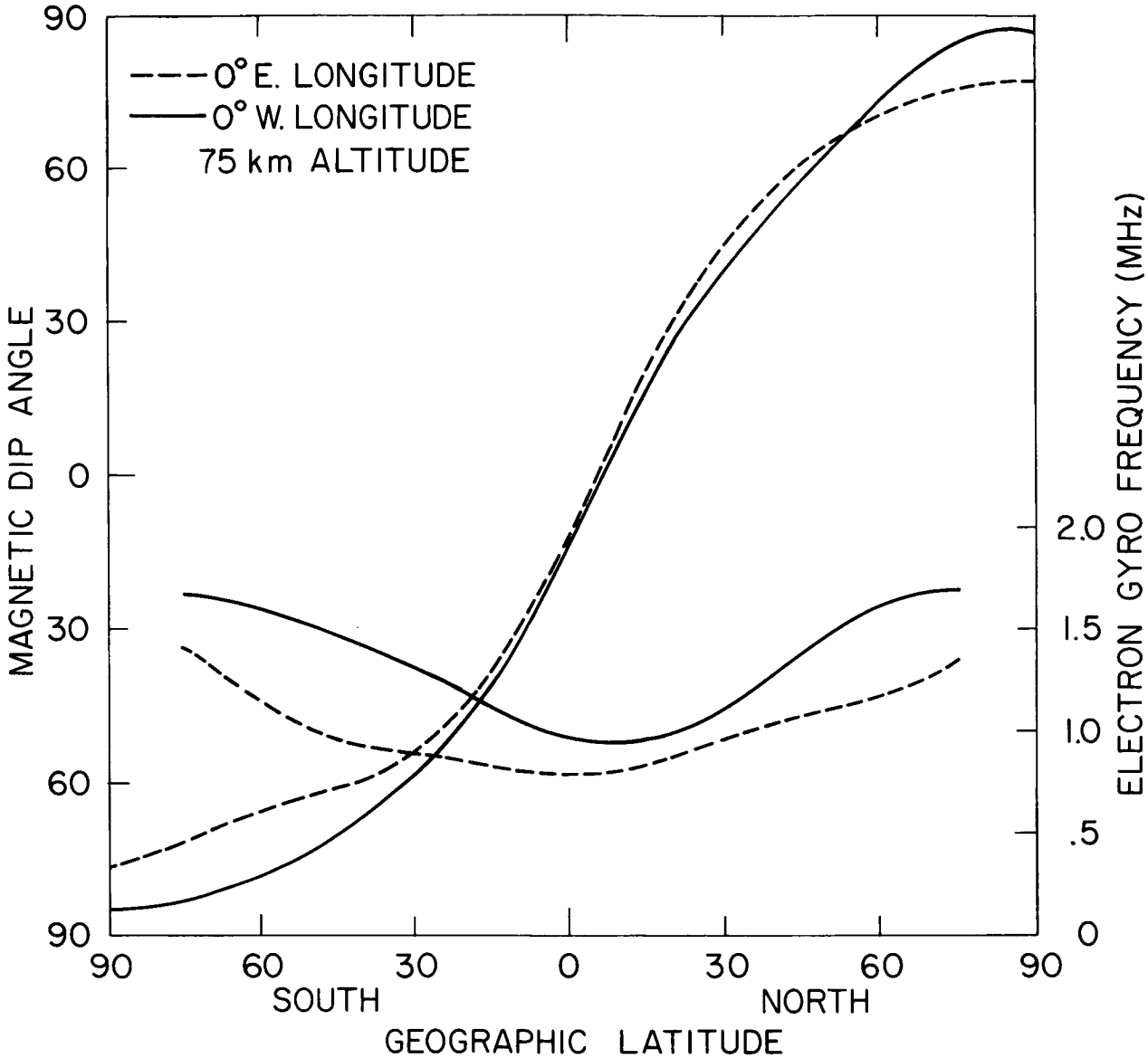

Figure 3.2 Variation along 0° E and 0° W longitudes of the electron gyrofrequency and dip angle at an altitude of 75 km.

conditions for the day of the launch were established from the ground-based measurements (Shirke and Rao, 1967). However one rather abnormal feature was noticed during the rocket flight, namely, the appearance of a sharp sporadic E layer near the 95 km level. Some features of the rocket measurements were discussed in Chapter 1. Further details will be discussed in a paper by Mechtly and Shirke (1967). Since the primary aim in carrying out the current investigations is the study of the latitudinal variation of absorption due to changes in the terrestrial magnetic field, the electron density profile has been modified to suit the present analysis. In effect, the sporadic E peak in electron density was suppressed while feeding the profile to the computer. This has permitted the study up to the 110 km level which would have otherwise been terminated close to 95 km.

A collision frequency model related to the pressure model given in CIRA (1965) was established by the rocket experiments. The model used for the current calculations is given by the expression

$$\nu_m = 6.74 \times 10^5 \, p \qquad (3.12)$$

where p is expressed in units of Newtons/meter^2. The electron density and collision frequency values used in the analysis are listed as a function of altitude in Appendix II.

Figure 3.3 shows the typical vertical distribution of absorption for the ordinary mode of propagation for 3 selected latitudes 15°, 35° and 55° N in the 75° east longitude zone. The calculations are made for an operating frequency of 3.0 MHz.

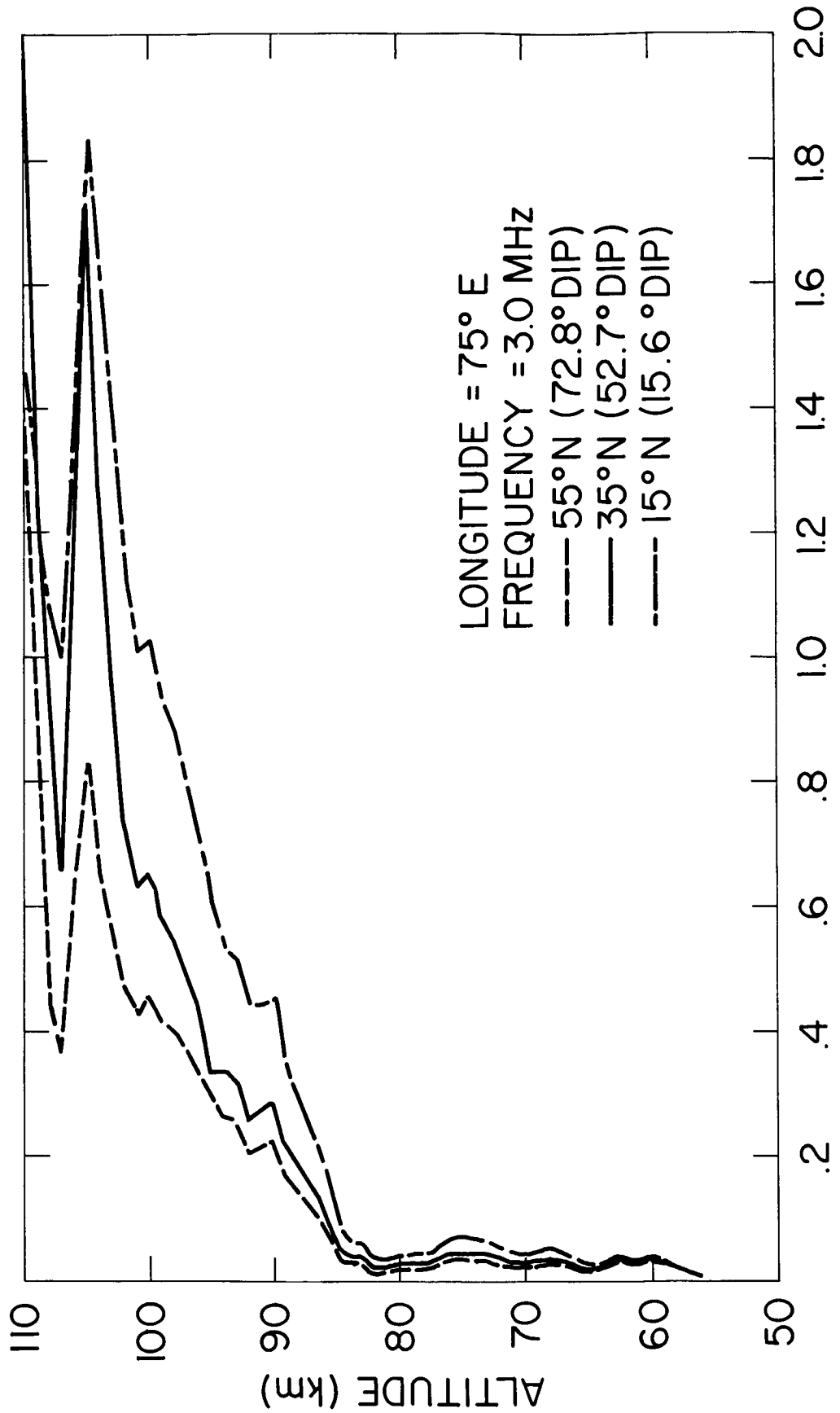

Figure 3.3 Vertical distribution of ordinary mode absorption on 3.0 MHz for different latitudes.

The progressive increase in absorption with decreasing latitude is clearly seen at each altitude except below about 62 km. As pointed out in Chapter 1, the normal absorption below 84 km is seen to be less than 10 percent of the total absorption up to 110 km. Above 55° N latitude there is not much change in absorption with further increase in latitude. This is so because both the gyrofrequency of electrons and the dip angle vary very little above this latitude.

Close to the level of reflection the absorption at all latitudes is seen increasing very rapidly with further increase of altitudes. For 3.0 MHz operation the sharp increase is seen to be close to 110 km. This is due to the deviative attenuation becoming large as the level of reflection is approached. An interesting feature, however, is the crossover of the 35° profile over the 15° one near 109 km. The consequences of such a behavior are discussed later, which has an important bearing on the 'geomagnetic anomaly' presented in Chapter 2.

Also seen in Figure 3.3 is a crossover of the absorption profiles at an altitude close to 60 km indicating that below this level the absorption for a given frequency is lower at higher latitudes compared to that at low latitudes.

Figure 3.4 shows the absorption characteristics for an operating frequency of 2.66 MHz corresponding to the same latitudes as shown in the previous diagram. As is to be expected from classical theory, the absorption is larger on the lower frequency at all altitudes. Once again a crossover in the absorption profiles is noticed at low altitudes, however the level at which the crossover occurs is slightly higher on the lower frequency. The level at which the crossover occurs is the one at which the collision frequency of electrons becomes equal to the operating frequency. As a collision frequency decreases

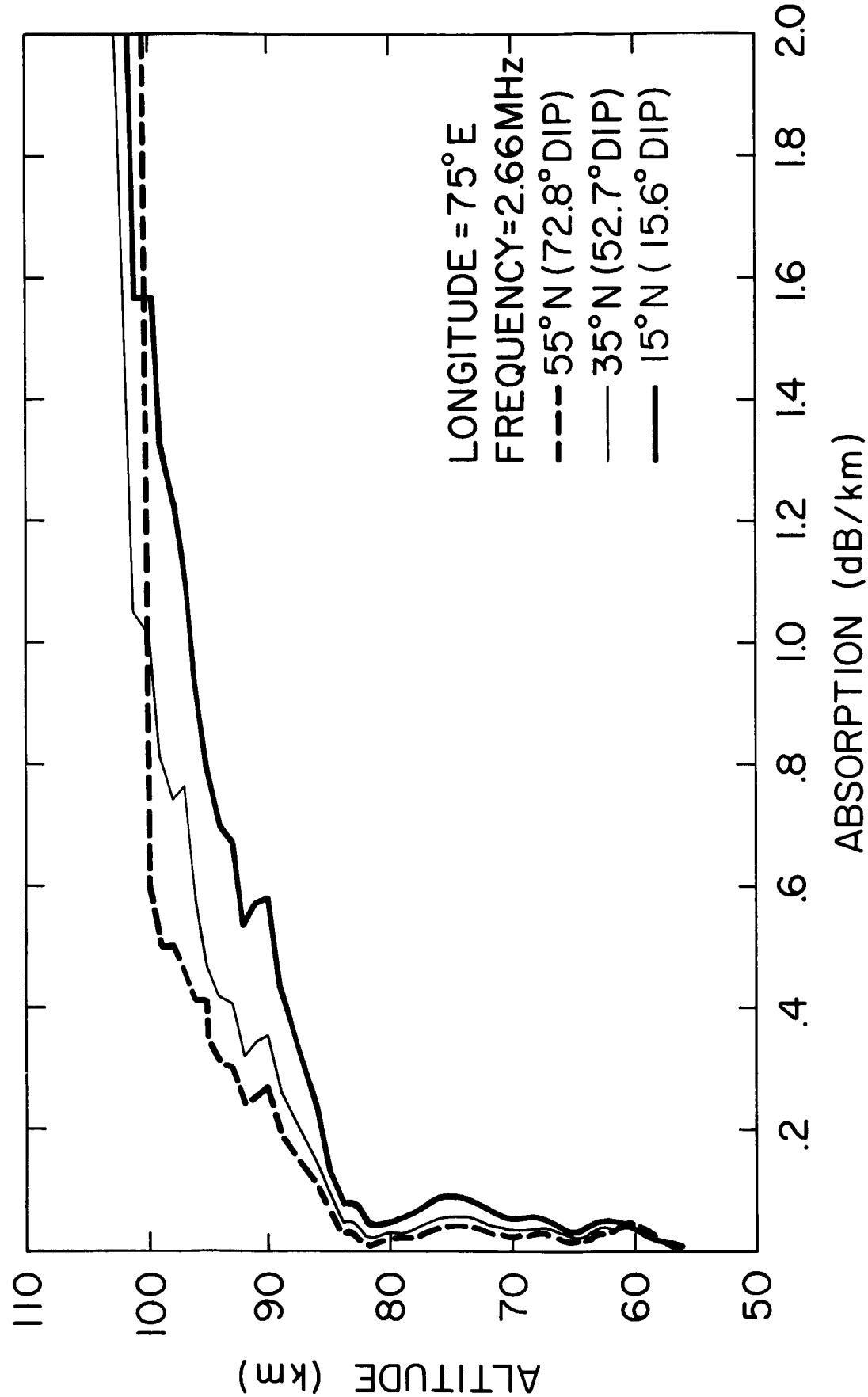

Figure 3.4 Vertical distribution of ordinary mode absorption on 2.66 MHz for different latitudes.

upward it should be expected that the crossover level would lift upward with a decrease in the operating frequency.

In order to investigate the frequency dependence of absorption as a function of altitude, the ratio of 2.66 MHz absorption to 3.0 MHz absorption is shown in Figure 3.5 for three latitudes. Around 60 km the ratio is seen to be close to 1.1 and is seen increasing with increasing altitude. At a given location for a given altitude the ratio increases with increasing latitude. According to the classical theory one expects an inverse frequency dependence of absorption at low altitudes changing over to an inverse square of frequency law at larger altitudes. For latitudes 15°, 35° and 55° N for which curves are shown, the inverse frequency law would give ratios of absorption on the two frequencies as 1.11, 1.09 and 1.08, respectively, and the inverse square law would give ratios 1.23, 1.19 and 1.16, respectively. In deriving these ratios the equivalent frequencies effective at these latitudes have been considered. It is interesting to note that the observed ratios exceed those expected from the inverse square law above about 74 km. Thus, around 90 km where an appreciable part of absorption takes place normally the appropriate index is 2.28 for the inverse frequency rather than 2.0 as noted in the classical work.

Returning to Figure 3.4 it might be noticed that similar to 3.0 MHz the absorption on 2.66 increases sharply as the level of reflection is approached which is a few km lower than for the 3.0 MHz operation. The crossover of characteristics is once again observed close to the level of reflection.

Figure 3.6 shows the latitudinal distribution of absorption per km at preselected levels in the ionosphere on an operating frequency of 3.0 MHz 75° E and 75° W. While the absorption is largest at the dip equator for an

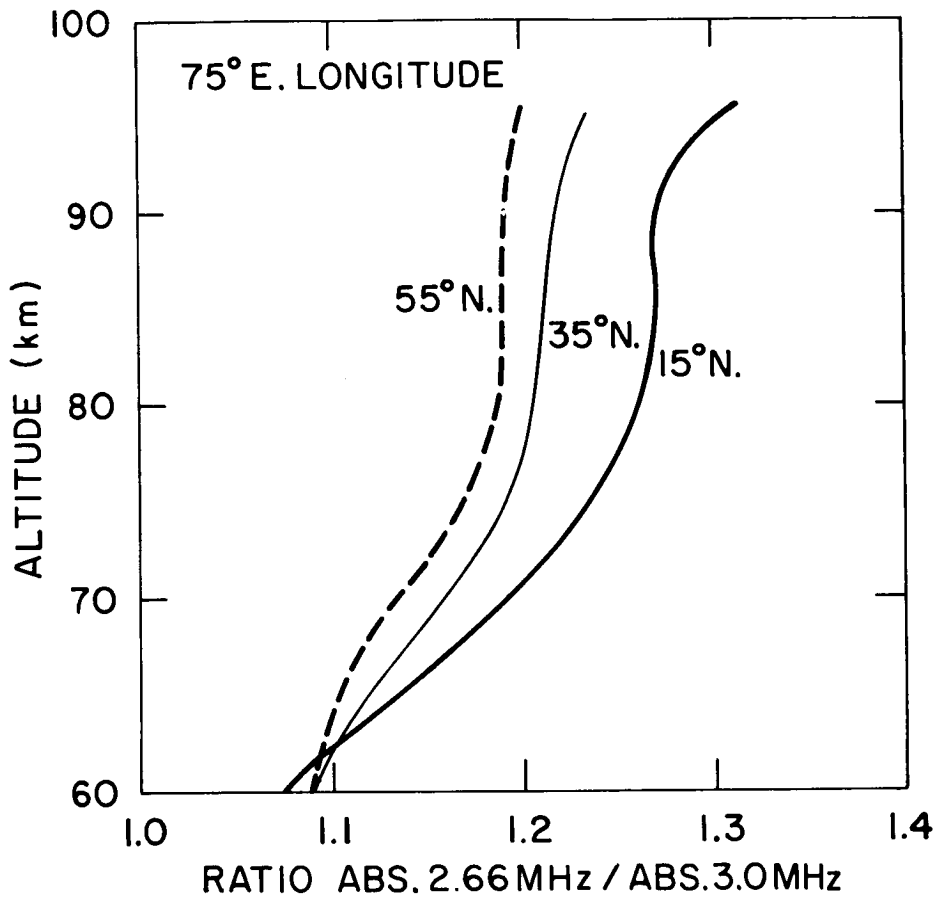

Figure 3.5 The ratio of ordinary mode absorption on 2.66 MHz to that on 3.0 MHz as a function of altitude.

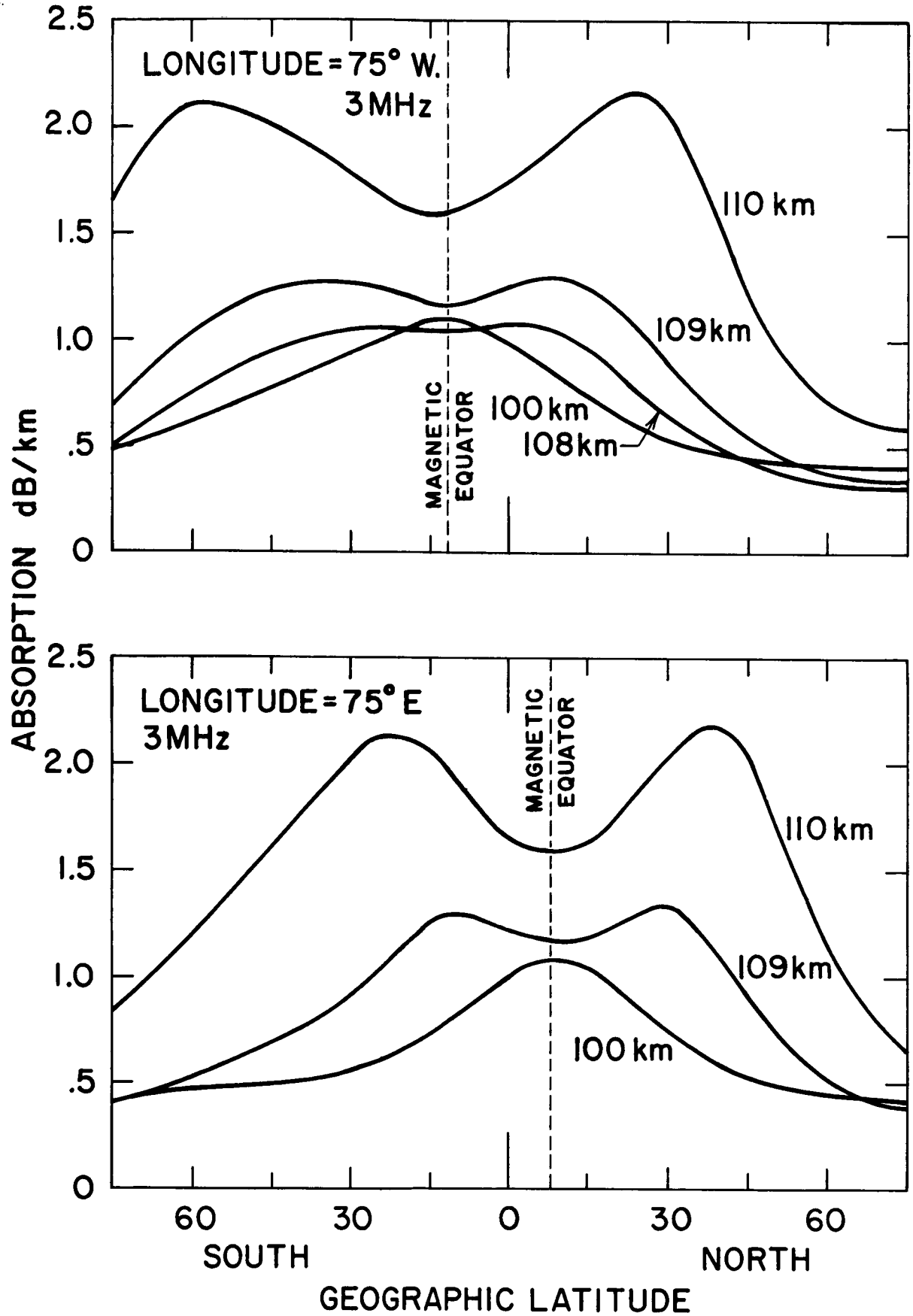

Figure 3.6 Latitudinal distribution of absorption per km at specific levels in the ionosphere.

altitude of 100 km, a double-hump characteristic is noticed around 110 km at both the longitude zones. At the higher altitude the maximum of absorption is situated close to a dip angle of 60° on either side of the equator for both the longitude zones. With decrease in altitude the maxima in absorption are seen shifting toward lower dip angles finally merging to form a single maxima at the dip equator at a lower altitude. It is interesting to note that the total absorption characteristics measured on board the ship USNS Croatan, and presented in Chapter 2, are very much similar to those seen at the 110 km level. The geomagnetic anomaly presented in Chapter 2 appears then to be a natural outcome of the generalized theory. The diurnal variation of total absorption observed on board the ship indicates that the double-hump feature is not present in the early morning hours. Since this feature is present only at levels close to the reflection of the waves, a change in this level with time of day might cause the type of diurnal variation observed on board the ship. More investigations are required on this aspect of the problem before the phenomena can be fully explained.

3.5 Latitudinal Variation of Differential Absorption

The latitudinal distribution of the total absorption is plotted in Figure 3.7 for a level where the refractive index falls to 0.8 from unity. Curves are drawn for both the ordinary and extraordinary modes of propagation and for longitudes 75° east and 75° west. The absorptions at the dip equator calculated using programs of the transverse case are seen to fit in smoothly with those calculated for neighboring latitudes using the program for the general case. For the ordinary mode the total absorption has also been shown up to an altitude of 110 km. Once again the frequency of operation has been chosen to be 3.0 MHz.

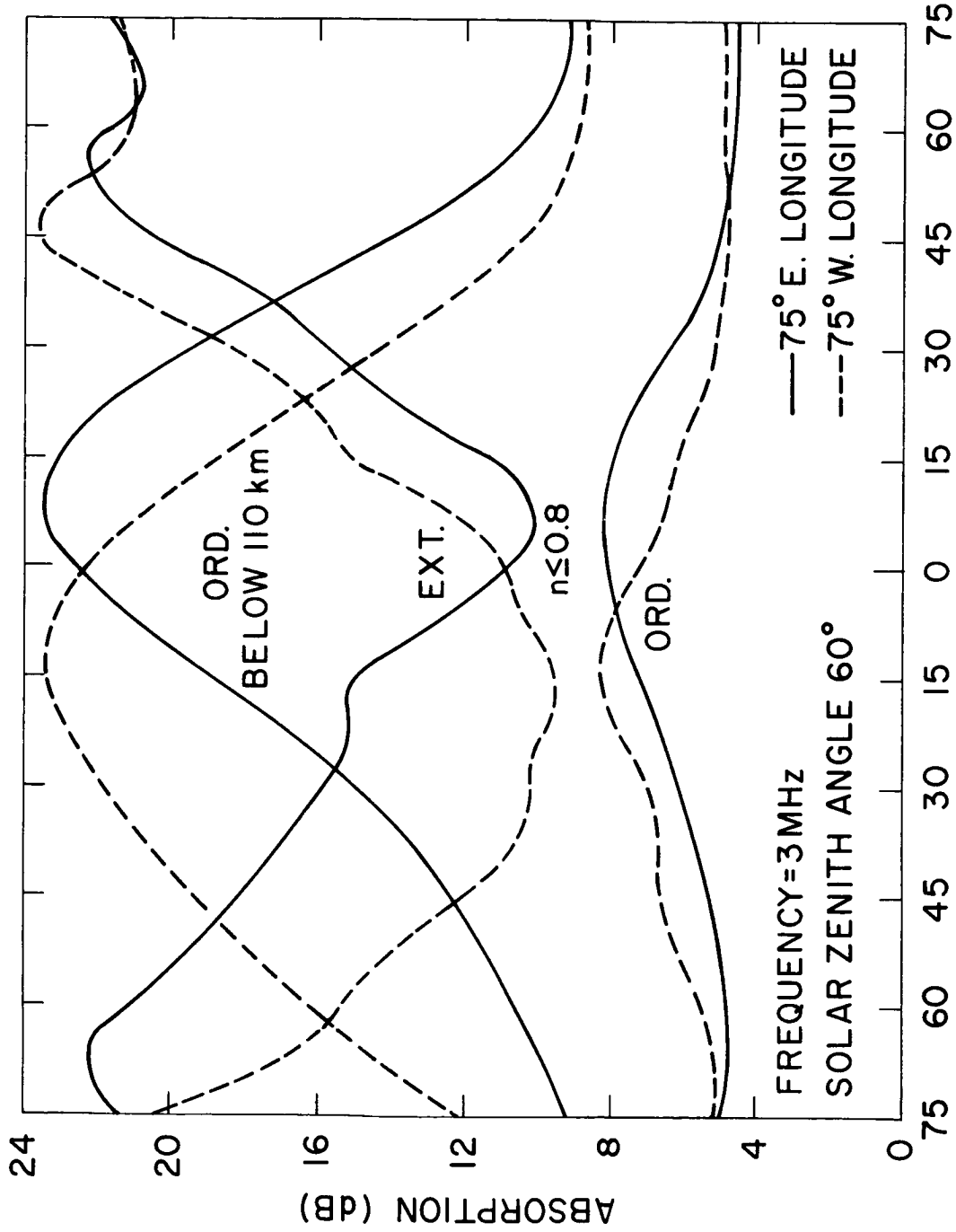

Figure 3.7 Latitudinal variation of total absorption on ordinary and extraordinary mode waves between levels where the corresponding refractive indices fall from unity to 0.8. Also shown are curves for total ordinary wave absorption below 110 km.

In the figure the total ordinary absorption up to 110 km is seen increasing uniformly toward the dip equator. The double-hump feature noted previously is not seen in the total absorption curve. This shows that the double-hump feature is restricted to a narrow range of altitudes below 110 km and has not affected the total absorption below this level. Besides, the shifting of the peaks in latitude with increasing altitude has the effect of smoothing out the peaks in the total absorption curves. It will be shown later that for a given frequency the level at which the ionospheric reflection takes place changes with latitude. This would have a further effect on the total absorption up to the level of reflection.

For the ordinary mode, the curve corresponding to the total absorption up to the level where the refractive index falls to 0.8 varies, moreover, similar to that for the total absorption up to 110 km. For the lower level, the absorption is about 8 dB at the dip equator and close to 5 dB at 55°. At the equator the absorption between the two levels under consideration is about two and a half times as large as below the lower level. At the higher latitude noted earlier the corresponding absorption is a little less than twice as much as below the lower level.

The extraordinary absorption curve corresponding to the lower reflection level shows just the reverse trend to that seen for the ordinary wave. While the absorption is largest at the equator for the ordinary mode and decreases with increasing latitudes, the extraordinary wave shows a minimum absorption at the magnetic equator and an increase with increasing latitudes. The extraordinary mode absorption is larger at all latitudes than the corresponding absorption on the ordinary mode. However, the difference between the two is by far the least at the equator and increases with increasing latitudes. This

effect has an important bearing on the measurements of partial reflection amplitude on the two ionic modes as a function of latitudes. It is evident from Figure 3.7 that for a given frequency and altitude the differential absorption would decrease substantially as the latitude decreases.

In Figure 3.8 is shown the ratio of the extraordinary to ordinary absorption as a function of altitude for the 3 MHz operation for a few selected latitudes in the 75° east longitude zone. Except for very low altitudes the ratio is seen to increase with increasing altitude at all the locations. For a given altitude the ratios are lowest at the equator and increase with increasing latitude. The wiggles in the curves are due to fluctuations in the electron density profiles as a function of altitude. Sharp increases in the curves above 95 km are due to large deviative type attenuation setting in on the extraordinary mode. An interesting feature is the crossover of all the curves at an altitude close to 60.5 km. As pointed out earlier, this level is governed by the collision frequency of electrons becoming identical to the operating frequency. Below this altitude the above ratio is less than unity and is reduced with a decrease in altitude or increase in latitude.

It is evident from the above discussion that at the higher latitudes the ratio of extraordinary to ordinary absorption is very low at the bottom of the ionosphere and undergoes changes of over one order of magnitude by the time the level of reflection of the extraordinary wave is reached. The change in the ratio over the same altitude range is less than 100 percent at 15° N which is about 7° away from the dip equator. If absorption were to be the only consideration, it is obvious that it is easier to make partial reflection measurements at lower latitudes than at higher ones. Since the partial reflection technique relies on making measurements on both ionic modes, the transmitted power would

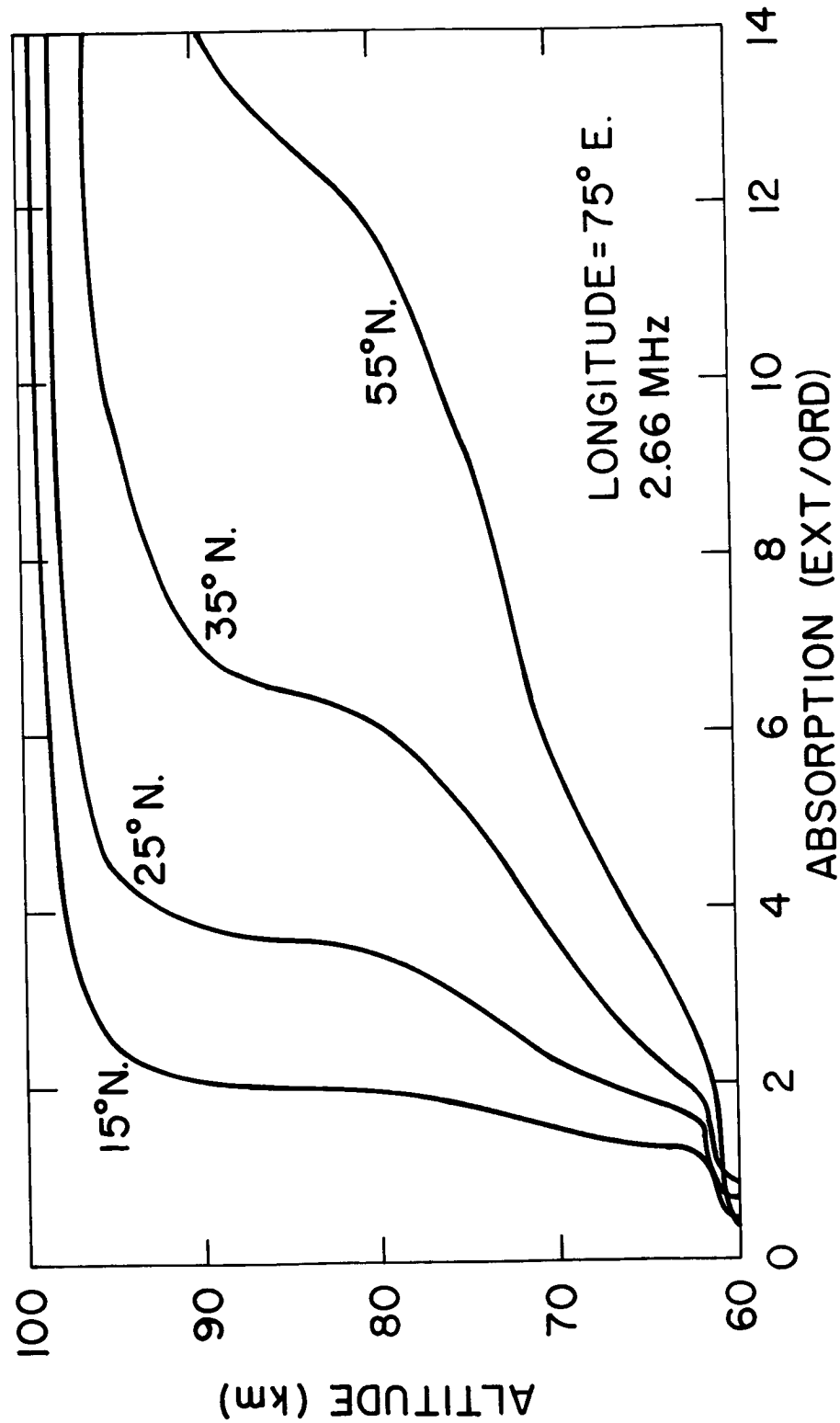

Figure 3.8 Ratio of 3 MHz extraordinary to ordinary wave absorption as a function of altitude at different latitudes.

also have to be larger at the higher latitudes to give an equal amount of received signal than at a lower latitude, provided the reflection coefficients of the ordinary and extraordinary modes were to remain constant as a function of latitude. However, the amplitude received from partially reflected echoes is a function of both the reflection coefficient and the absorption of the received signals. A study has therefore been undertaken of the changes occurring in the reflection coefficients as well as a function of latitude. The results of these investigations are presented a little later.

In Figure 3.9 curves are shown for the ratio of extraordinary to ordinary absorption for a frequency of 2.66 MHz. To facilitate comparison with 3.0 MHz operation the same geographic locations are chosen as for the previous figure.

It is evident from Figure 3.9 that the differential absorption increases with a decrease in frequency except at very low altitudes. If we were to compare Figures 3.8 and 3.9 for any given location the two sets of ratios one each for the two frequencies, differ more and more as the altitude increases. By an appropriate choice of frequency it should then be possible to achieve any desired level of differential absorption for a given location. However, measurements on a single frequency may not always cover the entire altitude region of interest. This may pose difficulties in instrumentation, especially so at higher latitudes where the variation of differential absorption with altitude is large as also the absorption on the extraordinary mode.

3.6 Refractive Indices on Ordinary and Extraordinary Modes of Propagation

As noted earlier, the refractive indices on the ordinary and extraordinary modes of propagation are computed as a function of height and latitude. The results are discussed in the following. In Figure 3.10 are shown the contours of constant indices for both modes of polarization as a function

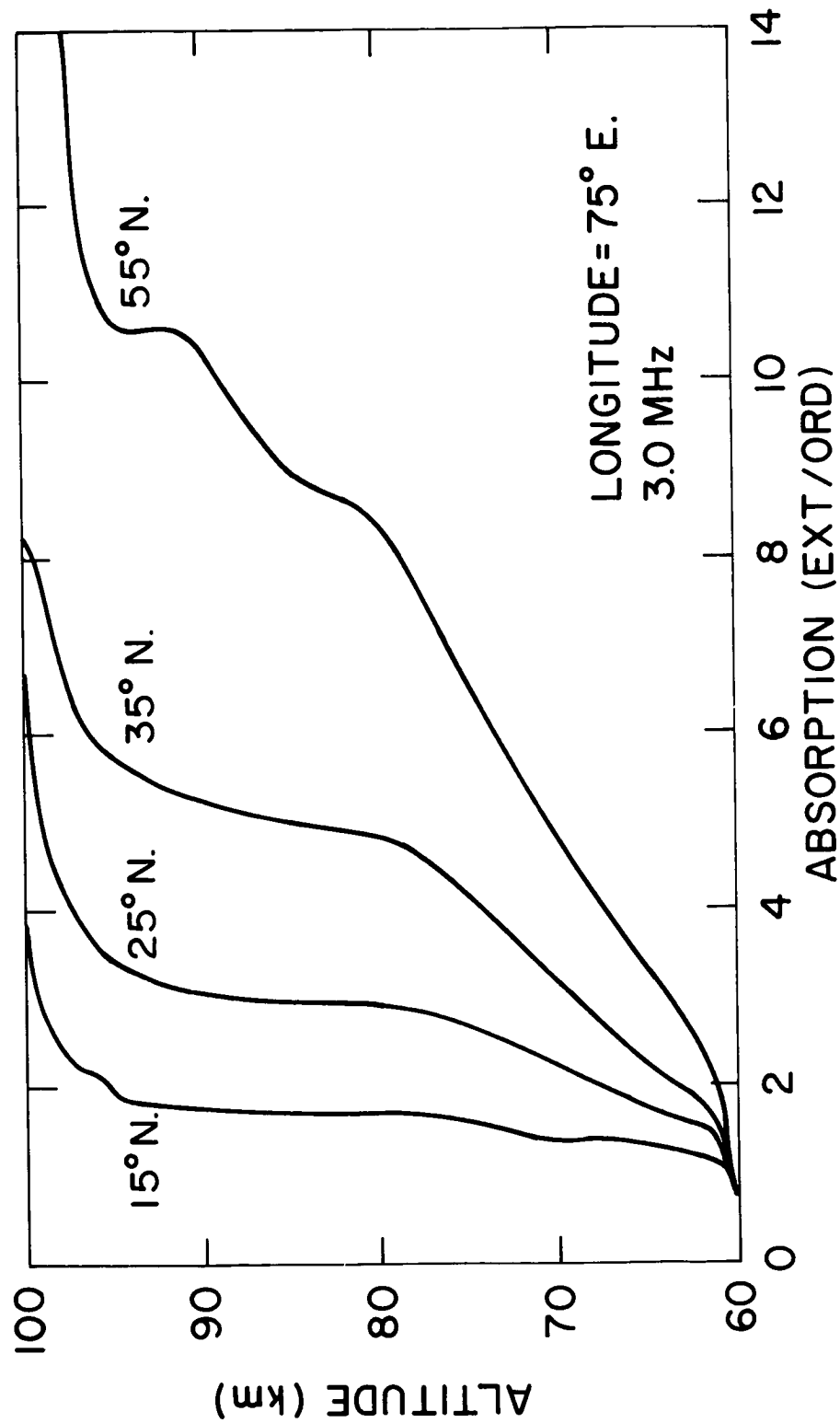

Figure 3.9 Ratio of 2.66 MHz extraordinary to ordinary wave absorption as a function of altitude for different latitudes.

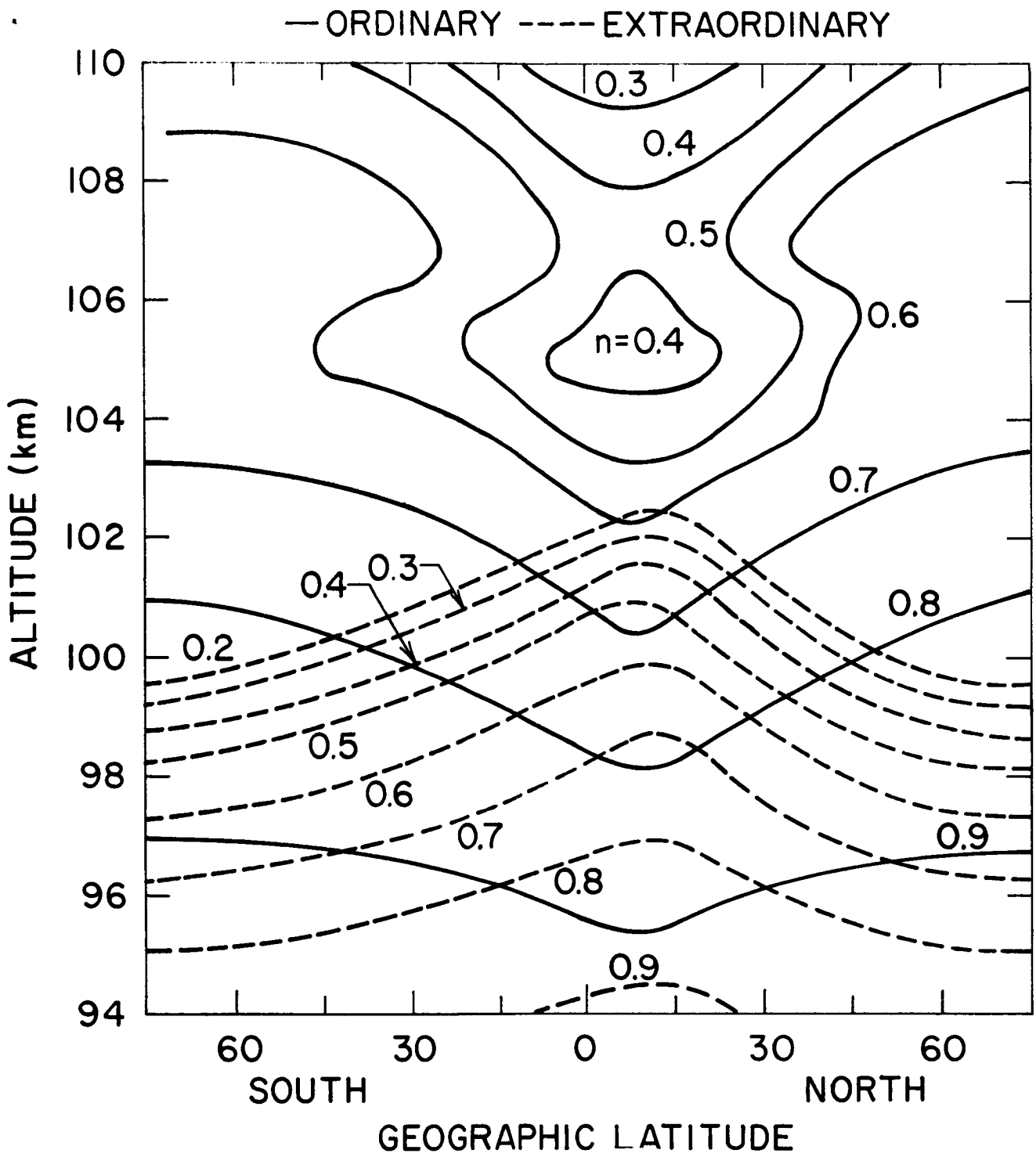

Figure 3.10 Contours showing height variation of constant refractive index levels for the ordinary and the extraordinary waves on 3.0 MHz.

of latitude and altitude. Once again a frequency of 3 MHz has been used. The results for the 75° east longitude have been shown. The contours of equal indices have been derived by noting the refractive index at each one km interval in altitude and 10° interval in latitude. In general, the contours are concave upwards for the ordinary and concave downwards for the extraordinary mode. The ordinary mode contours are seen distorted around the 106 km level. This is due to a ripple in the electron density profile at this altitude region.

It is interesting to note from Figure 3.10 that each of the ordinary wave contours in the region below 106 km is about 2 to 3 km lower in altitude at the equator compared to that at much higher latitudes. Conversely, the extraordinary wave gets reflected by about 2 to 3 km higher at the equator than at higher latitudes. Thus, the difference in the levels at which the ordinary and extraordinary waves get reflected is the least at the equator and increases with increasing latitude.

It is of interest to note that the refractive index for the ordinary wave at 110 km level falls moreover symmetrically with increase in latitude on either side of the dip equator. It might be recalled in this connection that the absorption (shown in Figure 3.6) per km at the same level was not varying smoothly as the refractive index, but showed a double-hump characteristic with a maximum of absorption close to 60° dip. In essence, this would mean that since the level of reflection is higher at higher latitudes there would be a larger contribution to the total absorption from latitudes farther away from the equator. Since the absorption characteristics are double-humped in nature at these altitudes, the additional absorption would have a double-hump characteristic to the total absorption up to the level of reflection. This lends strong support to the latitudinal distribution patterns of absorption observed on board the ship USNS Croatan and presented in Chapter 2.

3.7 Partial Reflection Coefficients

The effective reflection coefficient R_o of partially reflected echoes from a sharp boundary, where the complex refractive index changes from n'_2 to n'_1 is given by Budden (1961) by the following expression

$$R_o = \frac{n'_2 - n'_1}{n'_2 + n'_1} \simeq \frac{\delta n'}{n'} \quad . \tag{3.13}$$

A similar expression holds good for R_x, the reflection coefficient on the extraordinary mode. This is true for an isotropic medium, and is approximately true for an anisotropic medium when n'_1 and n'_2 are not close to unity. In the lower ionosphere the absorption index would be very low and to a first approximation, the complex refractive index would be close to the real part of the complex index. The reflection coefficient of partially reflected echoes from the lower ionosphere could then be considered to be proportional to δn, the corresponding change in the real part of the complex refractive index.

In practice the vertical amplitude distribution of partially reflected echoes would largely be governed by the presence of irregularities in the electron density profile. However, the relative amplitude of the reflection coefficients as a function of latitude could be investigated by studying a given electron density profile and by noting the changes which occur in the vertical gradients of the refractive indices for the two ionic modes.

Figures 3.11 and 3.12 show the vertical gradient of the refractive index for the ordinary and extraordinary modes of propagation, respectively, for an operating frequency of 2.66 MHz and for the latitudes 15 and 55° N in the 75° E longitude zone. The gradients change by over 3 to 4 orders of magnitude in an altitude range between 60 and 100 km. Considering the ordinary mode

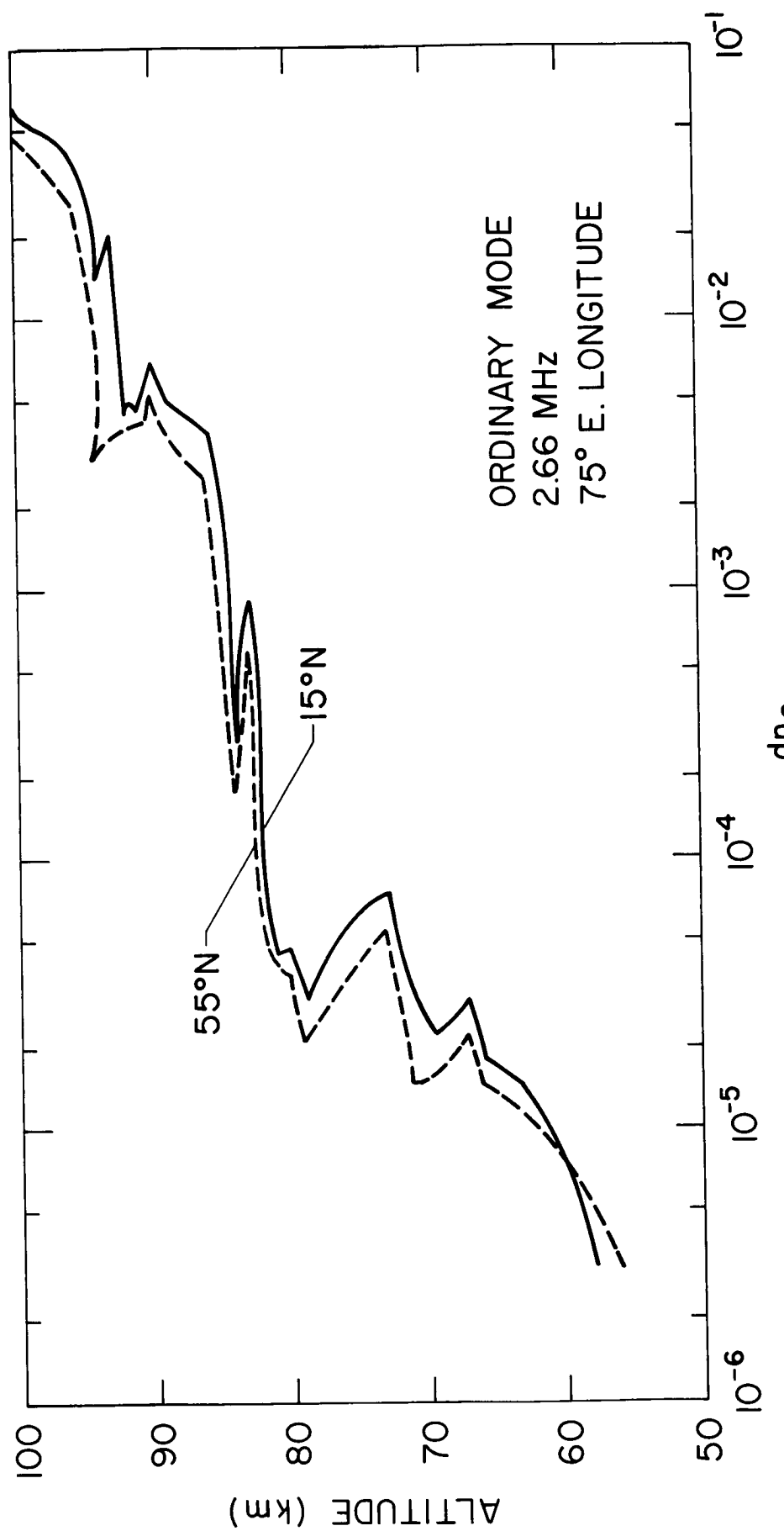

Figure 3.11 The vertical gradient in the ordinary wave refractive index for 2.66 MHz.

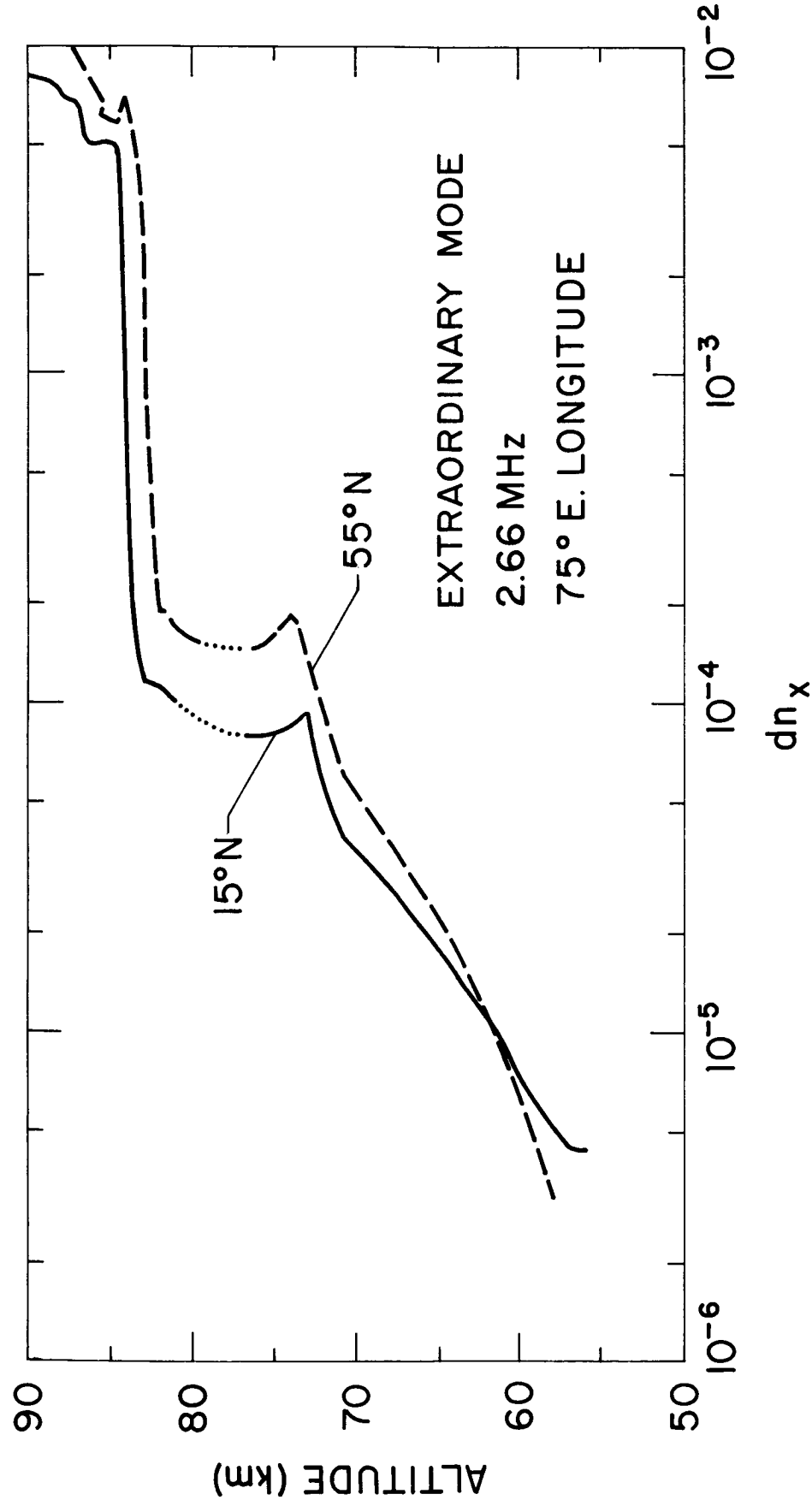

Figure 3.12 Vertical gradient of extraordinary wave refractive index on 2.66 MHz.

first, around 60 km the curves showing the gradients corresponding to latitudes 15° and 55° are found to cross over each other. Below this altitude the values are larger for the higher latitude whereas above the transition level the value of the gradient is larger for the lower latitude by about 60 percent compared to that at 55°. For the extraordinary mode as well, the curves cross over close to the 60 km level. Conversely to the ordinary case, the gradients are, in general, larger at the higher latitudes compared to those at the lower latitude above the crossover level and lower below the same. At the dip equator, for a given frequency the ratio of the reflection coefficients of partially reflected echoes on the extraordinary to the ordinary mode of propagation would be close to unity throughout the altitude regions of interest. At any other latitude the ratio would increase both with the increase of altitude as well with the increase in latitude. Thus, barring a few exceptions noted above, the extraordinary reflection coefficient would be by far larger than the ordinary coefficient.

3.8 Latitudinal Distribution of Faraday Rotation

The measurements on the Faraday rotation of radio waves has been used as an effective technique for the determination of electron densities using rocket and satellite signals. The results of the present analysis are extended to see the effect of the magnetic field on the rotation. When the refractive indices on the ordinary and extraordinary modes of propagation are not too far off from unity, it can be shown that the Faraday rotation on a given frequency is proportional to the quantity $(n_x - n_o)$, where n_x and n_o denote the real part of the complex refractive indices on the extraordinary and ordinary modes, respectively. The variation of the quantity $(n_x - n_o)$ is shown in Figure 3.13 as a function of altitude for 3 latitudes 15°, 35° and 55° N

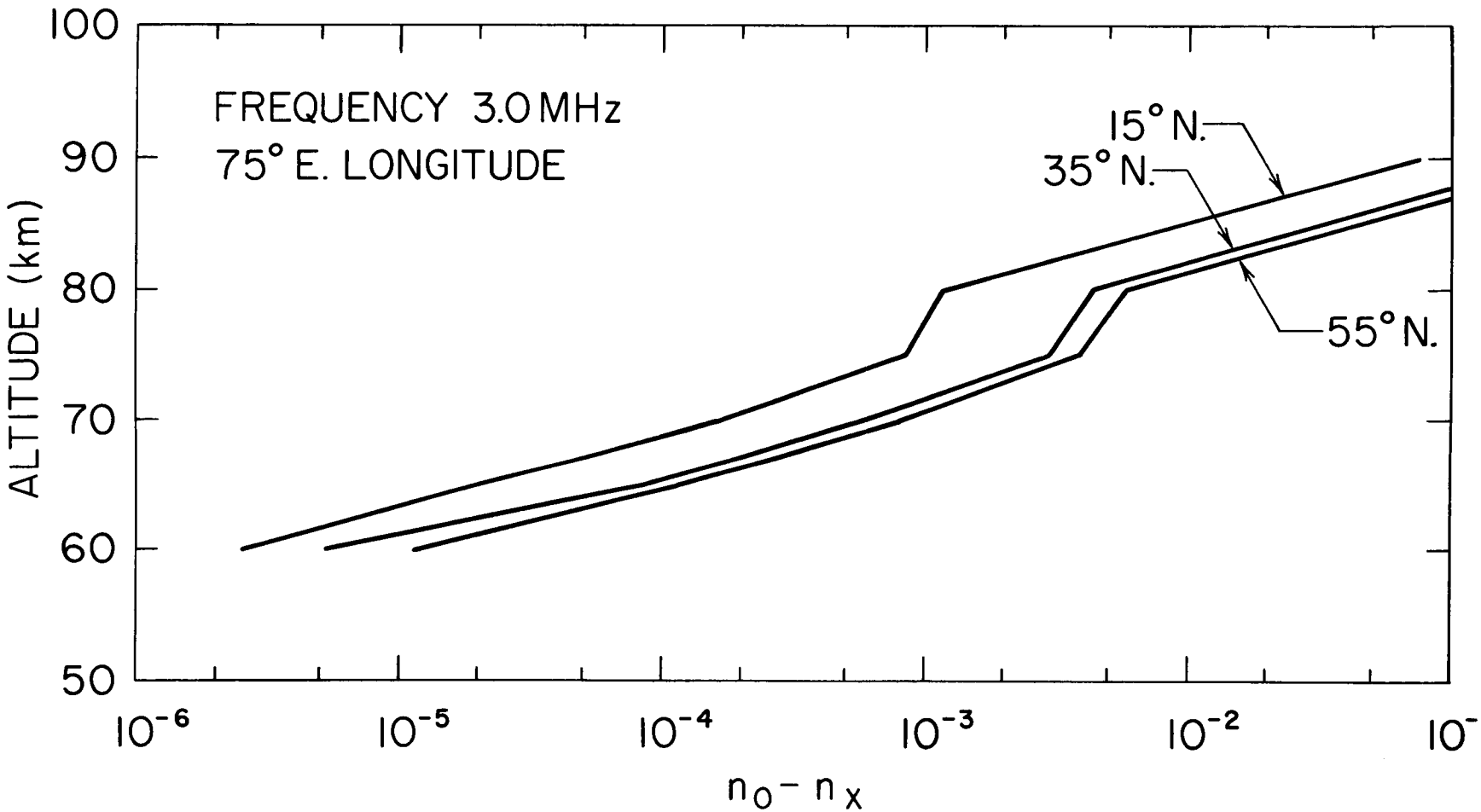

Figure 3.13 The variation of the quantity $(n_X - n_O)$ is shown as a function of altitude for different latitudes. n_X and n_O are the real parts of the complex refractive indices for the extraordinary and ordinary modes respectively.

in the 75° E longitude zone. The quantity (n_x-n_o) increases fairly smoothly with altitude by about 6 orders of magnitude between 60 to 100 km. In Figure 3.13 the variation up to about 90 km only is observable. A sudden change in the gradient of (n_x-n_o) is seen between 75 to 80 km due to a corresponding change in the electron density profile in this altitude range. With increase in latitude the curves shift toward the right by a constant amount. Thus, at 55° N the quantity (n_x-n_o) is about 5 times as large as at 15° N and about 1.3 times as large as at 35° N throughout the altitude region under consideration, except perhaps at very low altitudes where small departures from the above behavior are noticed. The latitudinal variation of Faraday rotation, as seen from the above characteristics, is different from the corresponding differential absorption variations which show a large altitude dependence.

3.9 Summary

The following are some of the conclusions drawn from the above analysis:

1. For a given altitude above a certain minimum level, the absorption on the ordinary mode of propagation is maximum at the dip equator and decreases toward higher latitudes except at regions close to the level of reflection of the waves.
2. Under similar conditions the absorption on the extraordinary mode is a minimum at the equator and increases toward higher latitudes.
3. The differential absorption is therefore a minimum at the equator and increases with increasing latitude.
4. For a given frequency of propagation the height at which the reflection takes place is about 3 km larger at the equator than at the polar regions for the ordinary mode.
5. Conversely, for the extraordinary mode the height of reflection is about 3 km lower at the equator than at high latitudes.

6. For a given frequency of operation the ratio of extraordinary to ordinary (EXT/ORD) absorption increases with increasing altitude at all latitudes except at the dip equator.

7. The ratio EXT/ORD increases more rapidly with height for increasing latitudes.

8. The ratio EXT/ORD is less than unity below a certain altitude where the collision frequency of electrons equals the operating frequency. For any altitude below this level the ratio decreases with further increase of latitude.

9. The altitude at which the ratio EXT/ORD becomes equal to unity decreases with increase in frequency of operation.

10. Above the transition level the ratio EXT/ORD decreases with increase in frequency of operation.

11. Classical law giving inverse frequency dependence of absorption needs modifications. For the case considered, the frequency index is close to (-2.28) rather than (-2.0) at 90 km around which level the bulk of the absorption normally takes place.

12. The quantity $(n_o - n_x)$ which in the lower ionosphere is proportional to the Faraday rotation of the signals, increases with increase in latitude. However, the ratio of this quantity at two latitudes does not change significantly with altitude.

13. The ordinary mode absorption per km near the level of reflection of the wave exhibits a double-hump characteristic. The maxima in absorption are situated, moreover, symmetrically with respect to the dip equator.

14. With decreasing altitude the maxima in absorption shifts toward the equator finally merging with each other to form a single hump at the equator.

15. The ratio of reflection coefficients for the ordinary and the extra-ordinary partially reflected echoes from the lower ionosphere is close to unity near the equator at all altitudes. For a given altitude the ordinary mode reflection coefficient decreases with increase of latitude while the reverse is the case for the extraordinary coefficient.

4. VERTICAL INCIDENCE ABSORPTION MEASUREMENTS AT URBANA

4.1 Introduction

One of the major interests of the Aeronomy Laboratory of the University of Illinois has been to perform *in situ* measurements of ionospheric parameters using rocket payloads. The number of rockets that could possibly be available for this purpose is, however, limited and it is essential to link the results so obtained with those from ground-based measurements spread over long periods. Several experiments have therefore been started at a field site in Urbana (40° 10' 03" N; 88° 09' 32" W) developed close to the University of Illinois. One of the earliest of these has been the measurement of ionospheric absorption of radio waves using vertical incidence transmissions.

Routine absorption measurements were commenced in June 1966, using an automatic recording system developed in the laboratory. Several aspects of absorption measurements are being investigated, including the short and long term variations. The analysis of the data is by no means complete at this stage and only a few of the preliminary results are presented in the following. One of the main objectives in doing so is to bring out some of the peculiarities associated with these measurements when an operating frequency close to the noon critical frequency of the E region was chosen for the observations. Finally, some of the plans for the future work in absorption measurements are briefly discussed.

4.2 Automatic Recording of Ionospheric Absorption

The A1 type of measurements of ionospheric absorption using ground-based transmissions would rely normally on some method of recording the amplitudes of the echoes reflected from the ionosphere. The manual method of noting the amplitudes at regular, short intervals is very tedious. Alternatively, the

echo amplitudes could be photographed successively and scaled at a convenient time. Such a method of recording had been employed during the measurements on board the USNS Croatan, results of which were described in Chapter 2.

The method of recording has proved extremely cumbersome and is not practicable for routine type of work. An automatic absorption recording system has therefore been designed and constructed in the laboratory. In essence, the system measures the mean amplitudes of the desired echoes. It employs a feedback system such that the signal applied to the receiver AGC bus point is linearly proportional to the difference between the mean echo amplitude and a fixed reference voltage. The receiver AGC characteristics being approximately logarithmic, the AGC voltage is proportional to the absorption level and can be recorded using a pen recorder. The design and other considerations regarding the system have been dealt with adequately by Appel and Bowhill (1965) and will not be discussed further here.

The frequency of operation was chosen to be 3.0 MHz from the commencement of the experiment until January 1967, at which time it was altered to 2.66 MHz. The equipment used for absorption measurements is also being utilized for partial reflection recording from lower altitudes on both modes of polarization. The recent change in the frequency was mainly to comply with the requirements of the partial reflection experiment.

The choice of 3.03 MHz for the earlier operation was made to investigate mainly the E region of the ionosphere. During the course of these measurements the daytime E layer critical frequencies have not remained too far off from the operating frequency of 3.03 MHz. When the experiment was initiated it was felt that a study of the absorption characteristics using this frequency for operation would give a better insight into the variations of the deviative component of absorption. As will be seen in the following these expectations have been realized to a large extent.

The equipment and method used for the recording are similar to those described in Chapter 1 for studies at Wallops Island. Only a few alterations made over the previous system are noted in the following. The changes have been incorporated mainly to improve the stability of the equipment and the reading accuracy of the recording system.

In the new system the receiver power supply is fed from a constant voltage transformer thus minimizing the line voltage fluctuations. The high wattage requirements have not permitted the use of a similar device for the transmitter power supplies. However the changes taking place in the RF output level of the final amplifier used in the transmitter are noted fairly frequently and are taken care of while estimating the absolute value of absorption.

The transmitter uses a pulse repetition frequency of 5 cps at which rate it is found to give the best stability of operation. The 3.03 MHz measurements were made earlier using a 30 cps pulse rate. The frequency of arc-overs in the final stage of the transmitter has been found to have reduced considerably following the changeover in the duty cycle. The transmitter is operated usually with a 50 μsec pulse-width and realizes peak powers of the order of 25-35 kw.

The final recording of the echo amplitudes is made using a Varian Recorder with a 16 cm wide chart paper. The changeover from a 6.5 cm wide Amprobe recording to the new one has greatly improved the reading accuracy of the system. Use of field effect transistors in the final amplifier stage has linearized the dB scale to a large extent. The dynamic range of the recording system has also been increased to 55 dB. This has greatly reduced the necessity of controlling manually the external attenuator settings in the receiving system.

Provision has been made to calibrate the receiving system to a large extent automatically. Once every hour or so the receiving antenna is disconnected from the receiver and is replaced by a standard signal generator. An automatic switching sequence then introduces pre-set values of attenuation in the system. This calibrates the receiving system in terms of a standard signal level. The overall system gain is calibrated according to the standard procedure using the one-hop and two-hop echoes from the ionosphere. Limited gain of the system prevents use of this method to periods when the ionospheric absorption is fairly low. To overcome this difficulty nighttime observations are made once a week at a time when the ionospheric absorption is negligibly small. An equipment constant is then derived as noted in Chapter 1 using the first and second order echoes. The constant is then used at other times of the day when only the first order reflections are present.

An aerial system common to both receiver and transmitter was used previously for the 3.03 MHz operation. The system was similar to that described in Section 1.4. Since then a much larger antenna system has been constructed for the 2.66 MHz operation. In this system the receiving and transmitting aerials are isolated from each other. Each system consists of a total of 60 dipoles. Half of these are arranged in 6 rows, each row consisting of 5 half-wavelength dipoles. The alternate half-wavelengths are folded to give the proper current distribution over the entire array. Each system of aerials is mounted on 40 poles, each pole being 70' in height. An identical system of dipoles is mounted at right angles to each of the two arrays described earlier. Circular polarization of desired polarity is achieved then by introducing a phase lag of 90° in one of the array systems before mixing its output with that of the corresponding array mounted in space quadrature with it. The antenna system has an overall estimated gain of 40 dB over a single dipole and

an average beam-width of the order of 14° at half power points. The system described above is constructed mainly to obtain adequate gain on the partially reflected echoes from the lower ionosphere mentioned earlier. The absorption recordings on the E-region echoes, however, have been greatly improved due to the improved antenna design described above.

The absorption measurements are conducted on the ordinary mode of propagation alone. The recordings of amplitudes are made on a routine basis during the sunlit hours on week days. The scaling procedure followed is identical to that noted in Section 1.4. The median values of absorption are then computed for successive 10-minute intervals by noting the corresponding median chart reading and by using the equipment constant derived from the nighttime observations mentioned earlier.

4.3 Deviative and Nondeviative Absorption Components

One of the major difficulties in the interpretation of absorption measurements using a single frequency of operation is the separation of absorption in the different ionospheric regions. The problem has been solved to a certain extent in the present study by plotting the measured absorption as a function of the virtual height of reflection of the echoes. The absorption characteristics of the different ionospheric regions being different from each other the data points group themselves in different regions on the plot, thereby permitting a method of identifying the various regions. A few plots of data illustrating the points made above are shown in the next few diagrams. In Figure 4.1 the absorption values for each 10-minute interval during 0900 to 1300 hours CST have been reproduced for several days in October 1966. The data are for 3.03 MHz and correspond to a solar zenith angle variation between 50° to 60°.

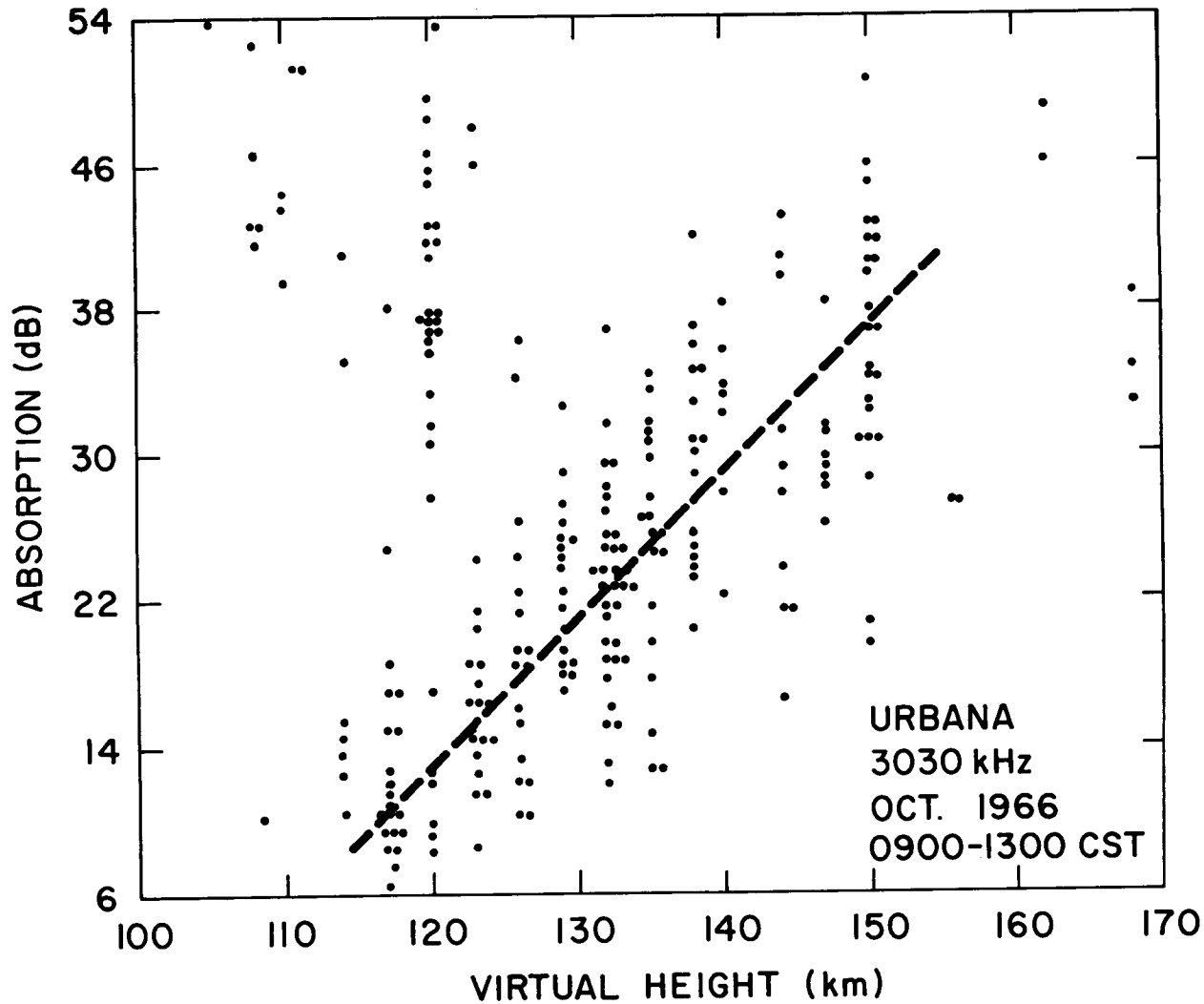

Figure 4.1 Plot of ionospheric absorption versus virtual height for October 1966. Each point refers to median value of absorption for a ten minute interval.

The bulk of the points are seen to fall in a zone crossing the plot diagonally. A dashed line has been drawn through these points for easy identification. In spite of the large scatter of data points a clear trend of increase in absorption with increase in virtual height is noticeable in this zone. The data points falling in this category are to be recognized as due to total reflection from a normal E layer. This, however, does not exclude the possibility of total reflections from the blanketing type sporadic E (Es) layer on some occasions. In fact the associated deviative absorption for this type of reflection is expected to be very low and the total absorption observed on such instances would then be also low. Some of the very low values of absorption observed in the mass plot are possibly due to this type of reflection.

Below a virtual height of 110 km the absorption is observed to be low. Above this level a good correlation is observed between the virtual height and the absorption values. This suggests that the varying component of absorption is associated some way with the increase in the virtual height of reflection of the echo. Changes in the virtual height could be due either to a change in the true height of reflection of the echo or due to a group retardation setting in close to the level of reflection. The question arises as to whether the bulk of the absorption seen varying with the virtual height is nondeviative or deviative in nature. The answer to this question has been attempted in the following.

The dashed line shown in Figure 4.1 gives the median distribution of absorption as a function of virtual height. The slope of this line is seen to be close to 0.8 dB per km. Knowing that the absorption at altitudes around 100 and above is proportional to the product of electron number density and electron collision frequency, the collision frequency required to give the

above gradient of absorption can be computed. For electron densities corresponding to 3.03 MHz the required collision frequency would be 2.7×10^4 collisions per second. The various models for the collision frequency available from rocket measurements indicate that a collision frequency of this order appears around 101 $\pm$ 3 km. With increasing altitude the collision frequency falls fairly rapidly. If the absorption were to be nondeviative then the vertical gradient of absorption would decrease with increase of altitude above a certain height. This is so because the increase in electron density with altitude is not as rapid as the corresponding decrease in collision frequency above a certain altitude. Normally the altitude at which the transition occurs is around 95 km as seen in Figure 1.8. Alternatively, for a given true height the deviative absorption would increase linearly with increase in group retardation giving a constant gradient of absorption per km of virtual height.

In Figure 4.1 the slope of the curve giving median absorption is observed to be, moreover, constant throughout the range of virtual heights shown. In view of the preceeding discussion then it can be concluded that the variable part of the observed absorption is mainly deviative in nature. Further, the observed gradient of absorption corresponds to an altitude region close to 101 km. Therefore the level at which the group retardation is taking place can be considered to be close to this altitude region.

The large scatter observed in the distribution of absorption values can be attributed partly to changes in the true level of reflection of the waves from the median value shown on some occasions. It is also probable that on occasions large nondeviative type attenuation sets in at altitudes below the true level of reflection. An intervening sporadic E layer can as well

introduce a further scatter in the data points. None of these causes, however, can explain the observed large vertical gradient of absorption with virtual height which has been attributed above to the deviative cause.

It would be recalled (Figure 1.4) that the observed vertical gradient of absorption at Wallops Island during an earlier set of measurements on the same operating frequency of 3.03 MHz was as low as 0.15 dB per km. Local measurements made during other periods also show gradients which are not always identical to that observed in Figure 4.1. This suggests that the level at which the deviative absorption sets in for a given frequency, undergoes variations with time and location. Using the technique discussed above it should be possible to keep track of these changes. Alternatively however, if the electron density distribution is known fairly accurately close to the level of reflection of the waves then it should be possible to determine the collision frequency of electrons in this region. A knowledge of the absorption and group retardation close to the level of reflection would be required for this purpose. A J5W ionosonde has been installed recently at the site of the absorption experiment. A true height analysis of ionograms should reveal the height of reflection at the operating frequency used for the absorption measurements as also the associated group retardation. It is planned that coordinated absorption measurements would be made in the near future to evaluate the collision frequency of electrons using the above technique.

4.4 Reflection Coefficient of Sporadic E (Es) Layer

In Figure 4.1 a group of data points are seen in the upper left hand corner of the plot. These correspond in fact to a reflection from the Es layer. The cluster of points in this region is shown better in Figure 4.2 wherein a mass plot has been shown for data during the four hours around

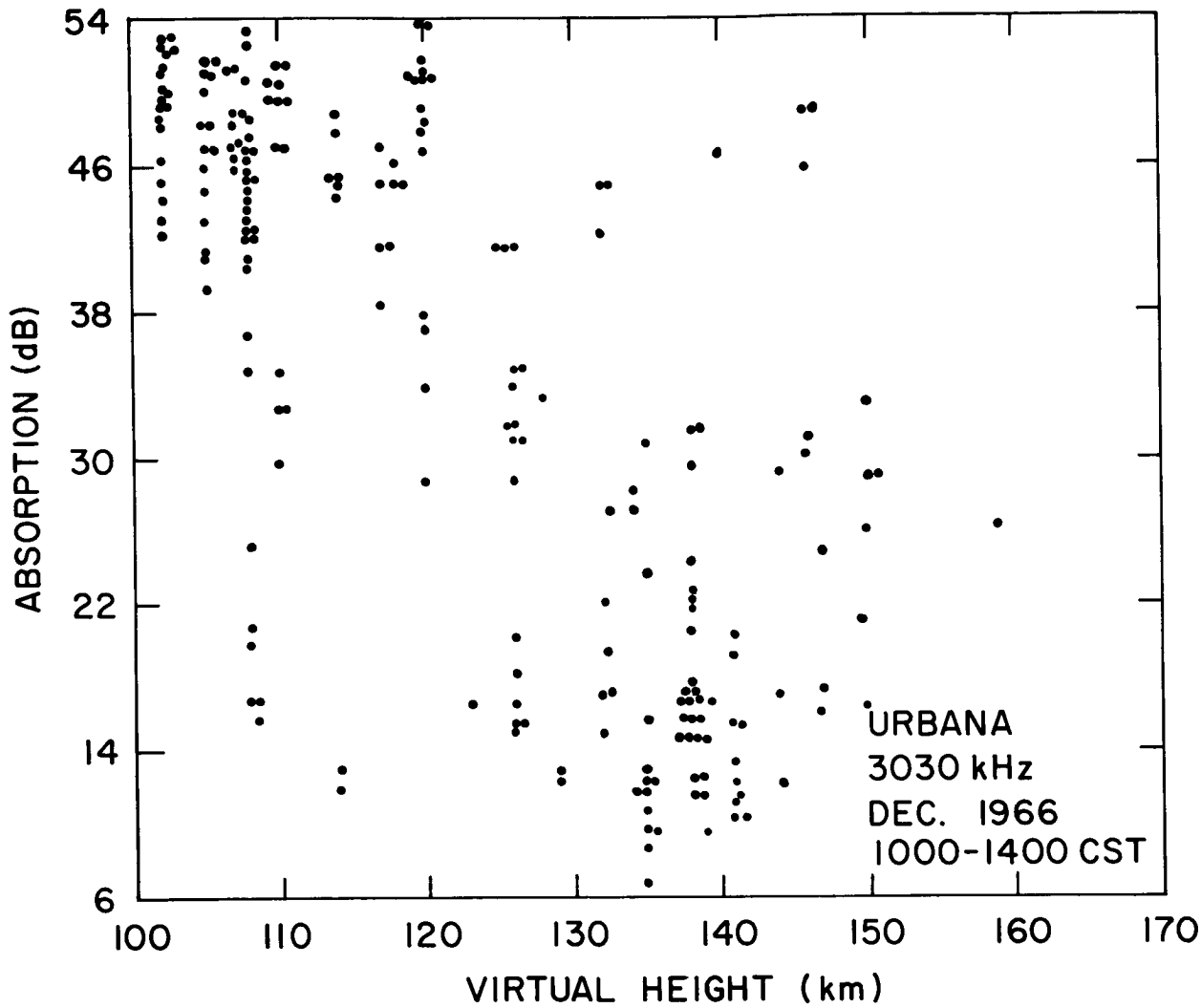

Figure 4.2 Ionospheric absorption on 3.03 MHz as a function of virtual height for December 1966. Cluster of points on top left hand corner correspond to Es level reflection.

noon in December 1966. The data points pertaining to the partial reflections from the Es layer are characterized by high values of absorption and are restricted usually to virtual heights less than 125 km. The occurrence frequency of Es is considerably larger in December than in October. The scatter seen in both months in the values of absorption might be due partly to changes in the absorption below the Es level from time to time, and partly to changes in the reflection coefficient of the Es layer itself.

The median value of absorption in December is seen to be around 48 dB corresponding to the Es type reflection. In Section 1.5 the normal winter noontime absorption corresponding to a virtual height of 110 km is shown to be close to 11 dB. Subtracting this from the total absorption, a remainder of close to 37 dB can be attributed to the partial nature of Es type reflection. This corresponds to a reflection coefficient of 0.015 as the median value.

In October the number of data points corresponding to the Es type reflection is very low. The median value of absorption for these points is about 5 dB less than in December giving a reflection coefficient of close to 0.06. The range of variability of Es reflection coefficient can be estimated from the data presented and from the data in other months to be from 0.009 to .01 with a median value around 0.015.

With the large amount of scatter in the data it is difficult to pick out the diurnal variation in the reflection coefficient of the Es layer. Attempts are continuing to investigate the diurnal and seasonal change in the reflection coefficient.

4.5 Evidence of 'Winter Anomaly' in Urbana

In Figure 4.3 is shown the mass plot of absorption against the virtual height for the summer months July and August 1966. The plot is characterized

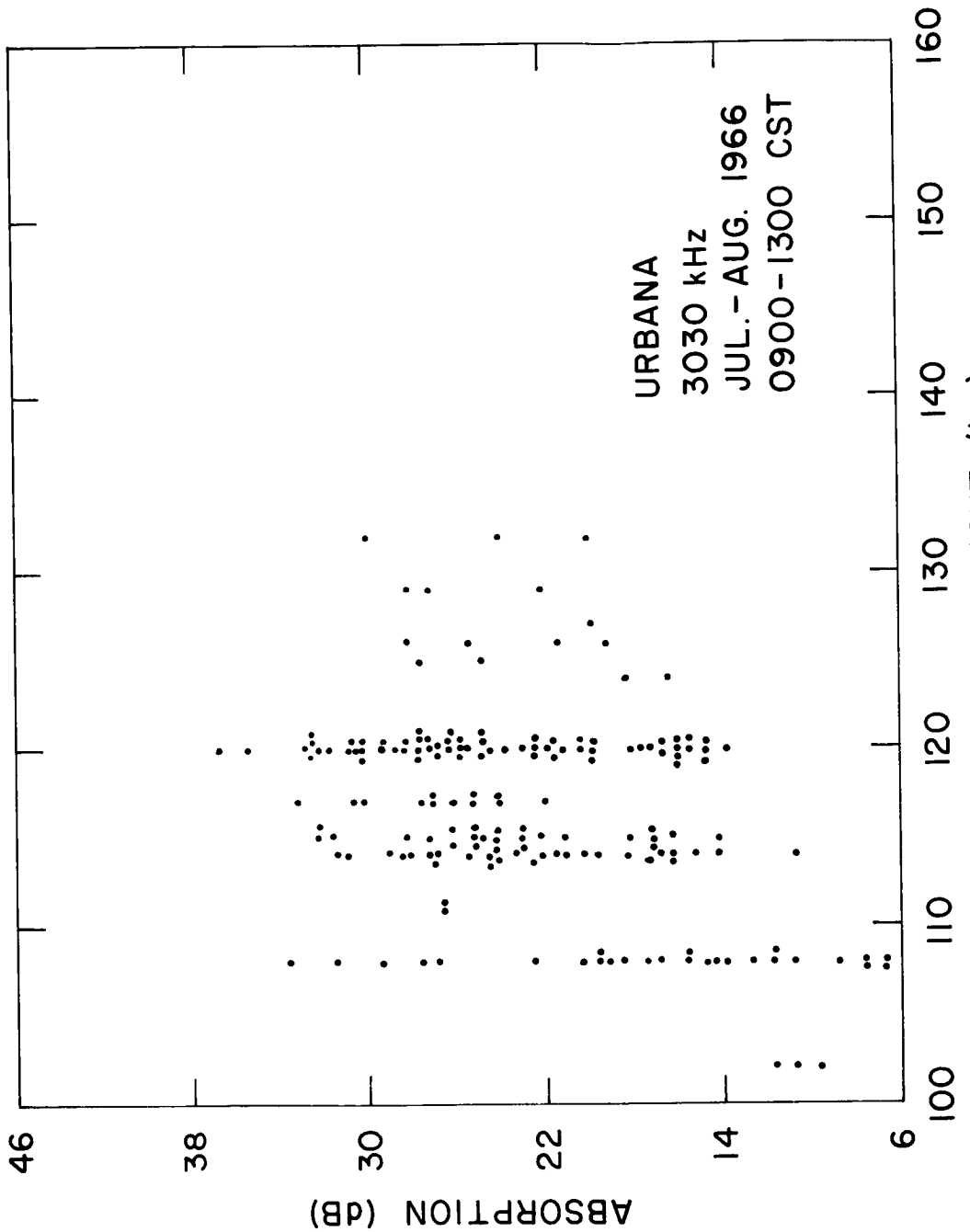

Figure 4.3 Absorption on 3.03 MHz versus virtual height for July and August 1966.

by a complete absence of Es type reflection. The scatter in the data points still persists, indicating that the scatter observed in other months as well could not have been solely due to intervening Es layer.

A comparison of Figures 4.2 and 4.3 indicates the presence of abnormally large absorption values on some days in December, corresponding to a whole range of virtual heights. These are in fact to be identified with the winter anomaly phenomena which is the subject of Chapter 1. The complete absence of this type of phenomena in the summer plot confirms the winter origin of this phenomena. With more data of this kind it would be feasible to undertake a detailed study involving the occurrence frequency, amplitude of excess absorption, diurnal variation of excess absorption etc. during the anomalous winter days. In view of the rather elaborate treatment on this topic in Chapter 1 the subject will not be discussed further here.

4.6 Diurnal and Seasonal Variation of Absorption

In order to study the diurnal and seasonal variation of absorption the following procedure has been adopted. Since the absorption has been varying so much in some months with the virtual height, the monthly data has been subdivided in successive 10 km virtual height intervals above 95 km. The median absorption values are then computed for each height interval for data points during successive one-hour periods.

In Figure 4.4 are shown some results of this analysis wherein the hourly median values of absorption are plotted as a function of the cosine of the solar zenith angle. The data corresponds to virtual height intervals between 115 to 125 and 125 to 135 km for the months July, August, September and October 1966. Logarithmic scales have been used on either axis. As noted in Chapter 1, the slope of the line joining the points corresponding to a given period would give the index of diurnal variation of absorption for that period.

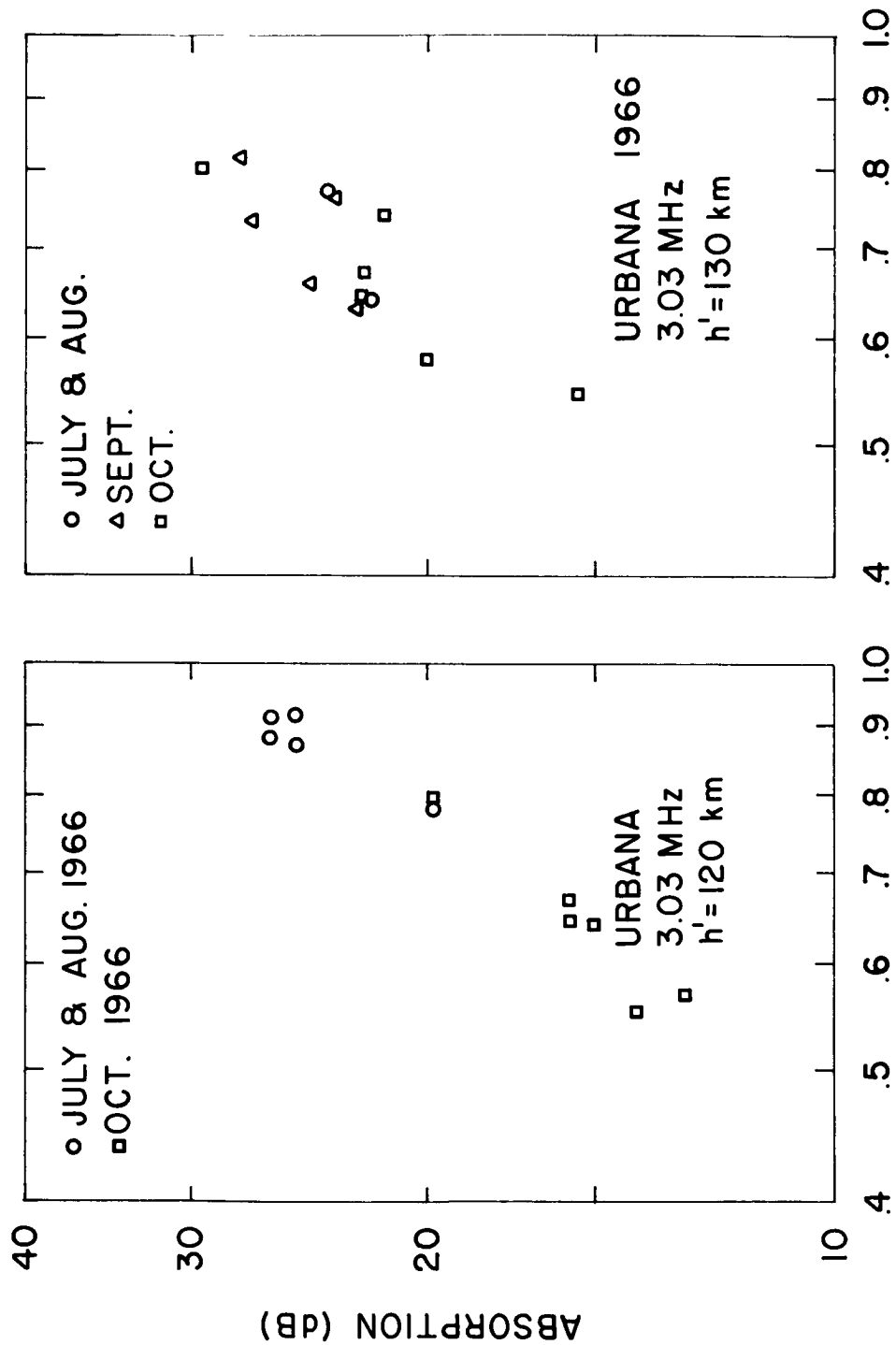

Figure 4.4 Absorption as a function of solar zenith angle corresponding to virtual height intervals 115 to 125 and 125 to 135 km.

In the plots shown the hourly data gets subdivided in so many height intervals that it has not always been possible to obtain a sufficient number of observations to give a statistically significant median value of absorption. For this reason only those points are shown for which the observation count is larger than 10. The range of solar zenith angles over which the analysis could be made is restricted considerably due to the choice of the operating frequency. For large solar zenith angles the E layer critical frequency decreases below the operating frequency of the absorption experiment and the conditions at the level of reflection of the waves change drastically. With the few data points available it is hard to draw continuous curves showing the diurnal variation. The scatter in the data points is also very large. Accurate determination of the indices is therefore not possible. The best fitting lines not shown in the diagram however give values for the diurnal index of absorption ranging from 1.5 to 2 for the different months shown for each of the two height intervals. The seasonal variation is seen to be of the same order as that of the diurnal variation since the curves corresponding to individual months are overlapping each other when extrapolated to cover identical ranges of the solar zenith angle.

Appleton and Piggott (1954) have given an index of variation close to 0.75 both for the diurnal and seasonal variation of absorption at a mid-latitude station. The large values of the indices noted above in the present case could possibly be explained on the basis of the variation in the true height of reflection of the echoes as a function of the solar zenith angle. A decrease in the true height of reflection corresponding to a decrease in the solar zenith angle would give more absorption per km of the virtual height transversed. For a given range of virtual heights then the absorption would

increase as the true height decreases. In essence then the indices are larger because of the predominantly deviative nature of the observed absorption.

4.7 Observations on 2.66 MHz

As noted earlier the frequency of operation has been changed to 2.66 MHz since February 1967. It is not intended to present the results of these measurements here. The change of frequency however has permitted elimination of certain effects dominant in the earlier frequency operation. With the lowering in the altitude of reflection of the echo the effects of the intervening Es layer are relatively less as also of the closeness of the critical frequency of the E region. For noon data the relative roles of the deviative and nondeviative components of absorption appear therefore to have been reversed on the lower frequency when compared to that on 3.03 MHz operation. With an increase in the E layer critical frequency with an increase in the sunspot number the nondeviative component is expected to accentuate still further and it would be interesting to follow the changes in the same as they occur.

4.8 Plans for Future Absorption Measurements

Several aspects of absorption measurements have been discussed so far. Some of the problems of interest are the reflection and transmission coefficient of the Es layer, the estimation of the level of optimum absorption and the associated determination of electron collision frequency. It would be worthwhile to know the long and short term variations of the collision frequency and electron density at specific altitudes in the ionosphere as also the precise determination of the deviative absorption with altitude. The use of a single frequency in making these measurements often leaves the interpretation of the results ambiguous. It is planned therefore to make absorption measurements on several frequencies on a routine basis. The frequencies chosen are

2030, 3030, 4030, 5030, 6030 and 8030 kHz. Efforts are underway to obtain the requisite authorization to operate on these frequencies. Provision is also being made to make the recording system more automatic by incorporating a device-making automatic recording of the virtual height of reflection alongside the amplitude measurements.

As has been noted earlier, an ionosonde has been installed at the site of operation of the absorption experiment. Provision has been made to use the ionosonde on fixed frequency modes so as to record the absorption on the frequencies listed above using some kind of a sequential programming. In order to cover the large range of frequency variation in a single receiver a new IF amplifier has been designed and constructed by the engineering personnel of the laboratory. A 1.0 MHz center frequency has been used for the amplifier. A tunable "front end" for the IF unit has also been designed consisting of two portions, one covering the 2.0 to 4.0 and the other, 4.0 to 8.0 MHz operation.

In addition to the various aspects of ionospheric absorption measurements listed above it would be interesting to study the frequency dependence of ionospheric absorption. It was pointed out in Chapter 3 that the classical formula giving an inverse square dependence of ionospheric absorption needs revision in view of the analysis undertaken using the generalized magnetoionic formulas. It would be of interest therefore to test the theory using measurements on some of the frequencies noted above.

The absorption on the larger frequencies listed will be relatively very low. However the purpose of making measurements on these frequencies is governed by a separate motive. With increasing altitude the electron-neutral particle collision frequency diminishes fairly rapidly and becomes very small by 140 km. Alternatively, however, the electron-ion collision frequency (ν_{ei})

becomes dominant as the altitude of maximum electron density in the F region is approached. Nicolet (1959) has given the following expression for the frequency

$$\nu_{ei} = [34 + 4.18 \log (T_e^3/N)]\, n_i/T_e^{3/2} \qquad (4.1)$$

wherein T_e is the electron temperature

N the electron number density

N_i the number density of ions.

At present the local F-region critical frequencies are approaching 10 MHz at noon. The curves for electron temperatures with altitude derived from ground-based backscatter radar measurements (private communication J. V. Evans 1967) suggests an electron temperature of close to 2400° K at noon at local latitudes. Calculations based on the above formula gives an electron-ion collision frequency of 533 collisions per second close to the level of maximum electron density noted above. This corresponds to a nondeviative absorption of 0.3 dB per km up and down path close to the level of reflection for an operating frequency of 10 MHz. This rate of absorption is normally encountered in the D region near 90 km level and is by no means negligible. It should be possible to record this order of absorption using some of the larger frequencies on which measurements are planned in the future. The multifrequency measurements in conjunction with the true height analysis of ionograms would then lead to the electron temperatures in the F region which are of considerable aeronomic interest.

Several aspects of ionospheric absorption measurements have been considered above. It is hoped that the continuation of the work as planned will go a long way in clearing up many of the unsolved problems of ionospheric absorption variations at middle latitudes.

APPENDIX I

Computer 7094 program for solving the generalized magnetoionic formulas for ordinary and extraordinary propagation. The program is not applicable for purely transverse or purely longitudinal propagation.

```
      DIMENSION A(55,3)
C     FRE= FREQUENCY IN MZ
C     ALTITUDE 75 KM. A(I,2)=COLLISION FREQ. A(I,3)= ELECTRON DENSITY
      C32F(X)=(X*(X*(X*(X+A1)+A2)+A3)+A4)/
     1 (X*(X*(X*(X*(X*(X+B1)+B2)+B3)+B4)+B5)+B6)
      C52F(X)=(X*(X*(X+D1)+D2)+D3)/(X*(X*(X*(X*(X+E1)+E2)+E3)+E4)+E5)
      RIT 7, 1C, A1,A2,A3,A4,B1,B2,B3,B4,B5,B6,D1,D2,D3,E1,E2,E3,E4,E5
   10 FORMAT (2X, 6E13.7)
      N=55
      DC11 I=1,N
      AAI=I
   11 A(I,1)=AAI+55.0
      RIT7,12,(A(I,2),I=1,N)
   12 FCRMAT (3X, 7E11.5)
      DO 13 I=1,N
   13 A(I,2)=A(I,2)*(6.74E+5)
      RIT7,14,(A(I,3),I=1,N)
   14 FCRMAT(3X,7E11.5)
      WCT6,8
    8 FORMAT(82H1                              HEIGHT IN KM      COLLISION FRE
     1QUENCY    ELECTRON DENSITY       )
      WCT6,20,(A(I,1),A(I,2),A(I,3),I=1,N)
   20 FORMAT(20X,2P3E20.5)
   15 RIT 7,16, ALAT,ALONG, DIP, S
   16 FORMAT (4F10.4)
      WOT6,18, ALAT,ALONG,DIP,S
   18 FORMAT(16H1      LATITUDE=,F8.2,5X,11H LONGITUDE=,F8.2,5X,
     1 16H DIP IN DIGREES=,F10.4,5X,22H GYRO FREQUENCY IN MZ=,F10.4  )
      WCT6,9
    9 FORMAT(1C7HO              HEIGHT IN KM      ABSORPTION DB ORD  ABSO
     1RPTION DB EXT.     REF. INDEX ORD      REF. INDEX EXT.      )
      ABSC1=0.0
      ABSX1=0.C
      ABSC2=0.C
      ABSX2=0.C
      SIP=ABSF(DIP)
      CN=SIN(SIP/57.294)
      SN= SQRT (1.0-CN**2)
      DO37 I=1,55
      FRE=3.0
      X1=(6.2832E+6)*FRE/A(I,2)
      X2=(6.2832E+6)*(FRE+S)/A(I,2)
      X3=(6.2832E+6)*(FRE-S)/A(I,2)
      W=506.8*A(I,3)/(FRE*A(I,2))
```

```
      AB=X1*C32F(X1)*W
      BA=2.5*C52F(X1)*W
      C=X3*C32F(X3)*W
      D=2.5*C52F(X3)*W
      E=X2*C32F(X2)*W
      F=2.5*C52F(X2)*W
      E1R= 1.0-AB
      E1I=-BA
      E2R=0.5*(F-D)
      E2I=0.5*(C-E)
      E3R=AB-0.5*(C+E)
      E3I=BA-C.5*(F+D)
      PR=2.*(E1R*(E1R+E3R)-E1I*(E1I+E3I))
      PI=2.*(E1I*(E1R+E3R)+E1R*(E1I+E3I))
      QR=E3R*(E1R+E3R)-E3I*(E1I+E3I)+E2R**2-E2I**2
      QI=E3I*(E1R+E3R)+E3R*(E1I+E3I)+2.*E2R*E2I
      CR=F-D-AB*F+AB*D+BA*C-BA*E
      CI=C-E-AB*C+AB*E+BA*D-BA*F
      DR=2.0-2.0*AB
      DI=-2.0*BA
      ER=2.0*AB-C-E
      EI=2.0*BA-F-D
      GR=(QR**2-QI**2)*SN**4-(CR**2-CI**2)*CN**2
      GI=2.0*QR*QI*SN**4-2.0*CR*CI*CN**2
      RR=0.70710678*SQRT(GR+SQRT(GR**2+GI**2))
      RI=GI/(2.0*RR)
      Z1=PR+QR*SN**2+RR
      Z2=PI+QI*SN**2+RI
      Y1=CR+ER*SN**2
      Y2=CI+EI*SN**2
      Z3=PR+QR*SN**2-RR
      Z4=PI+QI*SN**2-RI
      DN=Y1**2+Y2**2
      ZRC=(Z1*Y1+Z2*Y2)/DN
      ZIC=(Z1*Y2-Z2*Y1)/DN
      ZRX=(Z3*Y1+Z4*Y2)/DN
      ZIX=(Z3*Y2-Z4*Y1)/DN
      T1=SQRT(ZRC**2+ZIC**2)
      T2=SQRT(ZRX**2+ZIX**2)
      IF(ZRX+T2)25,25,26
25    RKX=0.0
      AKX=0.0
      GO TO 27
26    RKX=0.70710678*SQRT(ZRX+T2)
      AKX= 181.9166*ZIX*FRE/RKX
27    IF(ZRC+T1)28,28,29
28    RKC=0.0
      AKC=0.0
      GO TO 30
29    RKC=0.70710678*SQRT(ZRC+T1)
      AKC=181.9166*ZIC*FRE/RKC
30    WOTE,31,A(I,1),AKC,AKX,RKC,RKX
31    FORMAT(1CX,5E20.8)
      IF(RKC-C.8)33,32,32
32    ABSC1=ABSC1+AKC
      GO TC 34
```

```
   33    ABSC2=ABSC2+AKO
   34    IF(RKX-0.8)36,35,35
   35    ABSX1=ABSX1+AKX
         GO TO 37
   36    ABSX2=ABSX2+AKX
   37    CONTINUE
         WRITE(6,38)ABSO1,ABSX1
   38    FORMAT(30HO       TOTAL ABSORPTION DB     ,E20.8,E20.8)
         WRITE(6,39)ABSO2,ABSX2
   39    FORMAT(30X,2E20.8)
         GO TO 15
         END
```

APPENDIX II

The following values in computer notation dervied from Burke and Hara (1963), have been used as input to the computer programs.

A1 = 2.4653115E + 1
A2 = 1.1394160E + 2
A3 = 1.1287513E + 1
A4 = 2.3983474E - 2

B1 = 2.4656819E + 1
B2 = 1.2049512E + 2
B3 = 2.8958085E + 2
B4 = 1.4921254E + 2
B5 = 9.3877372E + 0
B6 = 1.8064128E - 2

D1 = 6.6945939E + 0
D2 = 1.6901002E + 1
D3 = 1.1630641E + 0

E1 = 6.6314497E + 0
E2 = 3.5355257E + 1
E3 = 6.8920505E + 1
E4 = 6.4093464E + 1
E5 = 4.3605732E + 0

A typical set of electron density and electron collision frequency values used in the program.

HEIGHT IN KM	COLLISION FREQUENCY	ELECTRON DENSITY
56.CCCCCE 00	25.34914E 06	57.5CC00E-01
57.CCCCCE 00	22.20156E 06	91.8C000E-01
58.CCCCCE 00	19.41794E 06	10.6CCCCE 00
59.CCCCCE 00	16.96458E 06	12.80CCCE 00
6C.CCCCCE 00	14.7943CE 06	14.9CCCCE 00
61.CCCCCE 00	12.88014E 06	18.10CCCE 00
62.CCCCCE 00	11.20188E 06	20.1CCCCE 00
63.CCCCCE 00	97.25820E 05	23.9CCCCE 00
64.CCCCCE 00	84.25CC0E 05	15.0CCCCE 00
65.CCCCCE 00	72.92680E 05	13.5CCCCE 00
66.CCCCCE 00	63.01226E 05	18.1CCCCE 00
67.CCCCCE 00	54.34462E 05	24.7CCCCE 00
68.CCCCCE 00	46.79582E 05	29.2CCCCE 00
69.CCCCCE 00	4C.22432E 05	29.2CCCCE 00
7C.CCCCCE 00	34.5088CE 05	29.7CCCCE 00
71.CCCCCE 00	29.54816E 05	35.CCCCCE 00
72.CCCCCE 00	25.24804E 05	45.CCCCCE 00
73.CCCCCE 00	21.52082E 05	58.6CCCCE 00
74.CCCCCE 00	18.29910E 05	73.6CCCCE 00
75.CCCCCE 00	15.52896E 05	84.9CCCCE 00
76.CCCCCE 00	13.143C0E 05	94.1CCCCE 00
77.CCCCCE 00	11.09404E 05	90.7CCCCE 00
78.CCCCCE 00	93.41640E 04	84.9CCCCE 00
79.CCCCCE 00	78.45360E 04	90.7CCCCE 00
8C.CCCCCE 00	65.68130E 04	10.1CCCCE 01
81.CCCCCE 00	54.92426E 04	10.1CCCCE 01
82.CCCCCE 00	45.92636E 04	11.5CCCCE 01
83.CCCCCE 00	38.41126E 04	26.8CCCCE 01
84.CCCCCE 00	32.12284E 04	31.7CCCCE 01
85.CCCCCE 00	26.86564E 04	67.0CCCCE 01
86.CCCCCE 00	22.47116E 04	13.8CCCCE 02
87.CCCCCE 00	18.79786E 04	21.2CCCCE 02
88.CCCCCE 00	15.72442E 04	30.6CCCCE 02
89.CCCCCE 00	13.15648E 04	42.CCCCCE 02
90.CCCCCE 00	11.00642E 04	66.3CCCCE 02
91.CCCCCE 00	92.20320E 03	77.CCCCCE 02
92.CCCCCE 00	77.44260E 03	84.9CCCCE 02
93.CCCCCE 00	65.19602E 03	12.4CCCCE 03
94.CCCCCE 00	55.02536E 03	15.CCCCCE 03
95.CCCCCE 00	46.55318E 03	19.5CCCCE 03
96.CCCCCE 00	39.47618E 03	26.CCCCCE 03
97.CCCCCE 00	33.55172E 03	33.CCCCCE 03
98.CCCCCE 00	28.57760E 03	40.CCCCCE 03
99.CCCCCE 00	24.39206E 03	46.5CCCCE 03
1C.CCCCCE 01	20.86C30E 03	56.2CCCCE 03
10.1CCCCE 01	17.89470E 03	60.3CCCCE 03
10.2CCCCE 01	15.4C090E 03	70.5CCCCE 03
10.3CCCCE 01	13.30476E 03	82.2CCCCE 03
10.4CCCCE 01	11.52540E 03	91.CCCCCE 03
10.5CCCCE 01	10.01564E 03	97.6CCCCE 03
10.6CCCCE 01	87.35C40E 02	94.8CCCCE 03
10.7CCCCE 01	76.36420E 02	86.2CCCCE 03
10.8CCCCE 01	66.92820E 02	94.2CCCCE 03
10.9CCCCE 01	58.81998E 02	99.8CCCCE 03
11.CCCCCE 01	51.83C60E 02	10.6CCCCE 04

A typical output from the computer corresponding to a station located at 75° N, 75° E. The computer program fails once, extremely low values of refractive indices are reached. Very large values of absorption per km noted at 100 km and above are not genuine.

LATITUDE= 75.00 LONGITUDE= 75.00 DIP IN DEGREES= -80.2951 GYRO FREQUENCY IN MZ= 1.5417

HEIGHT IN KM	ABSORPTION DB ORD	ABSORPTION DB EXT.	REF. INDEX ORD	REF. INDEX EXT.
.55999999E 02	.11144035E-01	.69657046E-02	.99999637E 00	.99999508E 00
.56999999E 02	.19625494E-01	.11611083E-01	.99999299E 00	.99999104E 00
.58000000E 02	.24906244E-01	.13878819E-01	.99999022E 00	.99998824E 00
.59000000E 02	.32907747E-01	.17188301E-01	.99998583E 00	.99998402E 00
.59999999E 02	.41717222E-01	.20318866E-01	.99998028E 00	.99997921E 00
.61000000E 02	.24801130E-01	.54879835E-01	.99997198E 00	.99997148E 00
.62000000E 02	.27365371E-01	.65552336E-01	.99996579E 00	.99996255E 00
.63000000E 02	.31952622E-01	.83230790E-01	.99995565E 00	.99994764E 00
.63999999E 02	.19449417E-01	.55332548E-01	.99996992E 00	.99996161E 00
.65000000E 02	.16768087E-01	.52250525E-01	.99997101E 00	.99995998E 00
.66000000E 02	.21263038E-01	.72768836E-01	.99995873E 00	.99993835E 00
.66999999E 02	.27095050E-01	.10202407E 00	.99994069E 00	.99990419E 00
.68000000E 02	.29541953E-01	.12244338E 00	.99992675E 00	.99987222E 00
.69000000E 02	.26920947E-01	.12272375E 00	.99992400E 00	.99985725E 00
.70000000E 02	.24669620E-01	.12342480E 00	.99992032E 00	.99983945E 00
.70999999E 02	.25917553E-01	.14178258E 00	.99990378E 00	.99979296E 00
.72000000E 02	.29420555E-01	.17507703E 00	.99987382E 00	.99971174E 00
.73000000E 02	.33522774E-01	.21562706E 00	.99983310E 00	.99959763E 00
.73999999E 02	.36546201E-01	.25218255E 00	.99978784E 00	.99946366E 00
.75000000E 02	.36349618E-01	.26679904E 00	.99975302E 00	.99934965E 00
.76000000E 02	.34516187E-01	.26717387E 00	.99972435E 00	.99924883E 00
.77000000E 02	.28340589E-01	.22937197E 00	.99973294E 00	.99925140E 00
.77999999E 02	.22490011E-01	.18877967E 00	.99974907E 00	.99929048E 00
.79000000E 02	.20279437E-01	.17527390E 00	.99973122E 00	.99921530E 00
.80000000E 02	.18975327E-01	.16781301E 00	.99970011E 00	.99911226E 00
.80999999E 02	.15908603E-01	.14316433E 00	.99969969E 00	.99910180E 00
.81999999E 02	.15174344E-01	.13835041E 00	.99965774E 00	.99896848E 00
.83000000E 02	.29627436E-01	.27296488E 00	.99920170E 00	.99757970E 00
.84000000E 02	.29337072E-01	.27225216E 00	.99905526E 00	.99712404E 00
.84999999E 02	.51945642E-01	.48555022E 00	.99800156E 00	.99389281E 00
.86000000E 02	.89725674E-01	.84551428E 00	.99587850E 00	.98735201E 00
.87000000E 02	.11560578E 00	.10974418E 01	.99366034E 00	.98047214E 00
.88000000E 02	.14002128E 00	.13399784E 01	.99083525E 00	.97165628E 00
.88999999E 02	.16140119E 00	.15586600E 01	.98739793E 00	.96085119E 00
.90000000E 02	.21483011E 00	.21130209E 01	.98003055E 00	.93741082E 00
.91000000E 02	.20974971E 00	.20810375E 01	.97676604E 00	.92688109E 00
.91999999E 02	.19475363E 00	.19449200E 01	.97435200E 00	.91902483E 00
.93000000E 02	.24260093E 00	.25031233E 01	.96230546E 00	.87916495E 00
.94000000E 02	.24989165E 00	.26407654E 01	.95420887E 00	.85160109E 00
.95000000E 02	.27920316E 00	.30901378E 01	.94002751E 00	.80162860E 00
.95999999E 02	.32327104E 00	.38816244E 01	.91914781E 00	.72326625E 00
.97000000E 02	.35831667E 00	.48386407E 01	.89610238E 00	.62781873E 00
.98000000E 02	.38080803E 00	.61172414E 01	.87242693E 00	.51462448E 00
.98999999E 02	.38891958E 00	.82578250E 01	.84982631E 00	.37992246E 00
.99999999E 03	.42156453E 00	.20969608E 03	.81486607E 00	.15602953E-01
.10100000E 03	.39670286E 00	.36817845E 03	.79959434E 00	.82211035E-02
.10200000E 03	.42500492E 00	.60546906E 03	.76012162E 00	.51240458E-02
.10299999E 03	.47108906E 00	.80060665E 03	.71162426E 00	.40770387E-02
.10399999E 03	.50669781E 00	.92976484E 03	.67186680E 00	.36503921E-02
.10500000E 03	.55701359E 00	.10303058E 04	.63873624E 00	.36031426E-02
.10600000E 03	.43328004E 00	.98603734E 03	.65329924E 00	.29214106E-02
.10699999E 03	.29645728E 00	.85993633E 03	.69399778E 00	.23488624E-02
.10800000E 03	.32504763E 00	.97731758E 03	.65630912E 00	.22124717E-02
.10900000E 03	.36817668E 00	.10688086E 04	.62648816E 00	.23233479E-02
.11000000E 03	.67575721E 00	.12449272E 04	.58219391E 00	.45641892E-02
TOTAL ABSORPTION DB	.45791420E 01	.23531355E 02		
	.44552270E 01	.91041432E 04		

APPENDIX III

Computer 7094 program applicable to ordinary wave transverse propagation.

```
C       ALTITUDE 75 KM, A(I,2)=COLLISION FREQ. A(I,3)= ELECTRON DENSITY
        DIMENSION A(55,3)
        C32F(X)=(X*(X*(X*(X+A1)+A2)+A3)+A4)/
      1 (X*(X*(X*(X*(X+B1)+B2)+B3)+B4)+B5)+B6)
        C52F(X)=(X*(X*(X+D1)+D2)+D3)/(X*(X*(X*(X*(X+E1)+E2)+E3)+E4)+E5)
        RIT 7, 10, A1,A2,A3,A4,B1,B2,B3,B4,B5,B6,D1,D2,D3,E1,E2,E3,E4,E5
   10   FORMAT (2X, 6E13.7)
        N=55
        DO 111=1,N
        AAI=I
   11   A(I,1)=AAI+55.0
        RIT7,12,(A(I,2),I=1,N)
   12   FORMAT (3X, 7E11.5)
        DO 13 I=1,N
   13   A(I,2)=A(I,2)*(6.74E+5)
        RIT7,14,(A(I,3),I=1,N)
   14   FORMAT(3X,7E11.5)
        D4=C.0
        D5=C.0
        FRE=3.0
        DO 5 I=1,N
        X1=(6.2832E+6)*(FRE/A(I,2))
        W=506.8*A(I,3)/(FRE*A(I,2))
        AB=X1*C32F(X1)*W
        BA=2.5*C52F(X1)*W
        E1R=1.0-AB
        E1I=BA
        T=SQRT(E1R**2+E1I**2)
        IF(E1R+T)3,3,2
   2    RKC=0.70710678*SQRT(E1R+T)
        ZKC=E1I/(2.0*RKO)
        GO TO 1
   3    ZKC=0.70710678*SQRT(-E1R+T)
        RKC=E1R/(2.0*ZKO)
   1    AKC=257.266*FRE*ZKO/0.70710678
        C=(A(I,2)*A(I,3))
        WCT6,4,A(I,1),A(I,2),A(I,3),C,AKO,RKO
   4    FORMAT(10X,6E20.8)
        IF (RKO-0.8)7,6,6
   6    D4=D4+AKO
        GO TO 8
   7    D5=D5+AKO
   8    CONTINUE
   5    CONTINUE
        WCT6,9,D4,D5
   9    FORMAT (90X,E20.8/90X,E20.8)
        CALL SYSTEM
        END
```

REFERENCES

Appel, R. L. and S. A. Bowhill (1965), An automatic recording system for the determination of ionospheric absorption, University of Illinois, Aeronomy Report No. 7.

Appleton, E. V. (1937), Regularities and irregularities in the ionosphere, I, Proc. Roy. Soc. *A162*, 451-479.

Appleton, E. V. (1947), Geomagnetic control of F2 layer ionization, Science *106*, 17.

Appleton, E. V. and W. R. Piggott (1948), Ionospheric absorption measurements throughout a sunspot cycle, General Assembly Proc., International Scientific Radio Union *7*, 320.

Appleton, E. V. and W. R. Piggott (1954), Ionospheric absorption measurements during a sunspot cycle, J. Atmosph. Terr. Phys. *5*, 141-172.

Belrose, J. S. and M. J. Burke (1964), Study of the lower ionosphere using partial reflections, Experimental technique and methods of analysis, J. Geophys. Res. *69*, 2799-2818.

Beynon, W. J. G. and K. Davis (1955), A study of vertical incidence ionospheric abosprtion at 2 mc/s, *The Physics of the Ionosphere--Report of 1954 Cambridge Conference*, Physical Society, London, 40-52.

Beynon, W. J. G. and E. S. O. Jones (1965), Meteorological influences in ionospheric absorption measurements, Proc. Roy. Soc. *A288*, 558-563.

Bowhill, S. A. (1965), IQSY rocket studies of the C, D, and E regions of the ionosphere, NASA-University Program Review Conference, 269-275.

Bowhill, S. A., E. A. Mechtly, C. F. Sechrist and L. G. Smith (1967), Rocket ionization measurements on a winter day of high absorption, *Space Research VII*, ed. R. L. Smith-Rose, North-Holland Publ. Co., Amsterdam, 246.

Bossolasco, M. and A. Elena (1963), Absorption de la couche, D et temperature de la mesosphere, C. R. Acad. Sci., Paris, *259*, 4491-4493.

Budden, K. G. (1961), *Radio Waves in the Ionosphere*, Cambridge University Press, London, 108.

Burke, M. J. and E. H. Hara (1963), Tables of the semiconductor integrals $C_p(x)$ and their approximations for use with the generalized Appleton-Hartree magnetoionic, formulas, DRTE Report No. 1113, Ottawa, Canada.

CIRA (1965), *COSPAR International Reference Atmosphere*, 1965, North-Holland Publ. Co., Amsterdam.

Davies, K. and E. L. Hagg (1955), Ionospheric absorption measurements at Prince Rupert, J. Atmosph. Terr. Phys. *6*, 18-32.

Dieminger, W. (1955), Short wave echoes from the lower ionosphere, Proc. Conf. Phys. Ionosphere, Physical Society, London, 53-57.

Dingle, R. B., D. Arndt and S. K. Roy (1956-57), The integrals $C_p(x)$ and $D_p(x)$ and their tabulation, Appl. Sci. Res. *6* (Sec. B), 245-252.

Eckhouse, R. H. (1964), A Fortran Computer program for determining the earth's magnetic field, Department of Electrical Engineering, University of Illinois (unpublished report).

Evans, J. V. (1967), Private communication.

Fligel, M. D. (1962), On the geographical distribution of ionospheric absorption, Ionospheric Res. *10*, 5-13.

Gardner, F. F. and J. L. Pawsey (1953), Study of the ionospheric D region using partial reflections, J. Atmosph. Terr. Phys. *3*, 321-344.

Gnanalingam, S. and K. Weekes (1955), D-region echoes with a radio wave of frequency 1.4 cm/s, Proc. Conf. Phys. Ionosphere, Physical Society, London, 63-70.

Gnanalingam, S. and P. H. J. Ratnasiri (1965), Private communication.

Gregory, J. B. (1965), The influence of atmospheric circulation on mesospheric electron density, J. Atmosph. Sci. *22*, 18-23.

Hartree, D. R. (1929), The propagation of electromagnetic waves in a stratified medium, Proc. Camb. Phil. Soc. *25*, 97-120.

Henry, G. W. (1966), Instrumentation and preliminary results from shipboard measurements of vertical incidence ionospheric absorption, University of Illinois, Aeronomy Report No. 13.

Lange-Hesse, G. (1953), 27 day variation in the absorption of the D region of the ionosphere over Singapore and Slough, J. Atmosph. Terr. Phys. *3*, 153-162.

Mechtly, E. A. and J. S. Shirke (1967), Rocket electron density measurements on winter days of anomalous and normal absorption (in preparation).

Mechtly, E. A., C. F. Sechrist, J. S. Shirke, K. Seino and J. S. Theon (1967), A coordinated experiment on the D region winter anomaly, I, Experimental results (in preparation).

Nicolet, M. (1959), Collision frequency of electrons in the terrestrial atmosphere, Phys. Fluids *2*, 95-99.

Phelps, A. V. and J. L. Pack (1959), Electron collision frequencies in nitrogen and in the lower ionosphere, Phys. Rev. Letters *3*, 340-341.

Piggott, W. R., W. J. G. Beynon and G. M. Brown (1957), The pulse reflection method of measuring ionospheric absorption, Ann. IGY *3*, 179-206.

Schmerling, E. R. (1958), An easily applied method for the reduction of h'-f records to N-h profiles including the effects of the earth's magnetic field, J. Atmosph. Terr. Phys. *12*, 8-15.

Schmerling, E. R. and C. A. Ventrice (1959), Coefficients for the rapid reduction of h'-f records to N-h profiles without computing aids, J. Atmosph. Terr. Phys. *14*, 249-261.

Sechrist, C. F. (1967), A theory of the winter absorption anomaly at middle latitudes, J. Atmosph. Terr. Phys. *29*, 113-136.

Sen, H. K. and A. A. Wyller (1960), On the generalization of the Appleton-Hartree magnetoionic formulas, J. Geophys. Res. *65*, 3931-3950.

Shapley, A. H. and W. J. G. Beynon (1965), Winter anomaly in ionospheric absorption and stratospheric warmings, Nature *206*, 1242-1243.

Shirke, J. S. (1959), Measurement of the ionospheric absorption on 2.5 mc/s at Ahmedabad, J. Inst. Telcom. Engr. *5*, 115-120.

Shirke, J. S. (1962), Ionospheric absorption on 2.5/2.6 mc/s at Ahmedabad, Proc. of IGY Symp., New Delhi, I, 142-148.

Shirke, J. S. and G. W. Henry (1967), Geomagnetic anomaly in ionospheric absorption at low latitudes observed on board USNS Croatan, Ann. Geophys. (in the press).

Shirke, J. S. and G. L. Narayana Rao (1967), Criteria for recognition of a winter day of high absorption, J. Geophys. Res. *72*, 2917-2927.

Skinner, N. J. and R. W. Wright (1956), Studies of ionospheric absorption at Ibadan, Nigeria during the period of minimum solar activity 1954-1955, J. Atmosph. Terr. Phys. *9*, 103-117.

Thomas, L. (1961), The winter anomaly in ionospheric absorption, J. Atmosph. Terr. Phys. *23*, 301-317.